Measurement of residual stress in materials using neutrons

*Proceedings of a technical meeting
held in Vienna 13-17 October, 2003*

IAEA
International Atomic Energy Agency

IAEA-TECDOC-1457

Measurement of residual stress in materials using neutrons

Proceedings of a technical meeting held in Vienna 13-17 October, 2003

IAEA

International Atomic Energy Agency

June 2005

MEASUREMENT OF RESIDUAL STRESS IN MATERIALS USING NEUTRONS
IAEA, VIENNA, 2005
IAEA-TECDOC-1457
ISBN 92–0–106305–9
ISSN 1011–4289

FOREWORD

Research reactors have played an important role in research and development in materials science and technology. The characterization, development and testing of engineering components form an area where neutrons have large potential as a probe. Measurement of residual stress is one such area where neutron diffraction has proved to be very fruitful. It is possible to design an instrument for a neutron beam on a medium flux research reactor with appropriate choice of parameters like resolution and beam intensity and components like collimators and detectors. The method has been used to measure residual stress distribution in large bearings of a crankshaft of car, strain distribution in the cross-section of a railway wheel and rail welds. The deformations in these components at microscopic level could lead to severe accidents. The testing of reliability of a product or the diagnosis of the failure of a component could thus be done effectively.

One of the objectives of the IAEA's project on effective utilization of research reactors is to promote the use of the existing research reactors based on their capabilities and is implemented through workshops and technical meetings. Measurement of residual stress is one of the techniques that find wide applications in materials development and testing. The Technical Meeting on Measurement of Residual Stress Using Neutrons was organized to meet this objective. This publication is the outcome of the deliberations during the meeting and the presentations by the participants and is addressed to the research reactor managers, users and designers of facilities for reactor utilization. It will especially benefit those seeking to develop new facilities or upgrade the existing ones to enhance the utilization of their research reactors.

Experts with a long experience in developing and using neutron beam instruments in high flux and medium flux research reactors participated in this technical meeting. They presented the design, development and utilization of the facilities at their respective centres and reviewed the current status of the residual stress measurements using neutron beams from research reactors. The sessions included brainstorming on the methodology and data analysis, characterization and standardization of the equipment and identifying the scope for further development. The IAEA thanks all the experts for their contribution to the technical meeting through presentation and detailed discussions on various aspects of the technique and in the preparation of the publication.

The IAEA officer responsible for this publication was S.K. Paranjpe of the Division of Physical and Chemical Sciences.

EDITORIAL NOTE

CONTENTS

SUMMARY

1.   Introduction

Research reactors have the potential to provide the necessary infrastructure for a wide range of scientific and technological developments around the world. Such reactors can act as centres of excellence for scientific studies in the field of Physics, chemistry, biology, geology, materials science and medicine as well as for industrial applications.

Neutron scattering has played an important role in studying structure and dynamics of condensed matter. The special nature of neutron interaction with matter provides important complementary and supplementary data to other techniques. The location of hydrogen atoms in the presence of heavy elements, for example, can only be determined by means of neutron diffraction studies. Crystal structures of biological systems, like amino acids and polypeptides, have been elucidated using single-crystal neutron diffraction. The behaviour of magnetic materials can also be explored for both scientific and industrial applications.

The large penetration depth and selective absorption of neutrons make them a powerful tool in NDT of materials. Residual stress formed in a material during manufacturing, welding, utilization or repairs can be measured by means of neutron diffraction. In fact neutron diffraction is the only NDT method, which can facilitate 3-D mapping of residual stress in a bulk component. Such studies can help to improve the manufacturing quality of engineering components and to optimise design criteria in applications. Anisotropies in thermal and electrical conductivities, for instance of fuel elements, and mechanical properties of materials depend on the textures developed during their preparation or thermal treatment. Textures can be studied using neutron diffraction techniques, which are developed and used in many research reactors.

The experimental technique, determination of residual stress, improvements in the instruments and standardization methods discussed during the technical meeting are described here.

2.   Review of the technique

Neutron diffraction (ND) as classical X ray diffraction (XRD) and strong X ray synchrotron diffraction (SD) are based on the same principle and are complementary. Due to their very nature, XRD is suitable for surface measurements, SD for shallow depths and thin specimens, and ND for bulk measurements within thick specimens. While ND and SD cannot provide for in-situ investigations and are only available in some 30 facilities worldwide, XRD can be applied in-situ and in a vast number of laboratories throughout the world. However, XRD is not practically useful for probing real industrial components, as it yields very localized information at the specimen surface, which usually is not representative of the bulk stress state.

This publication refers to the determination of residual and/or applied stresses in polycrystalline materials using neutron diffraction technique. The elastic strains are derived from the changes in the lattice spacings of the crystalline material. The stresses are then calculated through the incorporation of the elastic properties of the material given by the Hook's law. By translating the specimen through a highly collimated neutron beam, stresses within a small volume can be determined at different locations in the specimen.

2.1 Outline of diffraction principle – the Bragg law

When a crystalline material is illuminated with a neutron beam of wavelength λ, comparable with the inter-planer spacing d_{hkl}, a diffraction pattern is observed in which, the position of each plane (hkl) is obtained using the Bragg relation,

$$2 \, d_{hkl} \sin \theta_{hkl} = \lambda \qquad (1)$$

Figure 1 shows angle $2\theta_{hkl}$ at which the Bragg peak appears and is referenced to the incident beam direction. So each d_{hkl} is determined from the angle θ_{hkl} at which the reflection is observed.
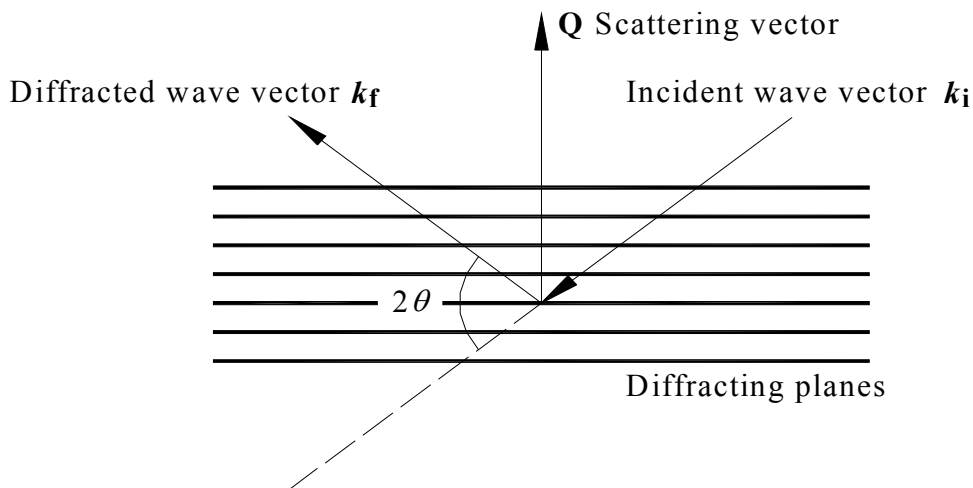

Figure 1. Schematic illustration of Bragg scattering.

3. Neutron sources

Neutron diffraction uses neutrons generated by fission or spallation. The former is predominantly employed in steady-state nuclear reactors and the latter usually in pulsed sources. In both cases the neutrons produced are moderated to bring their energies to the thermal range, i.e. $\lambda \geq 0.05$ nm. At continuous sources, a monochromatic beam of neutrons is produced by using a monochromating device to select a given neutron wavelength from the polychromatic beam. At pulsed sources, the neutron beam usually consists of a series of short pulses each containing a spectrum of wavelengths. The energy (and therefore wavelength) of each neutron can be determined from its velocity (time of flight methods TOF). Thus the entire diffraction pattern is recorded at any particular scattering angle.

4. Strain measurement

4.1 Steady state reactor

The strain is measured in the direction of the scattering vector, $Q = k_f - k_i$, which bisects the angle between incident and diffracted beams and is perpendicular to the diffracting planes as shown in Figure 1. Lattice spacings are determined from the measured angular position of the diffraction peak (Bragg reflection) by illuminating the specimen with a monochromatic collimated beam of neutrons. If the specimen contains no strain, the lattice spacings are the strain free (stress free) values for the material and are denoted by $d_{0,hkl}$. In a stressed

specimen, lattice spacings are altered and a shift in each Bragg peak position occurs and the elastic strains then are given by

$$\varepsilon_{hkl} = \frac{d_{hkl} - d_{0,hkl}}{d_{0,hkl}} = \frac{\Delta d_{hkl}}{d_{0,hkl}} = \frac{\sin\theta_{0,hkl}}{\sin\theta_{hkl}} - 1 \qquad (2)$$

The angle $\theta_{0,hkl}$ is the angle at which Bragg peak is observed from the strain free reference.

4.2. *Pulsed sources*

For TOF instruments, at a fixed scattering angle 2θ, the time-of-flight is proportional to the lattice spacing d_{hkl}, i. e.

$$t_{hkl} \propto \sin\theta \cdot d_{hkl} \qquad (3)$$

The elastic strain can then be calculated in any of the observed reflections in a manner analogous to that described in equation (2) so that for a fixed angle 2θ.

$$\varepsilon_{hkl} = \frac{\Delta d_{hkl}}{d_{0,hkl}} = \frac{t_{hkl} - t_{0,hkl}}{t_{0,hkl}} \qquad (4)$$

Where $t_{0,hkl}$ is the time of flight for the strain free reference. It should be noted that simultaneous recording of reflections of various lattice planes could facilitate analysing the data by multi-peak fitting or profile refinement method.

The angular resolution necessary to determine a strain ε is derived from the Bragg equation and is given by $\Delta\theta_{hkl} = -\varepsilon_{hkl}\tan\theta_{hkl}$. The necessary information comes from the shift of the peak and not from its absolute position value.

5. Neutron diffractometers

A polycrystalline sample consists of small crystallites, of the order of few µm, randomly oriented with respect to each other. When a monochromatic radiations fall on such a sample, the diffraction from a Brag plane results in the form of a cone, the Debye Scherrer cone, with semi-vortex angle 2θ. The intensity profile is recorded as a circle on a two dimensional detector (Figure 2).
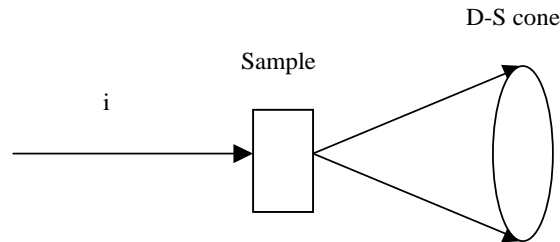
Figure 2. Diffraction from polycrystalline sample in a Debye Scherrer cone.

An instrument used for strain measurement at a reactor source is shown schematically in Figure 2. The polychromatic neutron beam is first monochromated to a chosen wavelength by diffraction from a suitable monochromator. The divergence and size of the monochromatic beam is suitably adjusted using appropriate neutron optical devices and is then diffracted from the specimen. In a similar way, the diffracted beam is shaped using suitable optical devices, before being captured by the neutron detector. The gauge volume over which the strain measurement is made is given by the intersection of the incident and diffracted beams (Figure 3). An example of a diffraction peak emanating from such an instrument is shown in Figure 4.
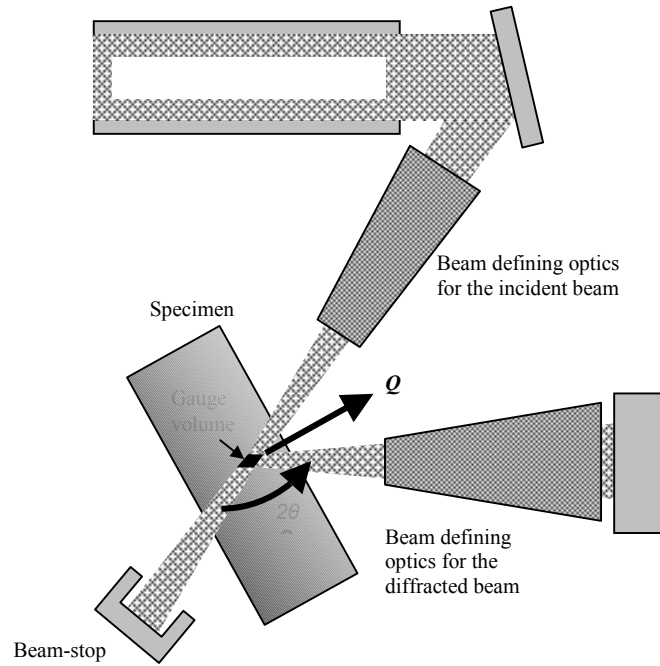
Figure 3. Schematic illustration of a typical continuous source based diffractometer for strain measurement.
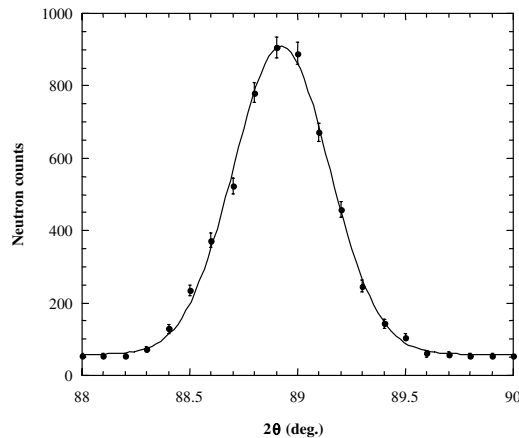
Figure 4. Example of a Bragg peak from a reactor (continuous source) based diffractometer fitted with a Gaussian distribution.

On a TOF-diffractometer each pulse provides a diffraction profile over a large range of lattice spacings. A typical TOF-diffractometer used for strain measurement at a pulsed source is shown in Figure 5.

6. Stress determination

Since neutron diffraction can measure the elastic strain within a defined volume in a crystalline solid, it is possible to calculate the mean stress in that volume provided the relevant elastic constants for the material are known.

4

Figure 5. Schematic of a typical pulsed source based diffractometer for strain measurement.

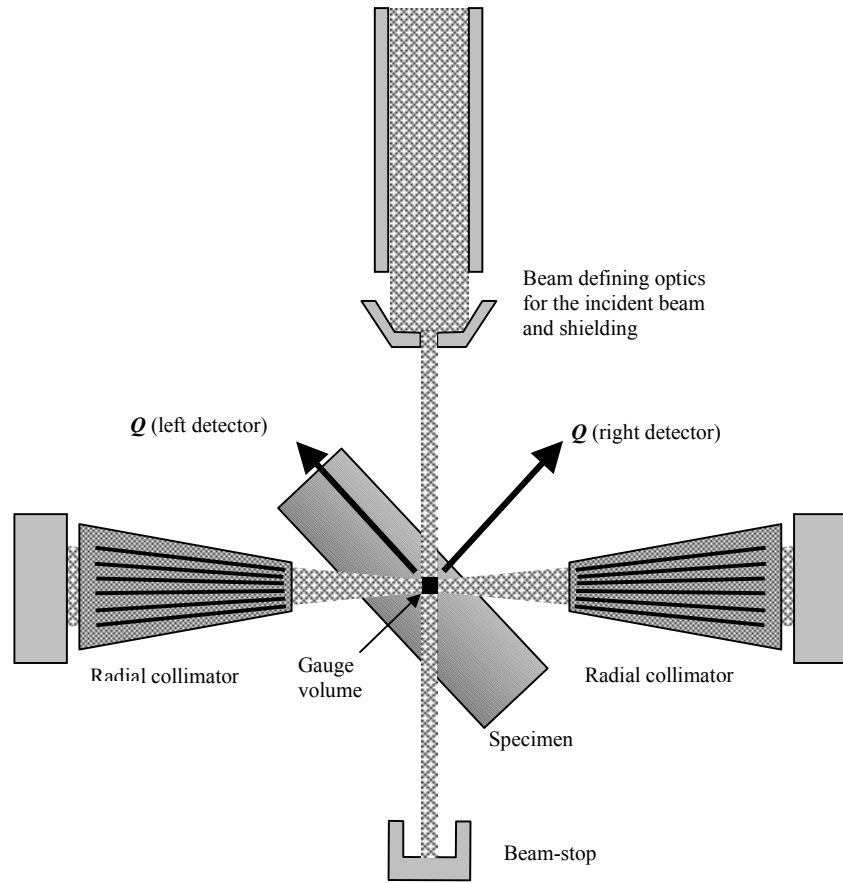Full determination of the strain tensor requires measurements of the elastic strain in at least six independent directions. If the principal strain directions within the specimen are known, measurements along these three directions are sufficient. For plane stress or plane strain conditions, a further reduction to two directions is possible. Measurement along one direction only is needed in the case of uni-axial loading.

Stresses and strains in a specimen are usually direction and position dependent. This leads to the need to measure strains at a number of locations in more than one direction. This in turn requires accurate positioning of the specimen with respect to the collimated neutron beam and the detectors. This is usually accomplished with linear translation and rotation tables, on which the specimen is mounted. By sequentially moving the specimen through the gauge volume the spatial variation in stress can be mapped.

Stress σ_{ij} and elastic strain ε_{kl} are second rank tensors and are related through elastic constants, $\underline{C}_{ijkl}$

$$\sigma_{ij} = \underline{C}_{ijkl}\,\varepsilon_{kl} \qquad\qquad (5)$$

However, equation (5) is often not practical for determining stresses from the diffraction technique. Diffraction measures *hkl*-specific lattice strains, which require *hkl* specific elastic constants for stress determination. In addition, shear strains cannot be measured directly by diffraction methods. In general, full determination of the strain tensor requires measurements of the elastic strain in at least six independent directions. Tilting and rotating the specimen as

5

shown in Figure 6 accomplish this. Finally, strong texture, prohibiting measurements of certain *hkl* reflections in certain directions, can give rise to the need of applying the same approach in order to obtain the full strain tensor.
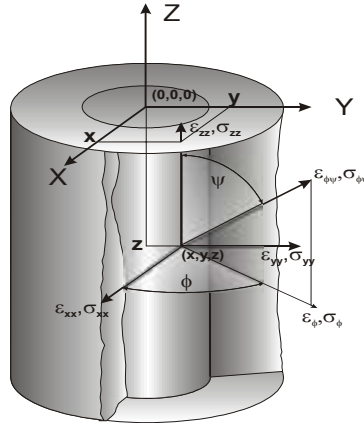

Figure 6. Stress and strain components in the direction of the scattering vector given by the tilt angles (ψ,φ) at a measurement point (x, y, z) in the specimen co-ordinate system (X, Y, Z).

The strain $\varepsilon_{\varphi\psi}$ is related to the stresses through

$$\varepsilon_{\varphi\psi} = \frac{d_{\varphi\psi} - d_0}{d_0} = \tfrac{1}{2} s_2(hkl) \times$$

$$\left[\begin{array}{l} \left(\sigma_{xx} \cos^2\varphi + \sigma_{yy} \sin^2\varphi + \sigma_{xy} \sin 2\varphi \right) \sin^2\psi + \\ \left(\sigma_{xz} \cos\varphi + \sigma_{yz} \sin\varphi \right) \sin 2\psi + \sigma_{zz} \cos^2\psi \end{array} \right] + s_1(hkl)\left(\sigma_{xx} + \sigma_{yy} + \sigma_{zz} \right) \tag{6}$$

If the number of strain measurements is greater than the number of unknown stress components in eq. (6) then a least square procedure is used to fit the calculated strains to the measured strains $\varepsilon_{\varphi\psi}$ with the stresses as fit parameters. The diffraction elastic constants $\tfrac{1}{2} s_2(hkl) = (1 + \nu_{hkl})/E_{hkl}$ and $s_1(hkl) = -\nu_{hkl} / E_{hkl}$ can be calculated using polycrystalline elasticity models. E_{hkl}, ν_{hkl} are the Elastic modulus and Poisson's ratio associated with *(hkl)*. Values for some common materials and diffraction planes *(hkl)* are given in Table 1.

Table 1: Values for diffraction elastic constants.

Specimen / Material	*hkl*	$\tfrac{1}{2} s_2(hkl)$ [10^{-6} MPa^{-1}]	$s_1(hkl)$ [10^{-6} MPa^{-1}]
Low alloy steel (iron)	211	5.72	-1.26
Low alloy steel (iron)	110	5.72	-1.26
Stainless steel, high nickel content	311	6.73	-1.59
Stainless steel, high nickel content	220	5.96	-1.33
Aluminium	311	19.57	-5.16
Aluminium	220	19.10	-5.00

7.   Instrument design

A strain diffractometer is basically similar to a conventional powder diffractometer with following special characteristics:

- The instrument requires the selection of a finite sampling volume over which measurements are made and a translation/rotation table for measurements at different locations and directions within the sampled specimen.

- The instrument evaluates the variations of lattice spacings within a sample with a spatial resolution of the order of a mm determined by the dimensions of the gauge volume.

- The diameter of the grains of polycrystalline aggregate probed should be about two orders of magnitude smaller than the dimensions of the gauge volume, which is geometrically defined by optical devices (slits, collimators) and scattering angle $2\theta_s$. The best geometrical choice corresponds to $2\theta_s=90°$, consequently the best choice is an intense Bragg peak at $2\theta_S$ near 90°. However, in some cases this may not be possible and a diffraction angle significantly different ($2\theta_s$ between 60° and 120°) has to be used.
- A wavelength in the range of 0.15-0.35 nm is necessary for the investigation of most commonly used crystalline materials.

- Beam parameters like divergence and $\Delta\lambda/\lambda$ should be adjusted such that the angular position of the sample reflections could be measured with a precision of 0.01^0 (which corresponds to a strain of 0.01% measured at $2\theta_s= 90°$).

7.1   Minimum requirements

Minimum fluxes at the sample position should be $> 5 \times 10^4$ n/cm^2/s provided that the instrumental background is very low. The full width at half maximum (FWHM) of the peak at a scattering angle of 90° should not be larger than 0.8°. Larger peak widths would require significantly longer counting times.

7.1.1 Monochromator

In order to obtain appropriate monochromatic beam characteristics either mosaic monochromators in combination with Soller collimators or bent perfect crystals can be used [1-5]. It is beneficial to use vertical and horizontal focusing. A substantial gain of the monochromatic beam flux can be achieved by vertical focusing without affecting the instrumental resolution. Similarly, horizontal focusing by means of bent perfect crystals can result in significant improvements of the resolution and diffraction peak height. The monochromator settings must not be changed during a measurement. Table 2 provides some guidance for selecting wavelength and sample reflections.

Table 2. Commonly used settings for sample d-spacings and monochromators

Specimen	hkl	d_s [nm]	λ required for $2\theta_s=90°$ [nm]	Possible monochromator choices and take-off angles					
				Cu-220	Cu-200	PG-002	PG-004	Ge-311	Si-220
Low alloy steel	211	0.118	0.167	82	55	29	60	59	52
Low alloy steel	110	0.204	0.288	N/A	107	51	119	116	97
Stainless steel, Nickel based alloys, copper	311	0.108	0.153	37	50	26	54	53	47
Stainless steel, Nickel based alloys, copper	220	0.127	0.180	45	60	31	65	64	56
Aluminium	311	0.122	0.173	43	57	30	62	61	53
Aluminium	220	0.143	0.202	53	68	35	74	73	64

7.1.2 Optical devices for beam definition

Optical devices are Soller collimators and apertures for the primary and the diffracted beams. The Soller collimator has a strong impact on the resolution and the intensity of the primary beam. Since the objective of a strain measurement is to determine the peak position accurately ($\leq 0.01\%$) the dimensions of the collimators should be selected such that a good compromise between intensity and peak width (FWHM) is found and the Figure of Merit (FM) is optimized.

$$\text{FM} \sim (\text{Peak Height}) / (\text{FWHM})^2 \qquad\qquad (7)$$

The peak height is defined to be background subtracted. This formula holds for peak to background ratios > 3. If this ratio is smaller than 3 then a larger sampling volume may be the solution. Shielding, especially around the monochromator and the detector is extremely important as it affects the instrumental background and, consequently, the peak to background ratio.

Primary beam apertures are made of neutron absorbing material such as boron, cadmium, Gd_2O_3, ^6Li or materials that contain sufficient concentrations of the aforementioned elements (BN, B_4C, borated polyethylene). The width and the height of the apertures define the dimensions of the primary and the diffracted beams. The openings and the distance from the sample of both the primary and the diffracted beam apertures should not be changed during an experiment because such changes would invariably cause shifts of the angular position of the reflected beam. If a change in the configuration of the apertures is necessary then a re-alignment is necessary as well. It is also important to position the slits as close to the specimen as possible.

7.1.3 Sample table

In order to measure strains at specific locations in the specimen, it has to be moved through the fixed gauge volume. The positioning accuracy is application dependent and should be to within one tenth of the minimum gauge volume dimension. For large specimens/sampling volumes less accuracy may be sufficient. The initial positioning of the sample can be achieved using optical instruments such as theodolites or mechanical means. The sample table should be able to move in three orthogonal directions and to rotate around the vertical axis (ω-rotation) of the instrument. The travel range in all three directions and the weight bearing capability must be chosen on the basis of the anticipated experiments. Many specimens at operating stress diffractometers weigh less than 20 kg, and typical travels are of the order of 100 mm.

7.1.4 Detector

Measurements with a single cell or point detector are possible but very time consuming. It is advisable to use at least a one dimensional Position Sensitive Detector (PSD) able to capture an entire diffraction peak. One or two dimensional PSDs facilitate simultaneous recording of data over a range of angle. A linear or one-dimensional PSD consists of an anode wire set axially with respect to a cylindrical tube, which acts as a cathode. The detector is placed normal to the scattered beam and output signal is collected from both the ends of the anode. Various methods, like charge division, rise time, delay line, are used for position decoding and scattered neutron spectra is recorded over the range of angle subtended by the detector at the sample center. A two dimensional detector comprises assembly of two orthogonal networks of one-dimensional detectors. The position decoding is similar to the one in linear detectors. Such detectors cover a wide angular range (linear PSD) and a Debye Scherer cone in a diffraction experiment or x-y plane of scattering vector (**Q**) in general (two dimensional detector). These detectors enhance the effective throughput of an experiment at times by an order of magnitude.

8. Data analysis

The peak angular position is usually obtained by fitting the experimental peak profile with an appropriate function, e.g. a Gaussian or a pseudo-Voigt function. The fitting algorithm should also provide an estimate of the statistical error of the peak position, which determines the statistical error of the strain measurement ($\Delta d/d$).

9. Instrument alignment, calibration and positioning

The apertures should be aligned such that the centroid of the gauge volume lies on the rotation axis ω. It is advisable to keep the wavelength constant throughout a measurement and that the detector angular response has been calibrated. It is though necessary that d_0 and d are measured during the same experiment. The positioning of the specimen can be achieved by optical (specimen fiduciary marks) or mechanical means (dial gauges or callipers); it can also be positioned relative to the gauge volume using neutron scans (entering curve).

Accurate specimen alignment is particularly important when scanning through steep strain gradients, interfaces, surfaces or when large translation scans are required.

10. Determination of a reference value for the d spacing

In order to determine elastic strains it is necessary to have a reference d-value, relative to which the strains can be determined. In some cases it is possible to determine a strain free lattice spacing d_0. In other cases only a reference lattice spacing may be known. The optimum method for determining d_0 depends on the particular application. Methods include:

- Measurement in the material at a position known to exhibit negligible strain
- Measurement on a representative powder of the material
- Measurement on small coupons cut from large blocks of the material
- Calculation of d_0 by imposing force and stress equilibrium
- Calculation of d_0 by ensuring zero stress near a free surface and normal to it

11. Recommendations for instrumental improvements

In the following, recommendations are made for the improvement of operating instruments. Significant gains can be achieved by using focusing monchromators and/or larger vertical detector coverage. Another option for significant improvement is the reduction of the instrumental background. Especially for long counting high instrumental background is the most serious limitation. Measures for reducing the background are fast neutron filters (saphire, silicon single crystal) and improved shielding around the monochromator and the detector (usually borated PE). Cadmium is very effective but should be avoided because it creates a high gamma background (gamma sensitivity of the detector). It is proposed to perform a Monte Carlo type analysis (McSTAS, VITESS, RESTRAX) to precisely identify effective ways for improvement.

12. Auxiliary equipment

For investigation of certain materials science problems the following equipment has proven very useful:

- Bending devices (elastic properties, fatigue).
- Load frame (elastic properties, fatigue, anisotropy of elastic and plastic properties).
- Eulerian Cradle (preferred orientation).
- Furnace (phase transformations, thermal stresses, stress relaxation).

Collaborative efforts or projects which would discuss the design of improved instrument, auxiliary equipment and a standardization methods with its implementation on reactors centres desirous of developing this technique will be useful for the effective utilization of research reactors will help in enhancing research reactor utilization.

13. Frequent problems encountered

The success and accuracy of residual stress measurements are influenced by positioning, inappropriate d_0, grain size, texture, partial illumination (such as at surfaces), d_0-variations (welding), plastic anisotropy, inhomogeneous attenuation.

14. Conclusion

Neutron diffractometer for residual stress measurements can be developed and fabricated for a medium flux reactor with appropriate choice of parameters and components. A well-standardized instrument can be a very important tool for applications in materials testing and improving the quality of engineering components.

REFERENCES

[1] POPOVICI, M., YELON, W.B., Focusing monochromators for Neutron Diffraction, Journal of Neutron Research **3** (1995) 1-25.

[2] MIKULA, P., VRANA, M., LUKAS, P., ŠARON, J., WAGNER, V., High-Resolution Neutron Powder Diffractometry on Samples of Small Dimensions, Materials Science Forum, **228-231** (1996) 269-274.

[3] MIKULA, P. LUKAS, P., VRANA, M., Bragg Diffraction Optics on Neutron Diffractometers, Physica B, **234-236,** (1997) 1058-1060.

[4] WITTE, D.A., KRAWITZ, A.D., WINHOLTZ, R.A., BERLINER, R.R., POPOVICI, M., An Instrument for Stress Measurement using Neutron Diffraction, Journal of Neutron Research **6** (1997) 217-232.

[5] MIKULA, P., VRANA, M., LUKAS, P., ŠAROUN, J., STRUNZ, P., ULLRICH, H.J., WAGNER, V., *"Neutron Diffractometer Exploiting Bragg Diffraction Optics – A High Resolution Strain Scanner"*, (Proc. of the 5th Int.Conf.on Residual Stresses ICRS-5, June 16-18, 1997, Linköping, Sweden), Vol. **2**, p. 721-725 (ERICSSON, T., ODEN, M., ANDERSSON, A., Eds).

BIBLIOGRAPHY

Polycrystalline Materials – Determination of Residual Stresses by Neutron Diffraction, ISO/TTA 3 S, ISO, Geneva (2001).

KRAWITZ, ARON D., Introduction to Diffraction in Materials Science and Engineering, John Wiley & Sons; (2001).

LODINI, ALAIN, FITZPATRICK, MICHAEL, Analysis of Residual Stress by Diffraction using Neutron and Synchrotron Radiation, (TAYLOR and FRANCIS, Eds), (2003).

NOYAN, I.N., COHEN, J.B., Residual Stress Measurement by Diffraction and Interpretation Springer-Verlag, New York (1987).

Residual stress measurements at LLB: An overview

J. Teixeira, M. Ceretti
Laboratoire Léon Brillouin, CEA Saclay, France

Abstract. Residual stresses can be evaluated from displacements of atoms at a microscopic scale. The changes of the distances between atoms correspond to shifts of Bragg reflections, which can be measured accurately by X ray or neutron diffraction. Collimation allows to probe separately small volumes and in this way to obtain a complete map of all the displacements in material. Neutron scattering has the advantage of a large penetration, due to small absorption by most of the elements. Instruments are permanently dedicated to this kind of studies in many neutron facilities. The principle of the technique is relatively easy and does not need very high fluxes. Because of its interest in metallurgical industries, the instrument becomes an attractive technique to be developed around medium flux research reactors.

1. Introduction

Materials are subject to forces and loads. As a result, their response is a deformation. Empirical diagrams represent the stress σ that must be applied to a sample in order to observe a stain ε. σ represents the applied force per unit of surface and has the dimensions of pressure. The more frequent units are GPa, Nm^{-2}, kbar and psi. The conversion is:

$$1 \text{ Gpa} = 10^9 \text{ Nm}^{-2} = 10 \text{ kbar} = 1.45 \times 10^5 \text{ psi}$$

ε is the relative increase of linear dimension in the direction of the applied force: $\varepsilon \equiv \Delta l / l_0$, where Δl is the change of the initial length l_0.
Diagrams representing $\sigma(\varepsilon)$ are extremely important to establish the mechanical properties of the material.

At low levels of deformation, stress and strain are proportional:
$$\sigma = E \varepsilon \qquad (1)$$

Figure 1. Typical Stress vs. Strain relation.

The constant of proportionality, E, is the Young's modulus. Typical values of E for metals spread from 45 GPa for magnesium up to 407 GPa for tungsten. For common steels E is of the order of 200 GPa (2 kbar must be applied in order to elongate of 0.1% the length of a steel rod).

At a microscopic level, crystalline solids have regular arrangements of atoms following well defined symmetry rules which allow the classification of different solids into a small number of crystallographic groups such as FCC (face-centred cubic), BCC (body-centred cubic), HCP (hexagonal close-packed), etc. In order to study such structural arrangements, scattering of particles or of electromagnetic radiation are the most convenient techniques, because they are sensitive to the correlation between atomic positions and average over very large volumes. The scattered intensity is the result of the interference of a large number of outgoing spherical waves from each atom of the sample when a plane wave is incident on them.
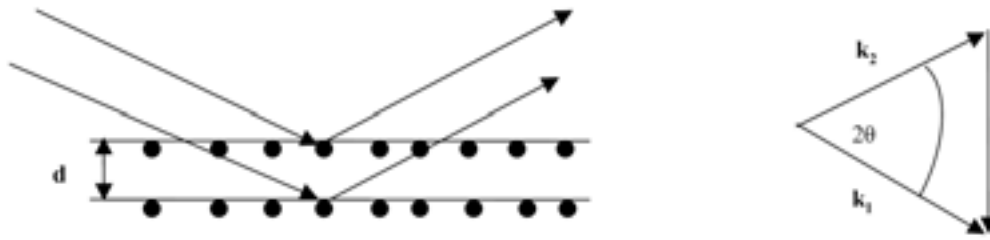
Figure 2. Representation of Bragg reflection from periodic array of atoms (left) with incident and scattered wave vectors k_1 and k_2 and scattering angle 2θ (right).

The Bragg law relates the relation between distance (*d*) between planes of atoms the incident angle θ and the wavelength λ of the radiation are related by the Bragg law:

$$2d \sin \theta = n\lambda \qquad (2)$$

Where *n* is an integer. The direction of the incident radiation is defined either by the Poynting vector in the case of electromagnetic radiation or the velocity *v* of the incident particle of mass *m* (which is related to λ by the de Broglie relation: $mv = h/\lambda$, where *h* is the Planck's constant).

Neutrons and X rays are the best probes to study the structure at the atomic level because their wavelengths have magnitudes comparable to inter-atomic distances and to the periodicity *d* of planes.
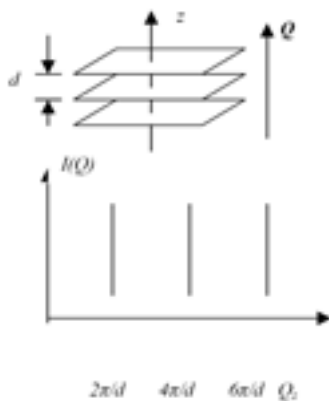
In a scattering process the exchange of momentum Q is given by:

$$Q = k_1 - k_2 \qquad (3)$$
$$Q = 4\pi \sin\theta/\lambda \qquad (4)$$

With this notation, the Bragg condition can be written:

$$Q = n \,(2\pi/d) \qquad (5)$$

Figure 3. Set of reflecting planes with Interplaner spacing d (upper) and intensity vs wave vector transfer (Q_Z) (lower) showing nonzero intensity at discrete values of Q_Z.

Since there are different sets of planes corresponding to different periodicities, the measurement of all "reflections" is a powerful technique to determine the crystal structure of a sample.

Most of the common materials are not perfect single crystals. The polycrystalline materials consist of small crystalline grains with a size typically of the order of μm, i.e. large compared

to inter-atomic distances but small as compared with the size of the sample. And are randomly oriented with respect to each other. As a consequence, the scattering is no more a fine spots but consists of circular lines, which can be seen as if a single monocrystal was turned in all directions. The scattered intensity, *I(Q)*, can be measured in one dimension. However, it will contain a superposition of a large number of reflections.

If we focus the attention in a well-defined line of *I(Q)*, its position Q_0 (or the corresponding angle θ) gives directly a distance of periodicity $d_0 = 2\pi /Q_0$. If in a small volume, the material is deformed, the distance *d* is slightly different from the nominal d_0.

For a piece of large dimensions, different regions are either under tension (ε>0) or under compression (ε<0). In the first (second) case the line moves to smaller (larger) values of Q.

$$\varepsilon = \left(\frac{d - d_0}{d_0}\right)_{hkl} = \left(\frac{\Delta d}{d_0}\right)_{hkl} = -\left(\frac{\Delta Q}{Q_0}\right)_{hkl} = -\frac{1}{2}\cot\theta_0.(\Delta 2\theta) \qquad (6)$$

The sensitivity of the technique is given by $-(d\theta/\varepsilon) = tg\ \theta$. It allows the detection of values of ε of the order of 10^{-2} to 10^{-5}.

In practice, the measurements are performed on one or two lines, the first of the powder spectrum of the sample. The scattering angle is fixed around 90°, probing planes oriented at 45° to the incident beam. One of the main advantages of neutron scattering is the large penetration depth (of the order of several cm) as compared to X rays. This property allows the study of pieces of very large size. With modern sources of X rays - synchrotron radiation- very short wavelengths and very intense beams are available yielding a larger depth of penetration than in conventional instruments but, in order to select the first intense lines of the spectrum, one must choose small diffraction angles. As a consequence the gauge volume under observation does not have the ideal cubic shape, but instead, it is a relatively long cylinder.

Source

Q

Detector
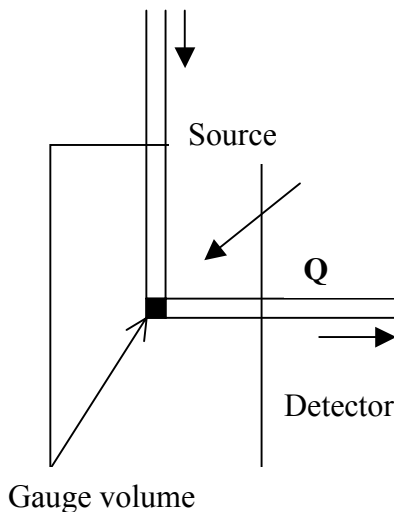
Gauge volume

The scattered intensity of a Bragg peak is relatively intense which allows the study of small gauge volume. Depending on this intensity and, mainly, on the depth, one may study gauge volumes of the order of 1 mm^3. Once defined the region of the sample to cover, successive measurements are done corresponding to a subdivision of the region in several small cubes. The selection of each small cube is achieved by an appropriate collimation of both the incident and scattered beams.

The instrument installed at the Laboratoire Léon Brillouin at Saclay is called Diane. It is installed on the guide G5 (cold neutrons).

Figure 4. Illustration of the Gauge volume as formed by the intersection of incident and scattered beam inside the sample.
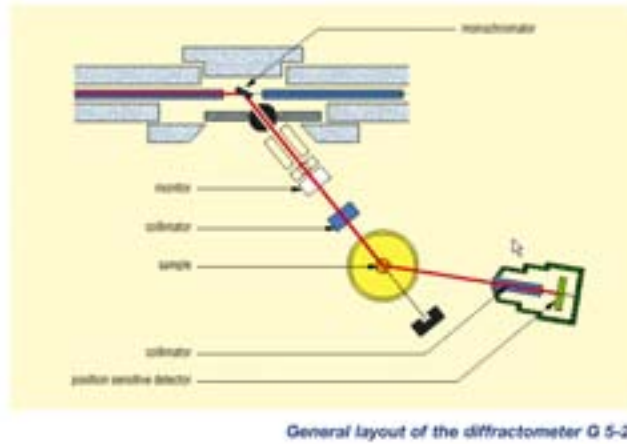
Figure 5. *General layout of the diffractometer G 5-2.*

The sketch of the instrument is represented in the above figure. The main characteristics of the instrument are given in the Table 1.

Table 1. Diana (G5.2)

Beam tube	Cold Neutron Guide G 5
Monochromator	Pyrolytic graphite (002) or (004)
Incident wavelength	$2.3\ \text{Å} \leq \lambda \leq 6\ \text{Å}$ continuously variable
Type of instrument	Two-axis
Detector	$100 \times 100\ \text{mm}^2$ EMBL (Grenoble outstation) ^{3}He PSD
Neutron flux at specimen	ca. $3.8 \times 10^6\ \text{n.cm}^{-2}\text{s}^{-1}$ at 3 Å
Angular ranges	$20° < 2\theta < 120°$, $\quad 0° < \omega < 360°$
Resolution	$\Delta d/d = 1.9 \times 10^{-3}$ at d = 2 Å ($\lambda = 2.8$ Å, using the (004) monochromator reflection)
Positioning table	with x, y and z movements : +/-75 mm x, y axes travel and 300 mm z-axis travel
Position repeatable	to 1 micron (x, y, z). Samples up to 500 kg in weight can be supported
Gauge dimensions	from 0.3 mm to 25 mm incident and outgoing beams variable in both dimensions.

Data collection and instrument Control system by PC
Ancillary equipment:
* Uni-axial loading rig : ± 20 kN dynamic loading for tension, compression and tension-compression. It can be mounted on the positioning table
* Eulerian cradle (inner diameter = 400 mm), $0 < \chi < 160°$ and $0 < \varphi < 360°$ for complete stress tensor determination.
* Four point bending device
* Furnace (T < 1000° C) for high temperature measurements

There is a position sensitive XY detector $100 \times 100\ \text{mm}^2$ with a resolution of 1.5 mm, which will be replaced by a new $200 \times 200\ \text{mm}^2$ detector. It allows the observation of the analysed lines with very good accuracy. In some cases two materials are observed simultaneous, for

example, in the case of welding or of metallic precipitates. The multi-detector allows very often the simultaneous observation of two lines corresponding to the two different materials.

Several times, one may be interested not only in the diagonal terms of the tensor matrix, but also in the off-diagonal terms, which correspond to shear stress:

$$\varepsilon_{ij} = S_{jikl}\sigma_{kl} \tag{7}$$

A complete evaluation of the stress tensor implies the evaluation of all the terms of the tensor, which requires the observation of the diffraction line at different positions of the sample. For this purpose, an Eulerian cradle with a diameter of 400 mm is installed on the instrument. Since the analysed pieces are very often very large (e.g. wheels of turbines, wings of planes, etc.) the positioning table can support charges of 500 kg and allows displacements of 7.5 cm in the horizontal plane and 30 cm along the vertical axis. An oven can be installed to perform experiments up to 1000° C.

2.   Conclusions

Measurements of deformations and stresses in materials of large size can be achieved relatively easily with neutron scattering techniques. The high penetration of the neutron beam in most metals allows a precise determination of residual stresses with a spatial resolution of the order of 1 mm. The low flux necessary for this technique makes it very attractive for installations with moderate neutron intensities.

REFERENCES

[1]. MACHERAUCH, E., KLOSS, K.H.,Proceedings of the International Conference on Residual Stresses, Garmisch-Partenkirchen (Germany), pp. 3-26, (1986).
[2]. WITHERS, P.J. , BHADESHIA, H.K.D.H., Residual Stress part 1-measurement techniques, *Mat. Science and Tech*. **17**, 355-365 (April 2001).
[3]. NOYAN, I.C., COHEN, J.B., Residual Stress Measurement by Diffraction and Interpretation, Materials Research Engineering, (Springer-Verlag ed) (1987).
[4]. ALLEN, J., HUTCHINGS, M.T., WINDSOR, C.G., ANDREANI, C., Neutron diffraction method for the study of residual stress fields, *Adv. in Phys*. **34**, 445-473 (1985).
[5]. CERETTI, M., KOCISI M., LODINI, A., Analysis of internal stress relaxation in an Al/SiC composite by neutron diffraction, *Science and Engineering of Composite Materials* **3**, 167-176 (1994).
[6]. CERETTI, M., MAGLI R., VANGI, D., Neutron diffraction study of stress field distribution in automotive gears, *Material Science Forum* **321-324**, 732 (2000).
[7]. CERETTI, M., Recent development for strain measurements at the LLB, *Physica B* **276-278**, 932-933 (2000).

Power of Bragg diffraction optics for high-resolution neutron diffractometers for strain/stress scanning

P. Mikula, M. Vrána, P. Lukáš
Nuclear Physics Institute, Řež, Czech Republic

Abstract. In this paper we introduce two high-resolution neutron diffraction techniques using Bragg diffraction optics based on cylindrically bent perfect crystals, which have been tested with the aim of their efficient exploitation for strain/stress and are routinely used in NPI Řež. Few presented experimental results demonstrate their experimental abilities for non-destructive testing and evaluation of a phase and deformation response of polycrystalline materials on residual stress or deformation loading. Two focusing double axis strain/stress diffractometers are operating at the medium flux reactor LVR-15 in Řež. Good luminosity of the diffractometers and a sufficiently high-resolution (*FWHM* of the instrumental $\delta d/d$ - profile can be less than 2×10^{-3} at d_{hkl}=0.2 nm) permit investigations of both the macro- and microstrains in the sample gauge volumes of several cubic millimetres with a sensitivity in the relative peak shift of 10^{-4} rad.

1. Introduction

Residual stresses or their development under applied external force can have a strong influence on the basic mechanical properties of materials. They displace atoms from their original positions in a crystalline material and neutron diffraction at a steady state source along with X ray diffraction can non-destructively reflect the resulting change of lattice constants with a sufficiently high precision by using the Bragg Diffraction Angle Analysis (BDAA) and/or by Energy-Dispersive Neutron-Transmission Diffraction (EDNTD).

Conventional neutron strain/stress scanners using the BDAA method (based on Bragg condition $2d_{hkl} \cdot \sin\theta_{hkl} = \lambda$; d_{hkl}-lattice distance, θ_{hkl} -Bragg angle, λ-the wavelength) are in fact powder diffractometers equipped with a mosaic monochromator and a system of Soller collimators and for high-resolution measurements they usually suffer from required luminosity. However, the dedicated diffractometers using Bragg diffraction optics provide substantially higher luminosity as well as better $\delta d/d_{hkl}$ resolution (*FWHM* – the Full Width at Half Maximum of the instrumental ($\delta d/d$)-profile can be of the order of 1×10^{-3}) [1-7] which results in figure of merit (FM) more than one order of magnitude better in favour of focusing diffractometers.

The EDNTD method is based on the measurement of a decrease of a beam intensity $I(\lambda)$ transmitted through a sample as a function the wavelength in a $\Delta\lambda$-range in the vicinity of the Bragg cut-off. The edge in this case can be observed when the wavelength is passing through the limit $\lambda=2d_{hkl}$, (d_{hkl} is the lattice spacing), below which particular reflection planes (*hkl*) begin to scatter neutrons. It means that no angular dependence of scattering is measured and only integrated intensity of this particular reflection can be determined for the transmitted beam for each value of λ. Mathematically, edge profile can be described by a Gaussian cumulative function (*FWHM* of the instrumental ($\delta d/d$)-profile can be of the order of 1×10^{-4}). As will be presented, using the Bragg diffraction optics, the EDNTD measurements, usually carried out only at the pulsed neutron beams [8], can be effectively carried out even at low and medium power reactors [9-11].

The excellent properties of focusing strain scanners permit one to investigate both the macrostrains with the sensitivity to $\Delta d/d$ changes down to 10^{-5} and microstrains by a peak profile or Bragg edge analysis in the gauge volumes of several mm^3. In principle, the substructural changes of e.g. dislocation density and average grain size in engineering

components after use can be investigated in situ, under loading by an external force. The stresses are not measured directly by diffraction techniques, but one measures strains defined as $\varepsilon = \Delta d/d_{o,hkl}$ ($d_{o,hkl}$ corresponds to the unstrained material), which are then converted to stresses using appropriate moduli. Then, the shift in the Bragg angle or of the position of the Bragg edge with respect to the strain-free material permits one to determine the average macrostrain over the irradiated gauge volume. Information on the microstrain (in the form of $\langle\varepsilon^2\rangle^{1/2}$) as well as dislocation density and grain size present in the irradiated gauge volume can be determined from a change of the width and the form of the diffraction peak or edge profile [12-16].

During the last years we have proposed and tested several modifications of the high resolution BDAA and EDNTD performances based on Bragg diffraction optics and those which have appeared as the most effective, are introduced.

2.   BDAA method, two-axis performance

The most spread high-resolution neutron diffraction two-axis performance (see Figure 1) consists basically of the following steps and properties [2,7]:

a. Monochromatic neutrons selected by a bent monochromator from the white spectrum are focused on a sample (real space focusing) making the luminosity of the device high.
b. The monochromatic beam is diffracted by a chosen volume element (determined by a pair of input and output slits) into the angle $\varphi = 2\theta_{hkl}$.
c. There is a strong correlation between the divergences α_0, α_1, α_2 and λ as
d. The quasiparallel diffracted beam is directly analysed by using a 1D-PSD.
e. No Soller collimators are required.

$$\alpha_1 = 2\eta(R_M) - \alpha_0; \qquad \alpha_2 = \alpha_1[2\,a_{SM}(1 - L_{MS}/2f_M) - 1] \qquad (1a)$$

$$\Delta\lambda/\lambda = \alpha_2 \cot\theta_M(1 - L_{MS}/2f_M)/[2\,a_{SM}(1 - L_{MS}/2f_M) - 1] \qquad (1b)$$
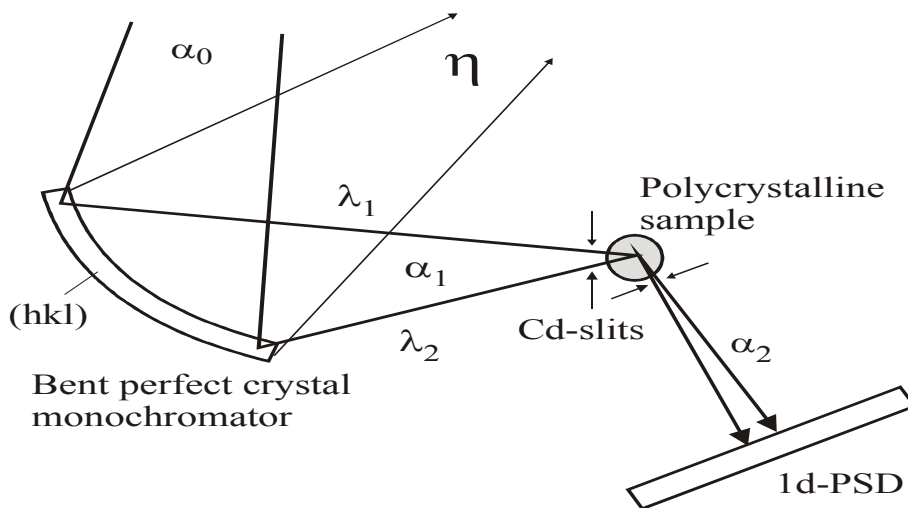

Figure 1. Schematic sketch of BDAA performance of the strain scanner.

Which all can be manipulated by changing the monochromator radius R_M ($\eta(R_M)$ is the total change of the angle of incidence (exit) over illuminated crystal length and a_{SM}=-tan θ_S/tan θ_M is the dispersion parameter). By setting a proper value of the radius R_M,

$$R_M= (2L_{MS}/\sin \theta_M)/(2 - 1/a_{SM}) \qquad (2)$$

$\alpha_2 = 0$ and a quasiparallel and highly luminous detector signal can by adjusted for a chosen scattering angle $\varphi = 2\theta_S$. Contrary to the conventional powder diffractometers equipped with mosaic monochromators, the minimum resolution e.g. at $2\theta_S = 90°$ can be achieved even for monochromator take-off angles far below $90°$.
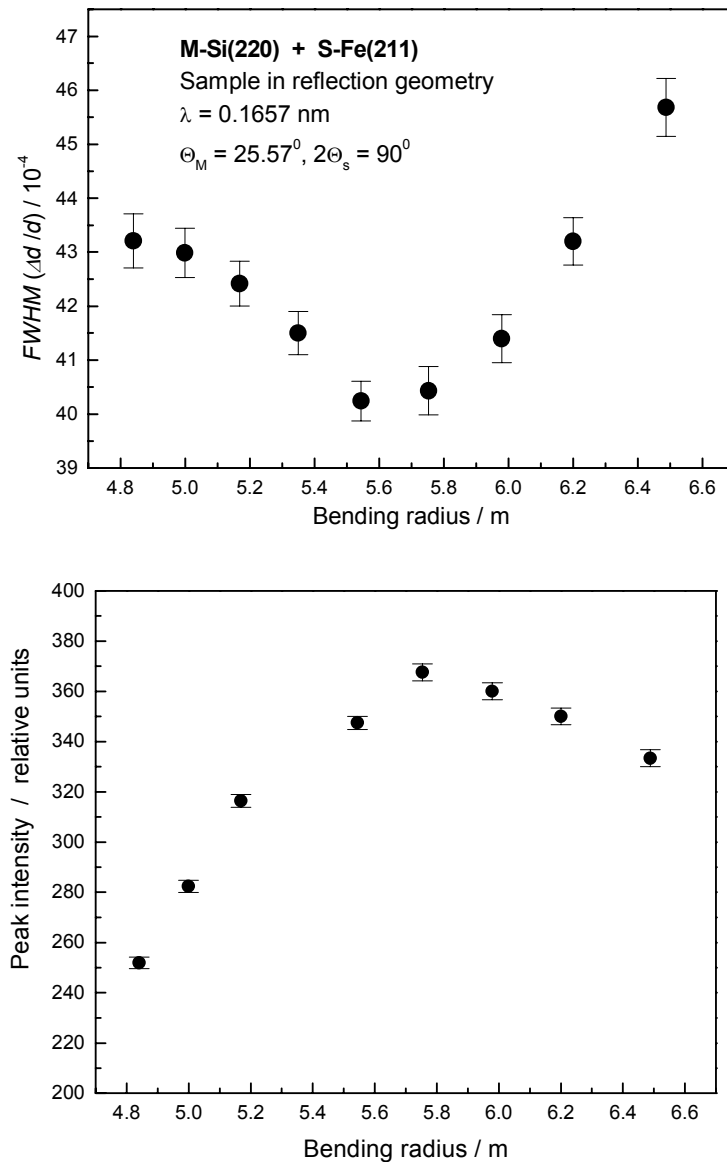
Figure 2. Optimization dependences determining the optimum radius for a given monochromator take-off angle and the scattering angle.

There are small resolution uncertainties $\Delta\alpha_{2t}$ and $\Delta\alpha_{2w}$ influencing the instrumental resolution which come from a non-negligible thickness t_M of the monochromator and from the finite width w of the irradiated volume of the sample determined by the input and output slits. Thus, for a point like sample, the monochromator of thickness t_M and the width of the sample w,

$$\Delta\alpha_{2t} = 2t_M\, a_{SM}\cot\theta_M / R_M ; \qquad \Delta\alpha_{2W} = w(2a_{SM} - 1)/L_{MS} \qquad (3)$$

Both of these parameters bring about the diffracted beam slightly divergent (quasiparallel) and directly determine the instrumental resolution. It is clear that it can be easily estimated and adjusted according to the experimental requirements. Of course, the total resolution of the instrument is strongly dependent on the spatial resolution of the 1d-PSD.

The employment of the Bragg diffraction optics resulted in an improvement of the luminosity and/or resolution of our dedicated strain scanners several times in comparison with the conventional counterparts. Moreover, recently, one of our two axis strain scanners has been equipped with a two-crystal-slab sandwich monochromator (when using combinations of Si (111)+Si (220) or Si (111)+Ge (311) reflections) which permits us to work simultaneously with two neutron wavelengths of 0.27 nm + 0.165 nm or 0.27 nm + 0.143 nm, respectively [5]. This fact enables us to investigate more sample-reflection profiles under the same experimental conditions within an angular range of scattering angles of $\Delta\varphi$ covered by one setting of the PSD. Thanks to a remote control of the bending device and a remote manipulation of the crystal curvature, the optimum focusing conditions can be achieved practically for any scattering angle $\varphi = 2\theta_{hkl}$. As a result of a compromise between the resolution and the luminosity, the two axis performances used in our laboratory work with the resolution $\delta d/d_{o,hkl} \cong 2\text{-}4\times 10^{-3}$ derived from the *FWHM* of the diffraction profiles taken with a well annealed standard samples. Several examples of measurements of residual strains are shown in Annex 1.

In addition, it should be mentioned that in principle, three-axis performance employing a focusing monochromator and a bent perfect analyser could be used for high-resolution strain measurements. Then, a cylindrically bent perfect analyser is set either in symmetric/slightly asymmetric diffraction geometry [9, 17-20] or in the fully asymmetric diffraction geometry in combination with 1D-PSD [20, 21]. The analysis of the beam diffracted by the gauge volume is in these cases performed in momentum space. Even though the three axis performances can provide a significantly higher ($\delta d/d$)-resolution the drawbacks coming from the employment of the additional diffraction component (analyser) make them rather impractical.

3. EDNTD method - one axis performance

The performance sketched in Figure 3 is the simplest one and by adjusting the monochromator take-off angle it can be used in a large range of the neutron wavelengths. A strong angular-wavelength correlation θ–λ in the beam passing through the slit can be expressed in the form as [10,11]

$$\lambda = \lambda_0[1 - \Delta\alpha_1\cot\theta_M\,(1 - L_{MS}/2f_M)]. \qquad (4)$$

Where $\Delta\alpha_1$ is an angular deviation of a neutron trajectory from the central beam within the α_1 divergence and $\lambda_0 = 2d_{hkl}$ is the value of the edge position (on the λ-scale) related to the

lattice planes (*hkl*). The resolution uncertainties Δx_t and Δx_W which come from the effective mosaicity of the bent perfect crystal and the width of the slit w, respectively, can be derived in the form [12]

$$\Delta x_t = w , \qquad \Delta x_w = w \ (\ 1 + 2L_{SD}/f_M) \qquad\qquad (5)$$

They make the θ–λ correlation imperfect and thus have an influence on the total smearing Δx of the Bragg edge as seen by PSD. The parameter Δx_t was derived for the case of the monochromator crystal thickness $t_M \geq W/\cos \theta_M$. For $t_M < w/\cos \theta_M$ an effective slit width w_{eff} should be introduced. The parameter Δx_w was derived for the case of an unlimited collimation of the incident polychromatic beam. However, in practice its impact can be considerably reduced for well-collimated beam in a guide tube having a divergence $\Delta\theta_o$. For $\Delta\theta_o \leq 2w/f_M$ we arrive at the estimation $\Delta x_w \leq \Delta\theta_o \ f_M(1+2L_{SD}/f_M)/2$. Fig. 4 demonstrates some basic characteristics of the one axis performance. Using a well annealed α-Fe (321) standard sample, a 4 mm thick monochromator and 2 mm wide slit, the ($\delta d/d$)-resolution (represented by the width of the edge profile) was about 1×10^{-3}.

In addition, we also mention possibility of the use of two-axis performance of the EDNTD method where the bent perfect crystal analyser is in symmetric or fully asymmetric diffraction geometry [9,11,18,22]. Also in this case both two-axis performances provide a higher ($\delta d/d$)-resolution, however, with the drawbacks again coming from the employment of the additional component-analyser.
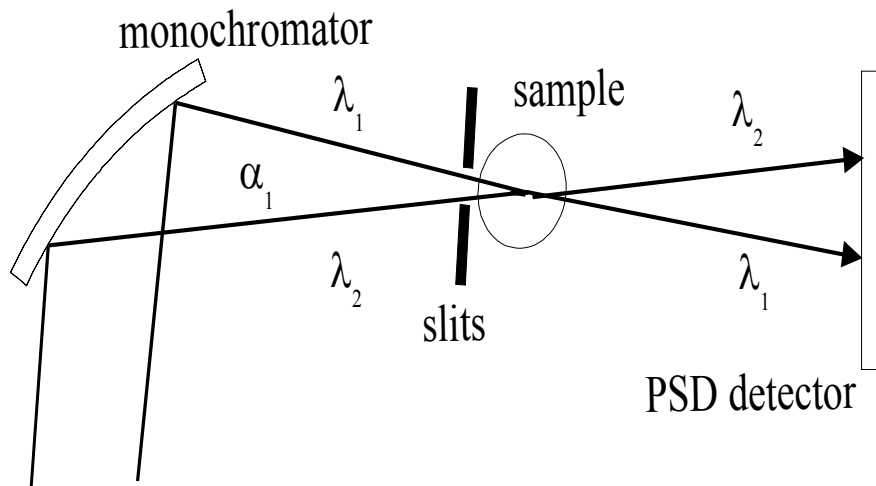

Figure 3. Schematic sketch of the one axis EDNTD-performance of the strain scanner.

In all the cases of the EDNTD methods following characteristics have been observed:

a.   The amplitude of the Bragg diffraction edge depends on the thickness of the sample.
b.   The steepness and the shape of the Bragg diffraction edge are determined dominantly by the $\Delta d/d$ distribution.

c.   Steepness of the edge can change with the thickness of the sample due to the multiple reflection effect.

d.   The resolution of the instrument permits to study macro-strain effects even below the value of 10^{-4} in $\varepsilon=\Delta d/d$ as well as some of the micro-strain characteristics from the edge profile analysis [15].

e.   The EDNTD techniques are limited to measurements of only one strain component parallel to the axis of the incident monochromatised beam.

f.   The introduced EDNTD techniques cannot be employed on a conventional diffractometer equipped with mosaic monochromator.
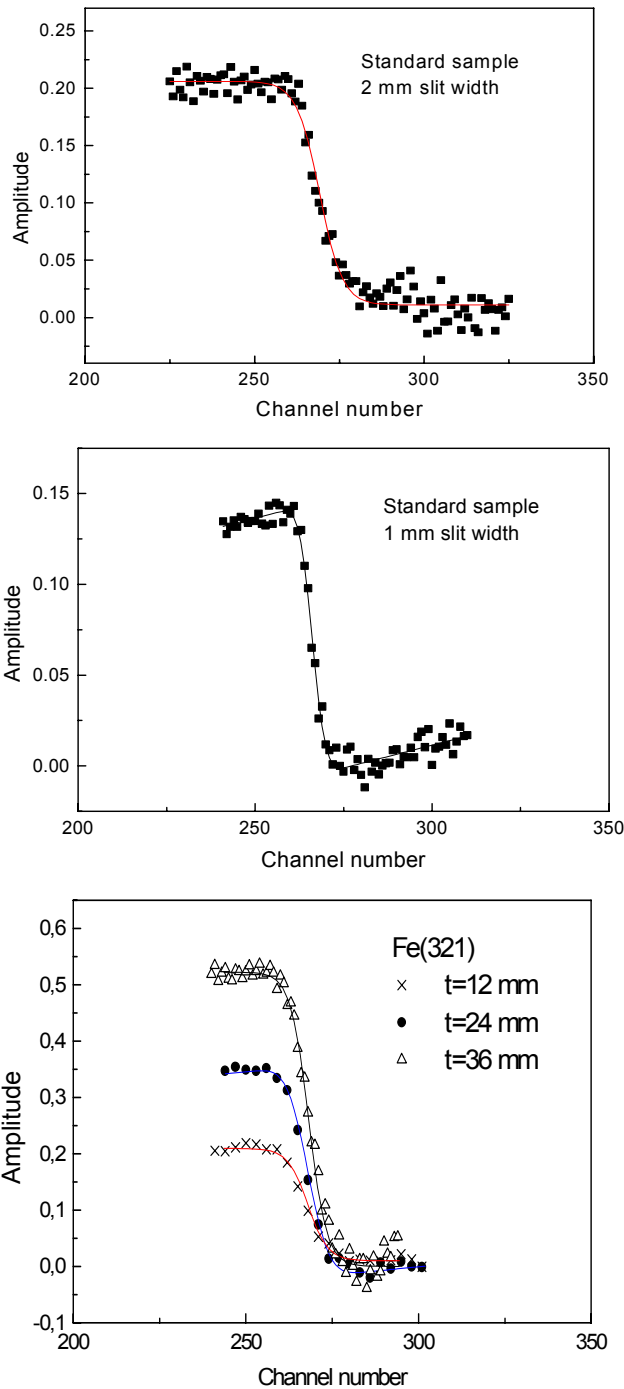
Figure 4. Bragg diffraction edges of 8 mm thick standard sample for different slit widths - (a),(b) and for different sample thicknesses - (c). (a)-FWHM(δθ)=12.5x 10⁻⁴ rad, (b)-FWHM(δθ)=7.7 x 10⁻⁴ rad.

An example of the use of EDNTD method - one axis performance - in the strain investigations is shown in Annex 2.

4. Discussion

This paper briefly describes two neutron diffractometer performances using Bragg diffraction optics for strain/stress scanning. In comparison with the conventional strain scanner equipped with a mosaic monochromator and a system of Soller collimators, our BDAA performance enabled us to improve the instrumental resolution and to increase the detector signal, simultaneously. The ($\delta d/d$)-resolution of the BDAA strain scanners of NPI Řež is about 2×10^{-3} (at $d_{hkl} = 0.2$ nm). Their luminosity permits us to perform peak-shift measurements with the sensitivity close to 10^{-5} on the ($\Delta d/d$)-scale for a reasonable measurement time even though we work at the medium-power research reactor. The only parameters, which influence the resolution of the instrument, are the effective mosaicity (linearly dependent on the thickness) of the bent perfect monochromator, widths of the slits and the spatial resolution of the position sensitive detector. Therefore, the resolution measured by *FWHM* of the diffraction profile or Bragg edge is a matter of a choice of these parameters with respect to the flux of the neutron source and the resulting detector signal. For further increase of the detector signal, in some cases a doubly bent monochromator using also vertical focusing (which has no influence on the resolution) can be used [23]. As can be seen from Figs. 1 and 3, the BDAA as well as EDNTD performances can be easily adapted to any conventional neutron diffractometer providing the appropriate wavelength. In the case of the EDNTD technique, basically, one axis diffractometer could be sufficient when having the possibility of changing the monochromator take-off angle. Monte Carlo simulations of resolution function and a detector signal can provide a great help in the course of the optimisation of the experimental performances [24]. Common feature of both focusing performances is a sufficiently high ($\delta d/d$)-resolution permitting also evaluation of micro-strains in plastically deformed polycrystalline samples. Of course, information about the strain state of art averaged within the irradiated sample volume is provided. Depending on the reactor power and the sample thickness, the cross-section of the incident/diffracted beam determined by the sample slits can be reduced to less than 10 mm^2, still keeping reasonable counting times.

REFERENCES

[1] POPOVICI, M., YELON, W.B., *Focusing Monochromators for Neutron Diffraction*, J. Neutron Research, **3**, 1-25 (1995).

[2] MIKULA, P., VRANA, M., LUKAS, P., ŠAROUN, J., WAGNER, V., *High-Resolution Neutron Powder Diffractometry on Samples of Small Dimensions*, Mat. Sc. Forum **228-231,** 269-274 (1996).

[3] MIKULA, P., VRANA, M., LUKAS, P., ŠAROUN, J., STRUNZ, P., ULLRICH, H.J., WAGNER, V., *Neutron Diffractometer Exploiting Bragg Diffraction Optics - A High Resolution Strain Scanner,* (Proc. of the 5th Int. Conf. on Residual Stresses ICRS-5, June 16-18, 1997, Linköping), Vol. **2**, p. 721-725 (Ericsson, T, ODEN, M., ANDERSSON, A., Eds)

[4] WITTE, D.A., KRAWITZ, A.D., WINHOLTZ, R.A., BERLINER, R.R., POPOVICI, M., *An Instrument for Stress Measurement using Neutron Diffraction*, J. Neutron Research, **6**, 217-232 (1998).

[5] VRANA, M., MIKULA, P., LUKAS, P., WAGNER, V., *Two Wavelength Sandwich Monochromator for Materials Research Experiments*, Physica, B **241-243,** 231-233 (1998).

[6] VRANA, M., MIKULA, P., LUKAS, P., DUBSKY, J., WAGNER, V., *New Developments in Instrumentation for Strain Scanning in NPI Řež*, Mat. Sc. Forum **321-324,** 338-344 (2000).

[7] MIKULA P., WAGNER, V., *Strain Scanning Using a Neutron Guide Diffractometer*, in the Proc. of the 5th European Conf. on Residual Stresses ECRS-5, Delft-Noordwijkerhout, Netherlands, 28-30 Sept. 1999, Mat. Sc. Forum, **347-349**, 113-118 (2000).

[8] PRIESMEYER, H.G., *Transmission Bragg-Edge Measurements, Measurement of Residual and Applied Stress Using Neutron Diffraction,* (Proc. NATO ARW Oxford), (HUTCHINGS, M.T., and KRAWITZ, A.D., KLUWER, DORDRECHT Eds), p. 389-394 (1992).

[9] VRANA, M., MIKULA, P., LUKAS, P., ŠAROUN J., STRUNZ, P., *High-Resolution Diffraction Techniques for Strain/Stress Measurements at a Steady State Reactor*, Acta Physica Hungarica, **75** (1994) 305-310.

[10] MIKULA, P., WAGNER, V., VRANA, M., *Bragg Diffraction Optics for Energy-Dispersive Neutron-Transmission Diffraction,* Physica B, **283,** 403-405 (2000).

[11] MIKULA, P., VRANA, M., LUKAS P., WAGNER, V., *High Resolution Neutron Diffraction Techniques for Strain Scanning*, Proc. of the Int. Symp. on "Recent Advances in Experimental Mechanics" - Session on "Neutron and Synchrotron Irradiation Stress Analysis", 14th US National Congress of Applied Mechanics, June 23-28, 2002, Virginia Tech., Blacksburg, VA, USA; Kluwer Academic Press, in Recent Advances in Experimental Mechanics, ed. E.GDOUTOS, Kluwer Academic Publisher, p. 457-466 (2002).

[12] LUKAS, P., KOURIL, Z., STRUNZ, P., MIKULA, P., VRANA M., WAGNER, V., *Microstrain Characterization of Metals Using High-Resolution Neutron Diffraction,* Physica B **234-236**, 956-958 (1997).

[13] KLIMANEK, P., KSCHIDOCK, T., MIKULA P., VRANA, V., *Substructure Analysis in Polycrystalline Materials by Means of Neutron Diffraction,* Physica B, **234-236**, 965-966 (1997).

[14] LUKAS, P., TOMOTA, Y., HATJO, S., ONO, M., VRANA, M., STRUNZ, P., KOURIL, Z., MIKULA, P., *Neutron Diffraction Investigation of Residual Strains α/γ Fe-Cr-Ni Alloys,* Proc. of the 5th Int. Conf. on Residual Stresses ICRS-5, June 16-18, 1997, Linköping, (ERICSSON, T., ODEN, M.,ANDERSON, A, Eds) Vol. **2**, p. 880-885.

[15] STRUNZ, P., LUKAS, P., MIKULA, P., WAGNER, V., KOURIL V., VRANA, M., *Data Evaluation Procedure for Energy-Dispersive Neutron-Transmission-Diffraction Geometry*, Ibid p. 688-693.

[16] LUKAS, P., ZRNIK, J., CERETTI, M., VRANA, M., MIKULA, P., STRUNZ, P., NEOV D., KEUERLEBER, J., *Neutron Diffraction as a Tool for Microstrain Characterization of Polycrystalline Ni-Base Super alloys after Thermal Fatigue*, Mat. Sc. Forum **321-324** 1048-1050 (2000).

[17] KULDA, J., MIKULA, P., LUKAS P., KOCSIS, M., *Utilisation of Bent Si Crystals for Elastic Strain Measurements,* Physica B, **180&181**, 1041-1043 (1992).

[18] MIKULA, P. LUKAS, P., VRANA, M., KLIMANEK, P., KSCHIDOCK, T., MACEK, K., JANOVEC, J., OSBORN, J.C., SWALLOWE, G.M., *Advanced Neutron Diffraction*

Techniques for Strain Measurements in Polycrystalline Materials, Journal de Physique IV, Colloque C7, **3**, 2183-2188 (1993).

[19]   VRANA, M., LUKAS, P., MIKULA P., KULDA, J., *Bragg Diffraction Optics in High Resolution Strain Measurements,* Nucl. Instrum. Methods A **338**, 125-131 (1994).

[20]   MIKULA, P., VRANA, M., LUKAS, P., ŠAROUN, J., STRUNZ, P., WAGNER, V., ALEFELD, B., *Bragg Optics for Strain/Stress Measurement Techniques*, Physica B, **213-214**, 845-847 (1995).

[21]   VRANA, M., MIKULA, P., LUKAS, P., DUBSKY, J., WAGNER*,* V., *New Developments in Instrumentation for Strain Scanning in NPI Řež,* In Proc. of the 6th European Powder Diffraction Conference EPDIC-6, Budapest, August 22-25, 1998, Hungary, Mat. Sc. Forum **321-324**, 338-344 (2000).

[22]   WAGNER, V., KOURIL, Z., LUKAS, P., MIKULA, P., VRANA, M., *Residual Strain/Stress Analysis by Means of Energy Dispersive Neutron Transmission Diffraction,* Proc. of 5th Int. Conf. on Applications of Nuclear Techniques "Neutrons in Research and Industry", June 9-15, 1996, Crete, SPIE **2867**, 168-171 (1997).

[23]   WAGNER, V., MIKULA, P., LUKAS, P., *A* Doubly Bent Si-Monochromator*,* Nucl. Instrum. Methods in Phys. Research A **338**, 53-59 (1994).

[24]   ŠAROUN, J., KULDA, J., *RESTRAX* - A Program for TAS Resolution Calculation and Scan Profile Simulation, Physica B, **234-236**, 1102-1104 (1997), and http://omega.ujf.cas.cz.
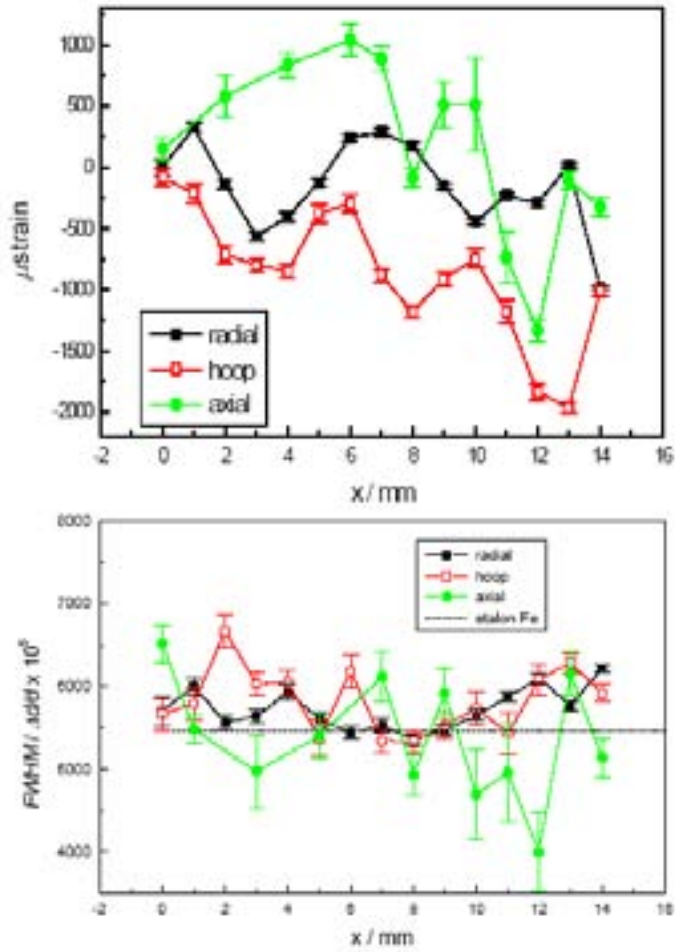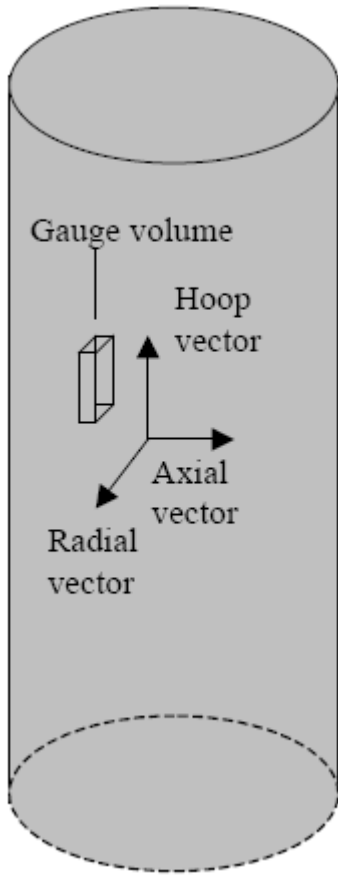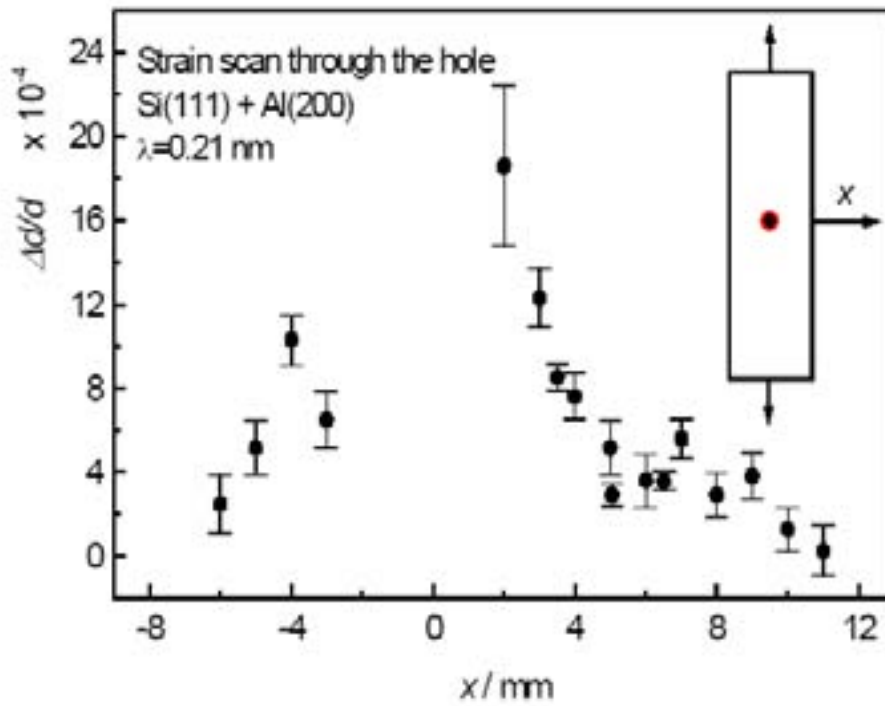
x- the distance from the rod axis

Effect of the fast quenching applied on a cylindrical austenitic rod X5 CrNi 18 9 (Φ=30 mm). Elastic strain and *FWHM* dependences on the distance from the rod axis; γ-Fe (111) reflection
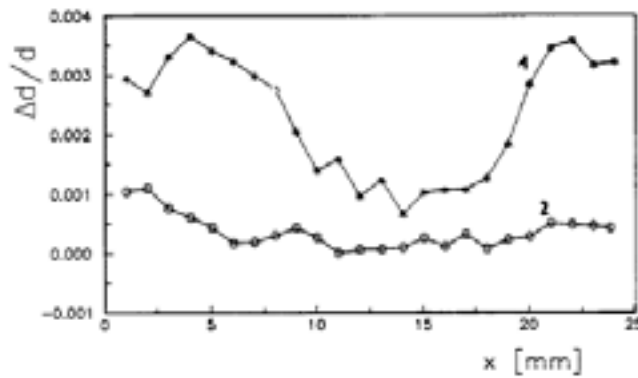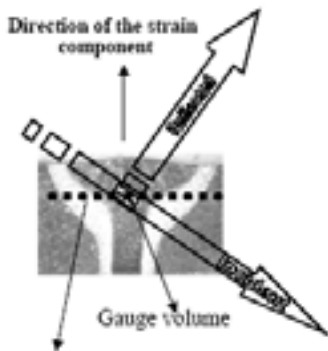

Strain scanning through the weld joint: Sample – high alloy stainless steel
1 – before annealing, 2 – after annealing

X-component strain scanning performed in the vicinity of the 5 mm diameter hole bored in the middle of an Al-plate of 2x25x130 mm^3 and then tensile deformed; gauge volume was 2x1x3 mm^3.
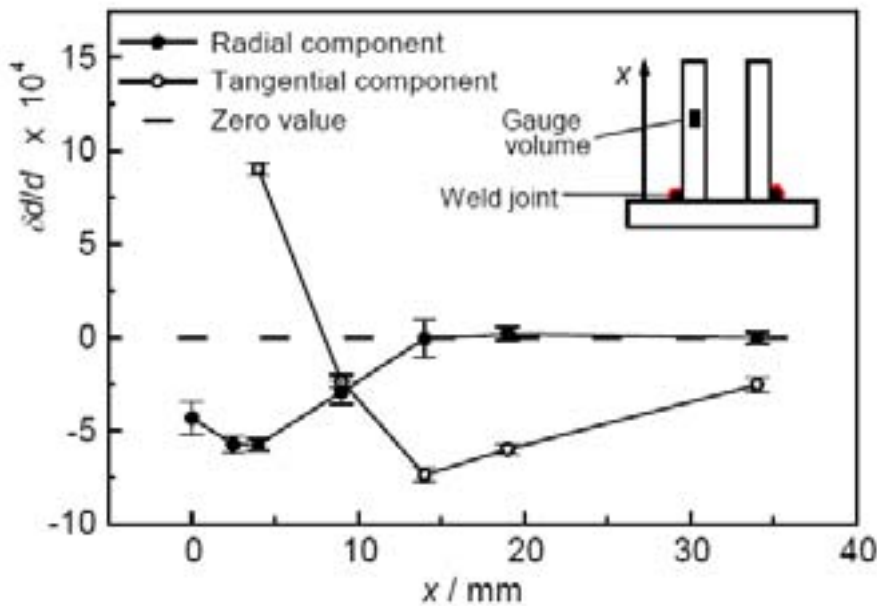

The dependence of the radial and hoop macrostrain component on the distance from the weld-joint of a 8 mm thick tube (Φ=85 mm) of ferritic steel welded on a 12 mm thick steel plate; gauge volume was 2x2x4 mm^3.
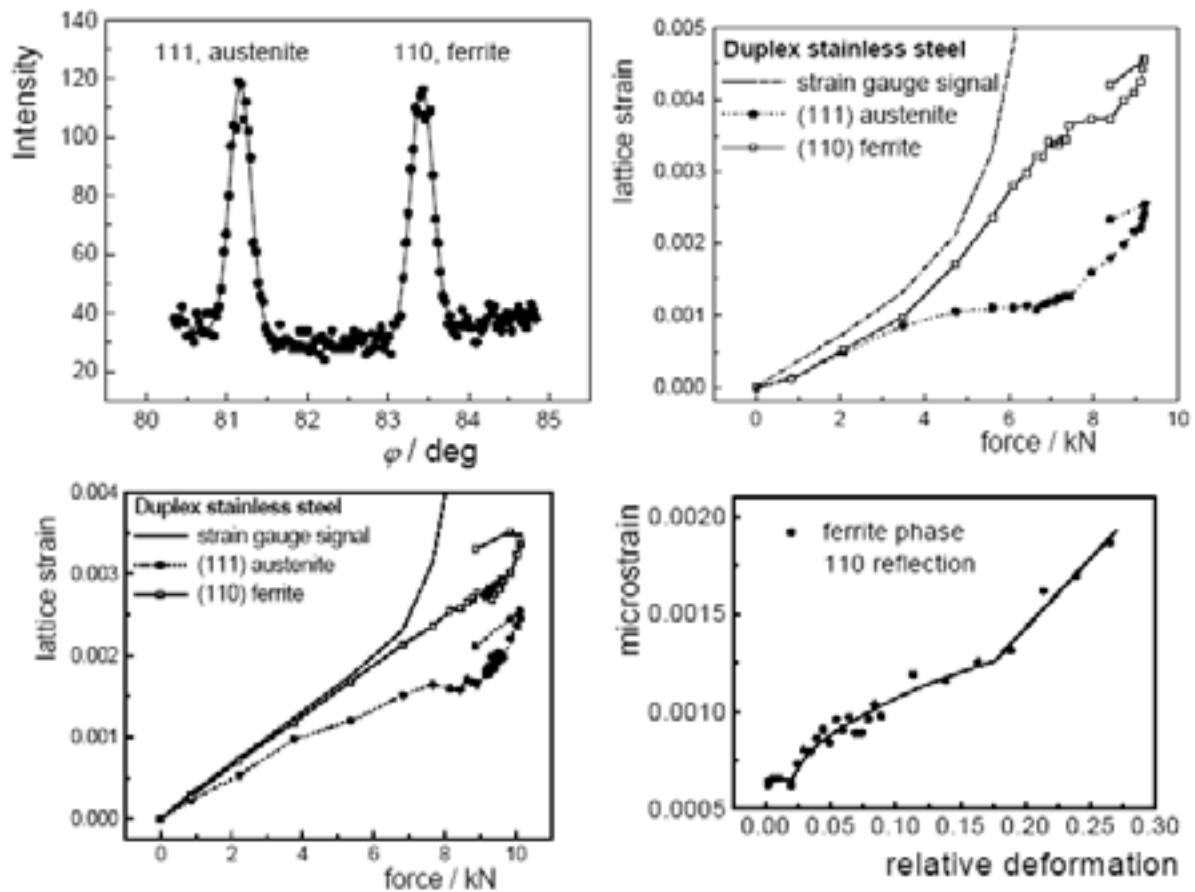
Structure response of two-phase stainless steel of different composition on external mechanical load applied in tension/compression rig. (a) – An example of the simultaneously measured diffraction profiles corresponding to both phases by PSD, (b) – lattice strain versus applied load for the material composition of 33% ferrite and 67% austenite, (c) – lattice strain versus applied load for the material composition of 67 % ferrite and 33 % austenite, (d) – mean value of microstrain $\langle \varepsilon^2 \rangle^{1/2}$ versus relative deformation as obtained from the profile analysis of the Fe(110) reflection of the ferritic phase.
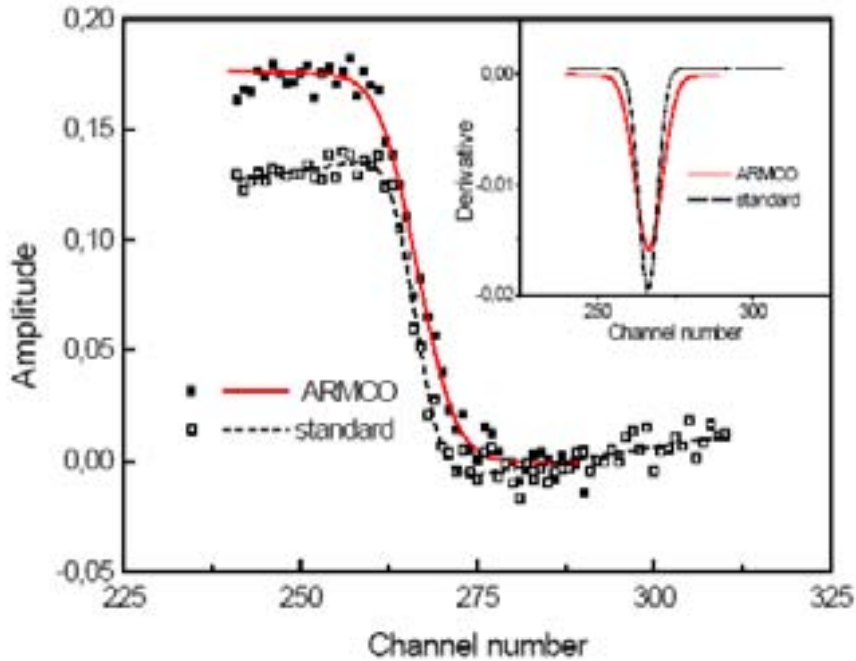
Fe(321) Bragg diffraction edge (*FWHM(δθ)*=1.2x10-3 rad) of a plastically deformed ARMCO steel (0.22% C, 0.64% Mn, 0.41% Si, 0.035% P, 0.04% S (in wt.%)) and, for a comparison, of the standard sample (*FWHM(δθ) = 7.7x10-4 rad*). The insert displaying the derivative of the amplitude shows the broadening of the edge more clearly; the slit width *W* = 1 mm.
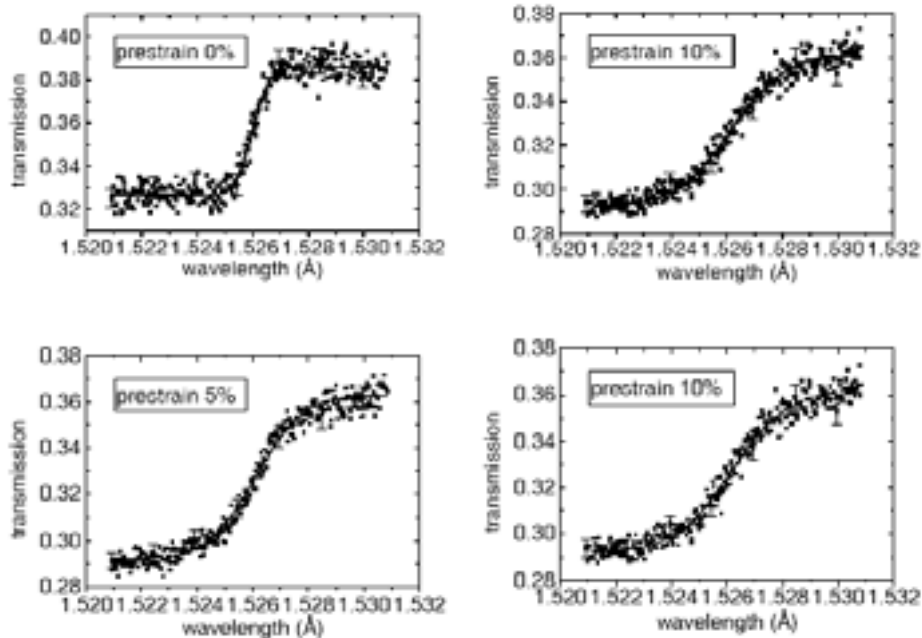
An example of the Fe (321) Bragg diffraction edges of a plastically deformed ARMCO steel samples (0.22% C, 0.64% Mn, 0.41% Si, 0.035% P, 0.04% S (in wt.%).

Research and standardization activities on neutron methods at HFR-Petten

A.G. Youtsos

EC - JRC - Institute for Energy (IE), Petten, Netherlands

Abstract. Thermal and sub-thermal neutrons are invaluable tools for investigations in fundamental, engineering and medical science. Most neutron applications are non-destructive, as neutrons penetrate deeply into most materials. In the engineering field, neutrons are nowadays mostly employed in residual stress analysis. At the High Flux Reactor in Petten, the Netherlands, neutron assisted experimental techniques such as neutron diffraction, neutron radiography and small angle neutron scattering are used for residual stress, micro-structural and defects analyses in nuclear structural components. Based on this and on similar infrastructures across Europe, a number of collaborative research activities aiming at standardization of neutron scattering techniques have been completed leading to international standards, while some other are still under way.

1. Introduction

The High Flux Reactor (HFR) at Petten (The Netherlands) is a multi-purpose reactor that has been operated since November 1961. It is owned and managed by the European Commission and operated under contract by the Nuclear Research and Consultancy Group (NRG, NL).

The HFR is a tank-in-pool type light water reactor with water as coolant and moderator. In core contains thirty-three fuel elements, six control rods, twenty-three beryllium reflector elements and nineteen irradiation positions, in 9x9 array. In the course of time the reactor and its facilities have been upgraded to meet increasing demands. The power of the reactor was raised from 20 MW to 30 MW in 1966 and subsequently to 45 MW in 1970.

A very extensive upgrading, involving the replacement of the reactor vessel and modification of the peripheral components took place in 1984. After a 14-month shutdown period, the reactor was restarted to 45 MW routine operation in February 1985. The HFR is in operation for approximately 270 days per year, divided into eleven cycles.

The HFR is a key European research infrastructure supporting human health and nuclear safety and providing various research and training opportunities on materials irradiations, fuel irradiations, isotope production and engineering and medical applications based on its neutron beam instruments.

Examples of current European Programmes executed at the HFR include the European Network on Neutron Techniques Standardization for Structural Integrity (NET), Ageing materials embrittlement studies (AMES), boron neutron capture therapy (BNCT) programme, Innovative reactor concepts, Transmutation studies, etc.

2. HFR Neutron diffraction facilities

2.1 *Overview of the HFR Neutron Beam Facilities*

In the HFR reactor 12 beam tubes are available for fundamental, engineering and medical research. Apart from those used for medical purposes, the neutron beams are used for various

types of non-destructive investigations on materials and components. The neutron flux available at the entrance windows of the beam tubes, are thermal neutron flux 9-10 x 10^{13} and fast neutron flux 3-10 x 10^{12} cm^{-2}s^{-1}.

The following eight HFR neutron beam instruments are currently used and/or are being refurbished:

- **HB3a triple-axis neutron spectrometer**: Suitable for neutron inelastic scattering.
- **HB3b Small-Angle Neutron Scattering instrument (SANS):** Suitable for particle dispersion, porosity, precipitation, structure of polymers, colloidal solutions, biological membranes etc.
- **HB4 Large Component Neutron Diffraction Facility:** Suitable for residual stress investigations in material specimens and structural components of up to 1000 kg.
- **HB5 Combined Powder and Stress Diffractometer:** Suitable for powder studies and residual stress investigations.
- **HB7: Prompt gamma-ray facility:** Suitable for isotope analysis. Primarily used for determination of low ^{10}B-concentrations in biological samples.
- **HB8:** Neutron Radiography facility.
- **HB11/12 BNCT:** Boron Neutron Capture Therapy. Treatment of certain types of malignant brain tumours (glioma).

2.1.1. HB4 Residual Stress Diffractometer - Large Component Neutron Diffraction Facility (LCNDF) - Fig. 1
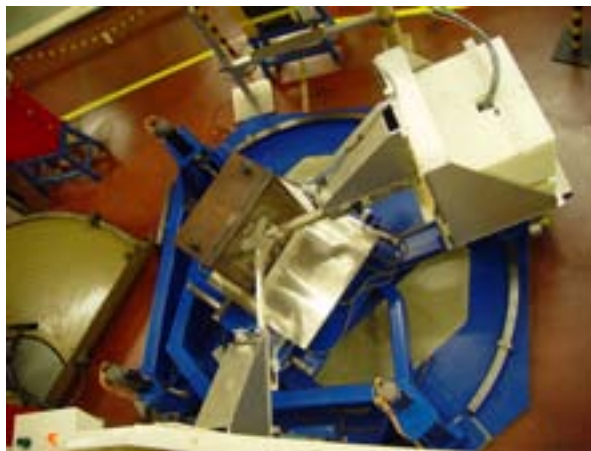

Figure 1. Large Component Neutron Diffraction Facility.

CHARACTERISTICS OF HB4 – LCNDF
- Unique European stress diffractometer for non-destructive evaluation of large structural components – up to 1000 kg
- It is equipped with a pyrolitic graphite (PG)-double monochromator – available wavelength in the range of 0.17 – 0.65 nm
- Maximum beam size at specimen: 10 .x 8.x 30 mm^3
- Maximum fluence rate at specimen: $\sim 10^{10}$ m^{-2}.s^{-1} (λ = 0.257 nm)

- Detector – AECL Research 32 wire position sensitive detector, ^{3}He operating at a resolution of 0.1° per wire
- Angular ranges: scattering angle 2Θ : –3° to + 123°
- Sample rotation angle: 0° to 360°
- Step size: 0.01°
- Sample displacements: x, y: -200 to + 200 mm, z: 300 mm
- Step size: 0.001 mm
- Control: LABView based control by standard PC

2.1.2 Applications of HB4 – LCNDF

- Residual stress analysis in welded components, specimen mass of up to 1000 kg possible, 50 mm thick steel structures can be tested

- Stress/strain measurements for validation of numerical models or qualification of other experimental stress measurement techniques

- Residual stress tensor mapping in structural components in support of reliable assessment of their structural integrity

- Phase distribution and average values of residual stresses in multi-phase materials such as ceramic matrix composites for their efficient design

- Evaluation of the performance of residual stress relief techniques such as post weld heat treatment

- Mapping of residual stresses across dissimilar material interfaces as in joints and coatings for the assessment of manufacturing processes.

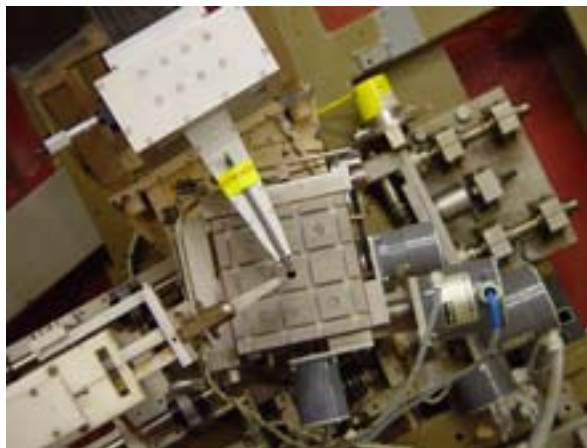## 2.2   HB5 Combined Powder and Stress Diffractometer – Figure 2

Figure 2. Combined Powder and Stress Diffractometer.

2.2.1 Characteristics of Combined Powder and Stress Diffractometer

Monochromator: Cu (111), take-off angle $2\Theta_M$: 32.7° or 76°
Incident Wavelength: at $2\Theta_M = 76°$: 0.257 nm
Angular ranges: 2Θ : –2° to +155°, ω: 0° or 360°
Step size: 0.05°
Detector: Ordela type PSD, solid angle covered by detector: 6.5°
Filters: Pyrolytic graphite for $\lambda = 0.257$ nm
Resolution: at $2\Theta = 76°$ with 30' collimation, $\Delta 2\Theta$ (FWHM)=0.6°
Maximum beam size at specimen: $2\times2\times6$ cm^3 (powder diffraction mode) and $5\times5\times30$ mm^3 (residual stress mode)
Maximum flux at specimen: ~ 10^{10} m^{-2}.s^{-1} ($\lambda = 0.257$ nm)
Sample displacements: x, y: -45 to +45 mm; z: 120 mm (residual stress mode)
Step size: 0.005 mm (residual stress mode)

2.2.2 Applications of HB5

- Measurements of residual stresses in small welded components, advanced materials and ceramic specimens
- Determination of crystal structures of a large variety of polycrystalline materials

2.3 Residual Stress Analysis based on the HFR Neutron Diffraction Facilities

2.3.1 Why neutrons?

Thermal and sub-thermal neutrons are used as testing tool in fundamental, engineering and medical science exploiting some unique features:
- High capability of penetration for most materials
- Neutron wavelength comparable to inter-atomic distances in crystalline materials
- High sensitivity for Hydrogen
- Neutrons facilitate non-destructive investigations

2.3.2 Neutrons as NDT tool in structural integrity assessment

Neutrons facilitate:
- Measurement of residual stresses, structure as well as micro-structure analyses and texture determination non-destructively through diffraction methods
- Defects analyses such as detection and measurement of precipitation's, voids, porosity, inclusions, cracks etc., through Small Angle Neutron Scattering (SANS) and Neutron Radiography

The EC-JRC High Flux Reactor (HFR) is equipped with five neutron beam instruments, which provide for efficient performance of such investigations - Residual stress analyses, in particular, have been extensively carried out during the last five years.
HFR investigations aim at:

- Evaluation of the effect of thermal and irradiation exposure to the evolution of microstructure, defects and internal stress in aged components and material specimens;

- Optimization process parameters for dissimilar metal welds;

- Optimization of current practice in repair welds;

- Evaluation of the performance of Post Weld Heat Treatment (PWHT) processes;

- Reconstitution of residual stress fields in oversize (too big for neutron diffraction test facilities) welded structural components through neutron diffraction testing of sub-parts, strain evolution measurement during cutting process, and numerical modeling;

- Assessing the influence of processes such as bending, rolling or shock quenching, on microstructure, defects and residual stress.

Numerical methods are also used in order to
- Scale up experimental data obtained on downscaled components,

- Develop sophisticated models for accurate determination of multi-pass welding residual stresses and finally,

- Analyse the impact of defects on structural integrity.

2.4 Testing campaigns and results on structural components at HFR-Petten

2.4.1 Residual stress measurement campaigns in welded specimens at the HFR/LCNDF

2.4.1.1. Bimetallic steel 25-mm thick piping welded component

The specimen investigated is a tube of 393 mm length, 168 mm outer diameter and 25 mm wall thickness. The weld has been applied circumferentially at mid-length. On the outer and inner surfaces the transition from the austenitic to the ferritic material is clearly visible. Measurements were performed at various locations within the weld, the buttering layer and the HAZs in three ortho-normal directions, i.e., tube hoop, axial and radial directions. In order to facilitate these measurements windows had to be cut into the component for providing access for the neutron guides. From the thus removed material a slice was then cut in order to provide for the reference coupons; these were wire eroded in the form of 6 x 6 mm^2 columns.

Thus, two reference specimens were made, one from the locations within the buttering layer and the ferritic steel HAZ and the other one representing the locations within the weld and the austenitic steel HAZ. Based on the assumption of macro-stress relief in the columns through cutting, these were used for reference measurements at each location in each direction. The most appropriate test procedure was found to be operating at a fixed scattering angle 2θ, while varying the neutron wavelength, using an adjustable double-monochromator, for the various material phases.

Material composition:
- 304L austenitic stainless steel
- A508Cl3 ferritic steel
- 308L austenitic steel for buttering and groove beads

Instrument settings for bimetallic weld specimen testing:
Gauge volume: 4 x 4 x 5 to 4 x 4 x 10 mm^3
Scattering angle: 76.150°
Crystallographic plane: ferrite (110)

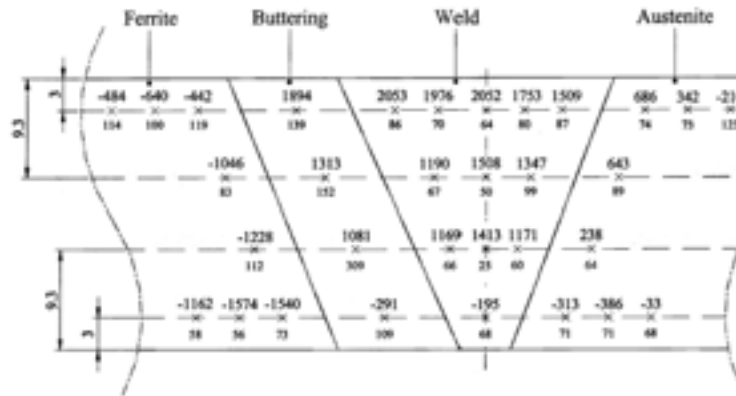*Figure 3. Hoop strains (με) and associated sampling error within the bimetallic weld specimen.*

Figure 3 shows an example of the measured internal strains (hoop direction) while Figures 4-6 show the resulting residual stresses in all three directions examined.
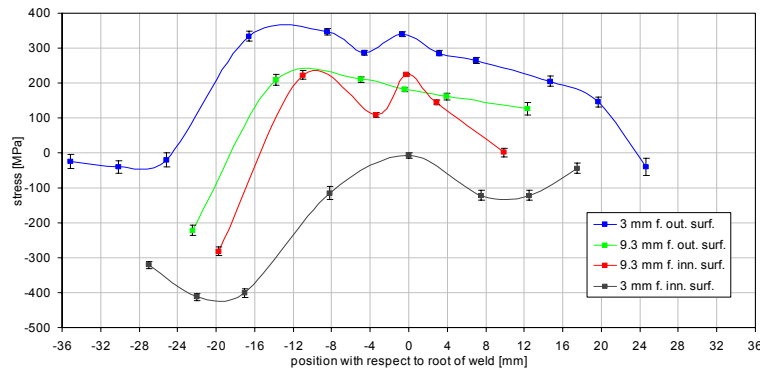

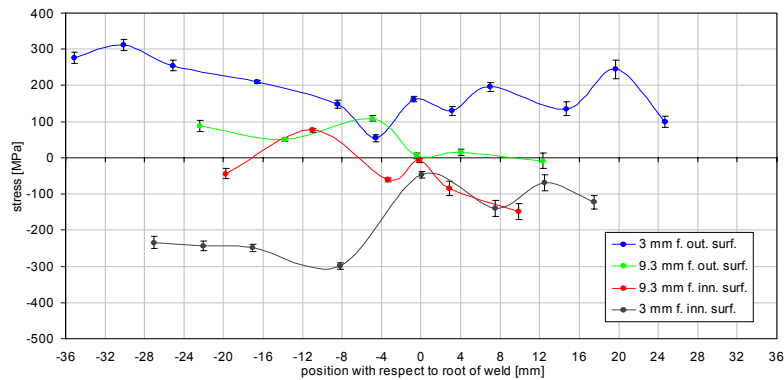*Figure 4. Hoop stresses across the bimetallic weld specimen.*

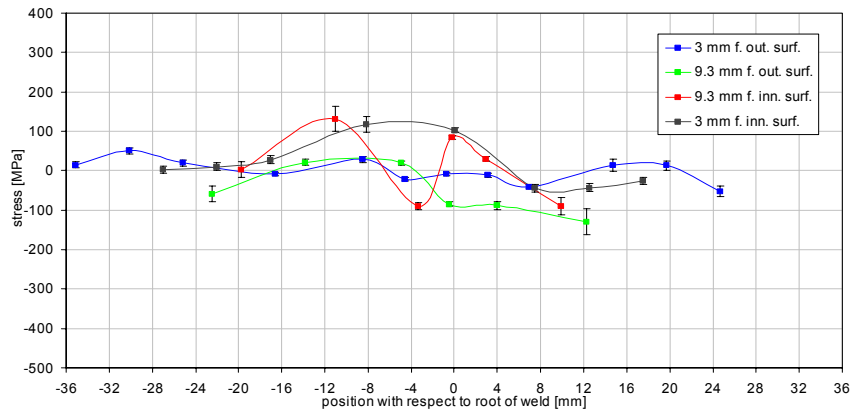Fig. 5 *Axial stresses across the bimetallic weld specimen*

Figure 6. Radial stresses across the bimetallic weld specimen.

2.4.2 Austenitic steel 66-mm thick piping welded component

The spatial distribution of residual stress in a thick section girth weld (432 mm outside diameter, 65 mm thick) joining two ex-service AISI type 316H austenitic stainless steel forgings was characterized by both neutron diffraction testing and numerical modelling. A neutron wavelength of 2.8 Å was employed rendering a scattering angle of about 84.5° with the austenitic (111) reflection plane. A large sampling volume (1.8 cm^3) was selected for measurements in the specimen radial, longitudinal and hoops directions. Seven locations through the piping wall in the HAZ were measured (nearly 20 mm from the weld centreline). Further measurements were made 6 and 20 mm below the outer specimen surface at various distances from the weld centreline. All hoop, longitudinal and radial direction strain measurements at mid-thickness of the specimen wall necessitated a total neutron path length within the steel of about 90 - 95 mm. This proved to be beyond the capabilities of the diffractometer because of the resulting severe neutron beam intensity attenuation. The above experimental campaign was repeated following completion of the PWHT of 2.5 hours at 750°C.
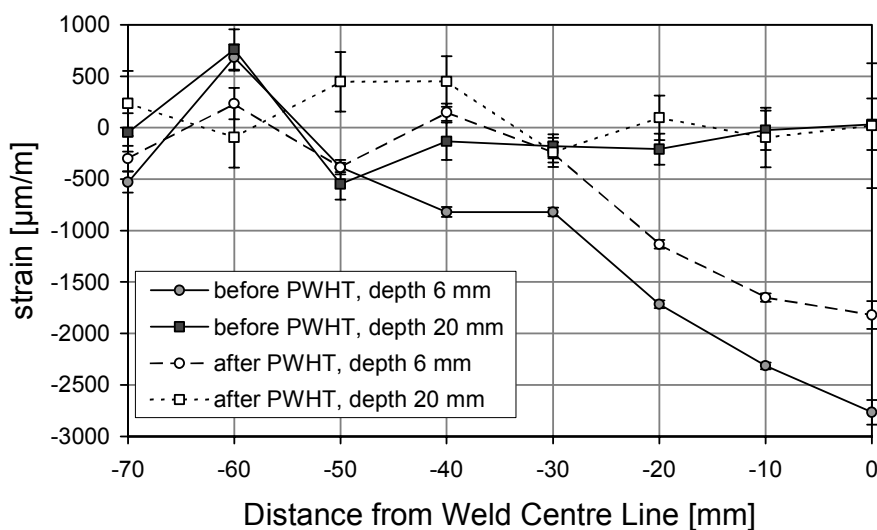

Figure 7. Radial apparent strains measured before and after PWHT at various distances from an austenitic steel girth weld centre line.

The strains presented in Figs. 7-9 are based on a unique reference value derived from measurements in the parent material far from the weld. Radial apparent strain results show relaxation in the order of 1000 με near the surface of the specimen, but minor change at locations up to 20 mm below the specimen surface (see Fig. 7). Fig. 8 shows the apparent radial strains before and after PWHT measured through thickness in the HAZ 20 mm from the weld centre line. The strain relief is positive for the test locations closer to the outer surface whereas is becomes negative at the inner surface. The difference in measured radial strains, that is the strain relief, is in good agreement with equivalent results based on Finite Element (FE) simulation performed by British Energy, as Fig. 9 clearly shows.
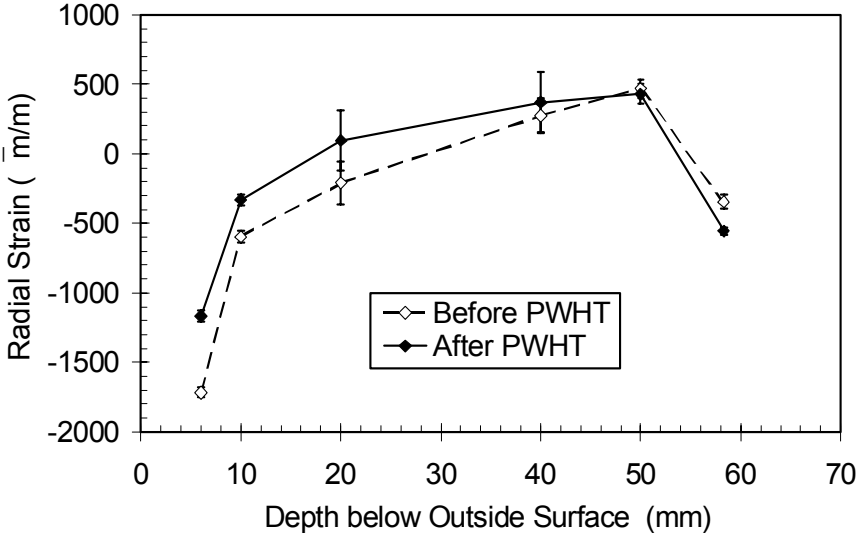

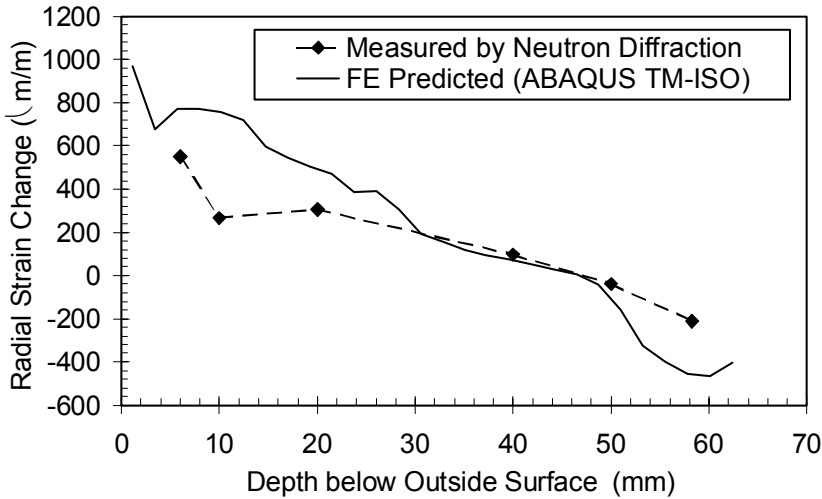Figure 8. Apparent radial strains in the HAZ of the austenitic steel girth weld.

Figure 9. Measured and predicted radial strain relief in the HAZ of the austeniticsteel girth weld.

Additional tests indicate that measurements, based on the selected sampling volume and wavelength, would have been feasible for up to 25-28 mm below the specimen surface locations, while beyond this depth the deteriorating quality and reliability of data seems to be prohibitive for neutron diffraction stress testing. This means that, and in agreement with

previous experience, reliable neutron diffraction data could be obtained for a piping wall thickness of up to 50 - 55 mm.

2.4.3 Ferritic steel welded plate specimen

Residual strains and stresses were measured at mid-length of a ferritic steel plate of 200 x 150 x 12.5 mm. A 12-pass TIG-weld was applied to the plate at mid- width. Various neutron diffraction laboratories worldwide tested the specimen and a comprehensive report on the obtained results is due to appear shortly.
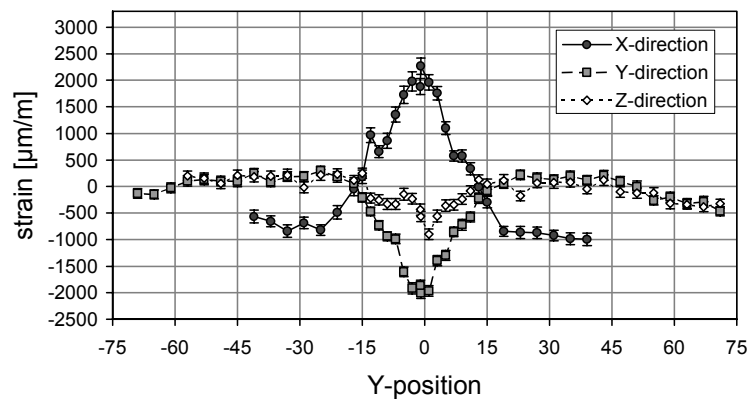

Figure 10. Ferritic steel weld strains in the weld longitudinal (X), weld transverse (Y) and plate normal (Z) directions.
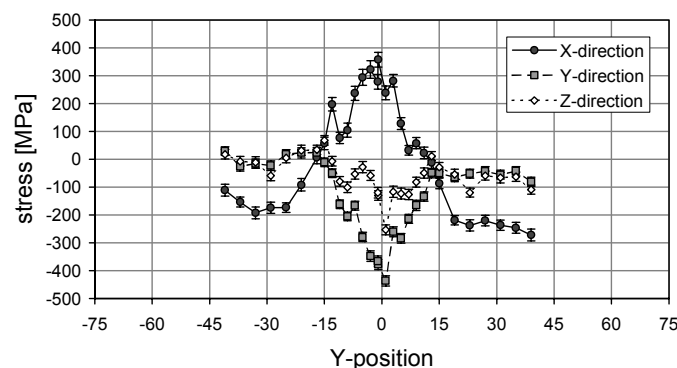

Figure 11. Ferritic steel weld stresses in the weld longitudinal (X), weld transverse (Y) and plate normal (Z) directions.

At JRC tests were performed using a 2 x 2 mm^2 gauge cross section and a neutron wavelength of 2.57 Å. Reference coupons in this case did not reveal significant variations in the stress free lattice parameter (d_0), thus an average was used as reference value for all tests. Figures 10 and 11 show the strains and stresses measured at the HFR-Petten at the plate mid-thickness in the weld longitudinal (X), weld transverse (Y) and plate normal (Z) directions.

2.4.4 Aluminium alloy plate friction stir welded specimen

Two Al-7010 plates of 6 mm thickness and 120 mm width were joined through friction stir welding. Strain measurements based on neutron diffraction were performed at ILL, Grenoble, France, and at HFR-Petten. The aluminium (111) reflection was chosen and an incident beam wavelength of about 0.299 and 0.257 nm respectively, giving rise to Bragg angles of about

79.4° and 67°. Both facilities employed gauge volumes of 1 x 1 mm^2 cross-section. An eventual variation in the reference parameter was not taken into account in this case.

Whereas the agreement between ILL and JRC results in the weld transverse direction is remarkably good (see Fig. 12), in the plate normal direction only a reasonable qualitative agreement could be established due to the unfavourable texture of the material. The alignment discrepancy between ILL and JRC results amounted to 0.5 to 0.75 mm. The good agreement in the data suggests uniformity of the stress distribution over a large range of the specimen.
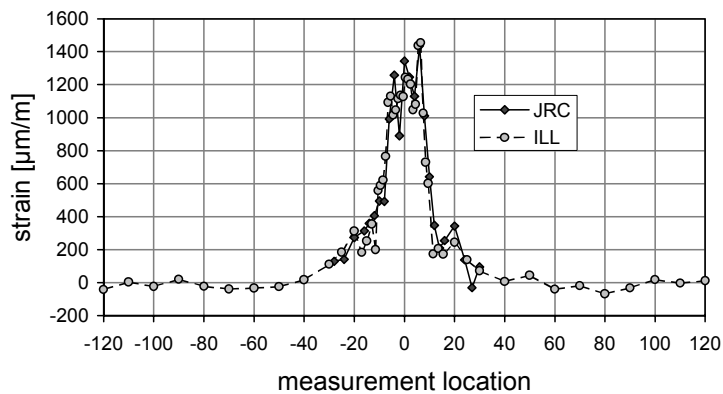

Figure 12. Aluminium alloy friction stir weld strains in the weld transverse direction and at mid-plane.

2.6 Standardization of Neutron Techniques at European and International Level - Neutron diffraction for residual stress analysis

2.6.1 European Project RESTAND – "Residual Stress Analysis using Neutron Diffraction"

Main objective: Development of industrial confidence in residual stress analysis based on neutron diffraction by demonstrating the usefulness of this method to a range of practical applications

Principal deliverable: Relevant draft code of practice

Partnership:

JRC — Commission of the European Communities – Joint Research Centre - Institute for Advanced Materials

CCLRC — Council for the Central Laboratory of the Research Councils, Rutherford Appleton Laboratory, ISIS Facility

HMI — Hahn-Meitner-Institut Berlin GmbH, Bereich Strukturforschung

Risoe — Risoe National Laboratory, Materials Department

UU — Uppsala University, Studsvik Neutron Research Laboratory

RR — Rolls-Royce plc

Sintec — Sintec Keramik GmbH

SKT — SKT Kohlenstofftechnik GmbH

VW — Volkswagen AG, Konzern Qualitätssicherung, Zentrallabor

BAe — British Aerospace Airbus Ltd.

AEA — AEA Technology plc., National NDT Centre

MANU — Manchester University

IMPCOL Imperial College of Science, Technology and Medicine, Department of Mechanical Engineering

Salford University of Salford, Telford Research Institute of Structures and Materials Engineering

ILL Institut Max von Laue - Paul Langevin

2.6.2 RESTAND scientific objectives

- To assemble the necessary technical information for the preparation of a suitable European standard for the non-destructive measurement of residual stress by neutron diffraction
- To use this technique to calibrate other methods, which are usually destructive or semi-destructive or, which can only measure near surface
- To resolve measurement problems which can lead to misinterpretation of data
- To bring about harmonization of the measurement method across Europe

2.6.3 Specimens examined within RESTAND

- Felt and fibre-reinforced composites for heat insulation and thermal shock resistance
- Induction hardened and deep-rolled crankshafts to represent complex shapes
- A quenched component
- Fusion, linear-friction and friction-stir welds for power generation and aerospace applications.

2.6.4 Accuracy achieved within RESTAND

From statistical analysis of the data, it has been established, in general, that
- A positional accuracy with a standard deviation of 0.1 mm can be achieved provided proper alignment procedures are adopted.
- Strains can be recorded away from surfaces to a tolerance of $\pm\ 10^{-4}$ corresponding to a stress of 7 to 20 MPa in most materials.
- Close to surfaces (or interfaces) and regions of variable microstructure, greater errors can be expected.

2.6.5 RESTAND Testing and evaluation

Five complementary methods have been extensively used to study residual stresses in a large range of material specimens and industrial components:
- Finite Element Modelling (Fig. 13)
- X ray Diffraction (Fig. 14)
- Synchrotron Diffraction (Fig. 15)
- MAPS (Magnetic Permeability Measurement System)
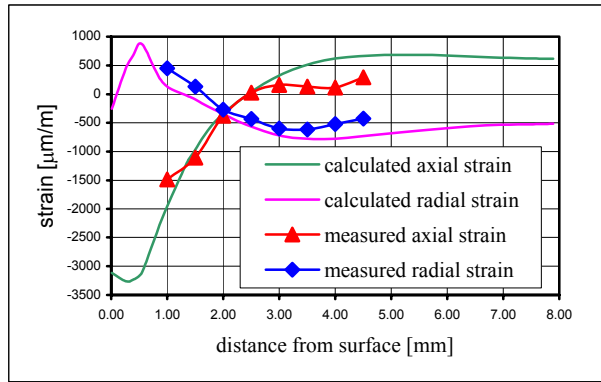- PALA (Positron Annihilation Line shape Analysis)

Figure 13. Comparison of FEM results and neutron diffraction data for strains in a deep rolled and induction hardened crankshaft section
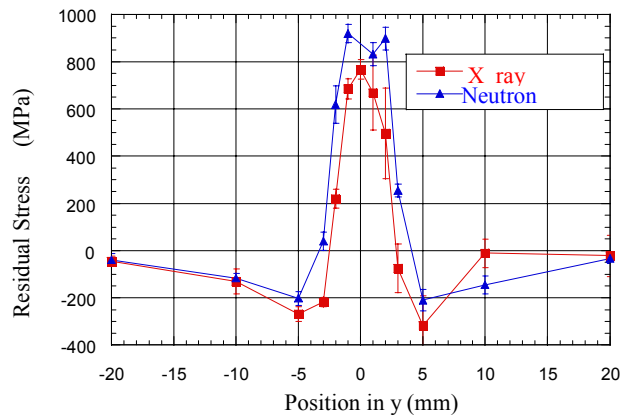

Figure 14. Comparison between X ray and neutron diffraction results for residual stress in a wasp alloy linear friction weld.
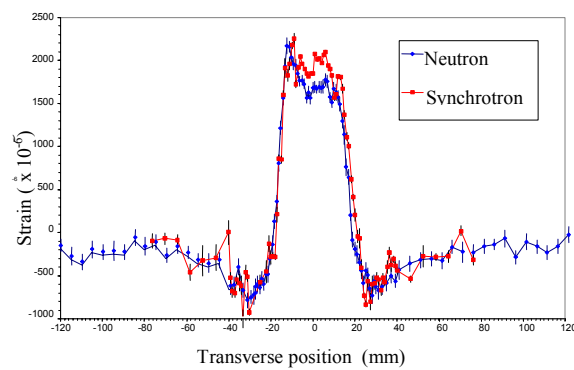

Figure 15. Comparison between neutron and synchrotron diffraction data for residual strain in the weld longitudinal direction of an Al alloy friction stir welded plate.

44

2.6.6 RESTAND Evaluation conclusions

- Neutron and synchrotron diffraction data are generally found to be in excellent agreement
- Neutron data and FEM predictions are found in very good agreement, provided that the predictive algorithms have been thoroughly calibrated based on reliable data
- Neutron diffraction data can be effectively used to validate the performance of FE Models
- Based on reliable neutron data and numerical models of verified performance, key material parameters could, under certain conditions, be determined through parametric studies
- Reliable numerical modelling can be very useful in the design of experimental programs
- PALA and MAPS (in ferromagnetic materials) can be considered as useful qualitative techniques
- MAPS can assist in the determination of the principal stress directions and magnitudes, which can be a time-consuming exercise by neutrons for cases without obvious symmetry
- PALA can assist in a quick estimation of the spatial extent of the residual stress field, thus enabling the experimentalist to confine the range of neutron diffraction investigation.

2.7 International Project VAMAS TWA 20 – Versailles Project on Advanced Materials and Standards Technical Working Area 20

Deliverable: Relevant draft code of practice.
Partnership: Neutron diffraction facilities

2.8 Joint RESTAND/VAMAS TWA 20 ROUND ROBINS

- A shrink-fit aluminum alloy ring and plug assembly (Fig. 16)
- A ceramic matrix composite
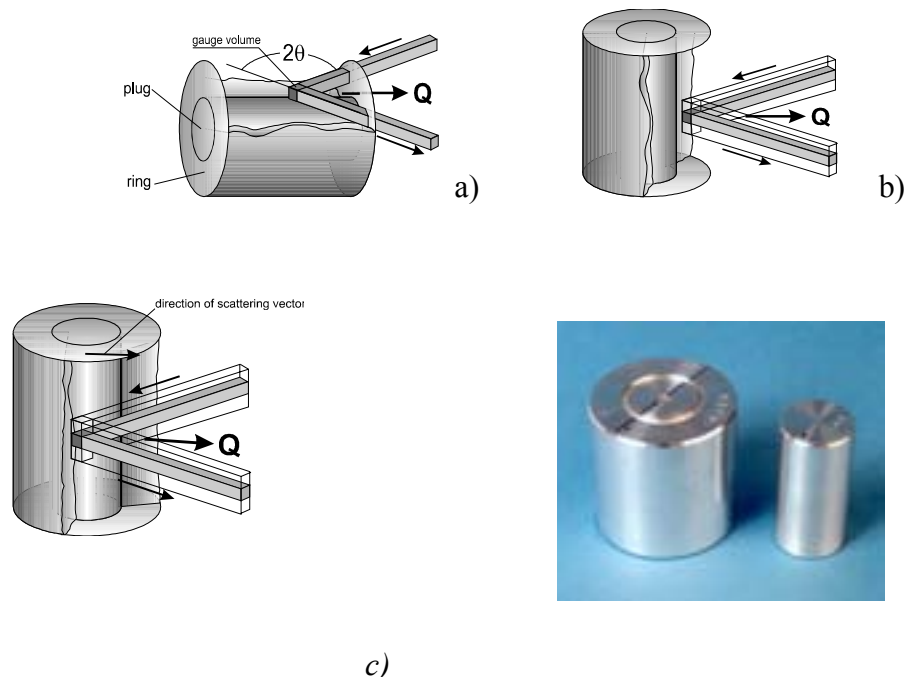- A nickel alloy shot-pinned plate
- A ferritic steel weldment

Figure 16. Schematic diagrams and photograph of ring and plug assembly a) axial direction b) radial direction and c) Hoop direction.

2.8.1 Conclusions based on 1ˢᵗ round robin (Figure 17)

- The experimental strain measurements from all facilities appear to agree with each other and with theory to within about +/- 200 με, and for three labs, even to within +/- 100 με
- The extra scatter in the other results seems to arise from a combination of systematic and statistical error in the determination of the peak, which cannot be completely removed by improving the counting statistics
- *Using a protocol to harmonize testing it would appear reasonable to expect that in the future data from all facilities could agree to within +/- 100 με*
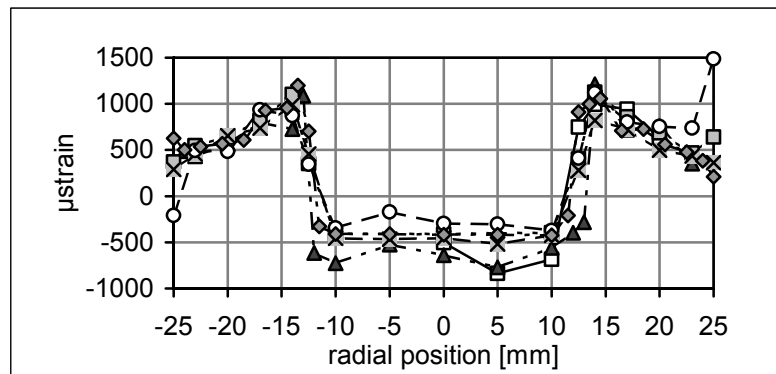

Figure 17. Hoop strains in Al alloy shrink fit ring & plug as measured by six neutron diffraction facilities within RESTAND

2.9   CEN/ISO Activities

The European Standards Committee on Non Destructive Testing (CEN/TC 138) added in October 2000 a New Work Item to its programme and established an Ad hoc Work Group (AHG7) for the development of a European Standard on **"test method for determining residual stress by neutron diffraction"**. Eight National Standards Organizations adopted the scope and appointed delegates to the new AHG7 (Resolution CEN/TC 138 No. 232) charged with the preparation of a pr ENV, based on an UK recommendation.

The International Standards Organization Committee on Non Destructive Testing (ISO/TC 135) adopted the same work item to its programme in June 2001 and thus AHG 7 was enlarged to include non-European experts. The Joint CEN/ISO AHG7 is charged with the task to draft an International Technical Specification under WI 21432.

2.10   AHG7 meetings

Kick-off meeting: Petten, The Netherlands, April 2001
2ⁿᵈ meeting: Athens, Greece, September 2001
3ʳᵈ meeting: Petten, January 2002
4ᵗʰ meeting: Blacksburg, Virginia, July 2002
5ᵗʰ meeting: Brussels, September 2002
6ᵗʰ meeting: London, January 2003
7ᵗʰ meeting: Corfu, Greece, May 2003

46

8th meeting: Grenoble, France, September 2003
The TS publication will be submitted to CEN and ISO by October 2003. It is expected that the International TS will be adopted by end 2004.

2.11 European Network on Neutron Techniques Standardization for Structural Integrity

NET was established in early 2002 and managed by JRC. Thirty-nine organizations from 7 member and 4 candidate countries of the EU and from Korea (observer) participate in its work programme.

2.11.1 NET Mission

- To support progress toward improved performance and safety of European energy production systems through the standardization and harmonisation of neutron based NDT methods within the enlarged EU.
- To provide a forum for training of young scientists, and sound advice to the EC policy makers.

2.11.2 NET Objectives

- To employ neutron based testing methods for gaining improved understanding as to how residual stresses and material degradation have to be taken into account in structural integrity analysis
- To harmonize the corresponding experimental methodologies

2.11.3 NET Scientific Activities

Within NET 3 Task Groups have been developed aiming at
- NET-TG1: Validation of 3D Finite Element Weld Simulation
- NET-TG2: Evaluation of novel repair welding methods for steel plates
- NET-TG3: Thermal ageing effects on duplex steel plates.

2.11.4 NET-TG1 Residual Stress Round Robin investigations

Neutron diffraction: CEA/LLB, HMI, ISIS, GKSS, NPI, NCSR, JRC
X ray diffraction: TU Berlin, Open University
FEA: BE, MBEL, UWE, UP, COMTES, JRC, MPA, KOPEC, TWI, IC

2.11.5 NET-TG2 Residual Stress Round Robin investigations

Neutron diffraction: HMI, ISIS, GKSS, NPI, JRC
X ray diffraction: TU Berlin, TU Warsaw, ENSAM, Open University
Destructive testing: MBEL, TWI (Block removal); IS, UB (Centre hole)
FEA: IS, UWE, UP, COMTES, JRC, MPA, IC

2.11.6 NET-TG3: Thermal ageing effects Round Robin investigations

Small Angle Neutron Scattering: CEA/LLB, GKSS, JRC and ISIS.
Initial harmonization of the performance of participating SANS facilities on thermal ageing effects investigations on a simple binary system, based on data obtained by more conventional methods.
Small Angle Neutron Scattering: CEA/LLB, GKSS, JRC and ISIS.
Investigation of thermal ageing effects (micro-structural analysis) on cast duplex stainless steels.

2.12   Concluding remarks

- Neutron diffraction proves to be a very suitable tool for non-destructive, through thickness mapping of residual stress in monolithic and bimetallic structural welds.
- Testing of the reference scattering angle at each location and in all measurement directions, throughout the weld pool and the HAZs, proves to be, in general, indispensable for reliable stress measurements.
- Reliable neutron diffraction data can be obtained for piping wall thickness of up to 50 - 55 mm at the HFR/LCNDF.
- Neutron, X ray and Synchrotron diffraction methods are complementary tools for NDE of residual stress
- Neutron and synchrotron diffraction data are generally found to be in excellent agreement
- Neutron data and Finite Element Method (FEM) predictions are found in very good agreement, provided that the predictive algorithms have been carefully and thoroughly calibrated based on reliable data
- Neutron diffraction data can be effectively used to validate the performance of FE Models
- Based on reliable neutron data and numerical models of verified performance, key material parameters could, under certain conditions, be determined through parametric studies
- Based on reliable scarce neutron data and numerical models of verified performance one can numerically predict strain and stress levels at locations where such measurements are missing.

2.13   NET Partners

BE - British Energy, BELLELI - Belleli Energy srl, CEA - Commissariat a l'Energie Atomique, LLB - Laboratoire Léon Brillouin, CNRS/ENSAM - Ecole Nationale Supirieure d'Arts et Métiers, COMTES - Complete Technological Service, EDF - Electricité de France, ETC - ETC Elettrotermochimica srl, FRAMATOME ANP, GAEC – Greek Atomic Energy Commission, GKSS - Universität Kiel/GKSS, HMI - Hahn-Meitner-Institut, HSE - Health & Safety Executive, IC - Imperial College of Science, Technology and Medicine, IFIN - Institute Of Physics & Nuclear Engg., INASMET - Materials Research Centre, INR - Pitesti - Nuclear Research Institute, IS -Institut de Soudure, ISIS - Pulsed Neutron & Muon Source, Rutherford Appleton Laboratory, KOPEC - Korea Power Engineering Company, KRU - University of Krakow, MBEL - Mitsui-Babcock, MPA - Staatliche Materialprüfanstalt, NCSR-D - National Centre for Scientific Research "Demokritos", NPI - Nuclear Physics Institute, OU - Open University, SERCO - SERCO ASSURANCE, SVUM - Statni Vyskumny Ustav Materialu, TUB - Technische Universität Berlin, TUK - Technika Univerzita v Kosiciach, TUW - Technische Universität Wien, TUM/FRM II:Technische

Universität Munchen, TWI - The Welding Institute, UB - University of Bristol, UMAN - University of Manchester, UP – University of Patras, UWE - University of Western England, VUJE Trnava – Engineering, Design and Research Organization, WUT - Politechnika Warszawska ,VUZ - Vyskumny Ustav Zvaracsky.

ACKNOWLEDGEMENTS

REFERENCES

[1] "High Flux reactor (HFR) Petten – Characteristics of the Installation and the Irradiation Facilities", (AHLF, J., ZURITA, A, Eds.) EUR 15151 EN, pp. 1-196 (1993).

[2] "High Technology Composites in Advanced Applications", *Proceedings of the COMP'95 - 4th International Symposium jointly with the 5th Euro-Japanese Colloquium on Advanced Composite Materials,* University of Patras, Greece and Institute for Advanced Materials, Petten, the Netherlands, (PAIPETIS, S.A., YOUTSOS, A.G., Eds.), pp. 1-582 (1995).

[3] YOUTSOS, A.G., OHMS, C., TIMKE, T., "Residual stress investigations by neutron diffraction at the JRC-Petten", *Physica B: Physics of Condensed Matter*, Vol. 234-236 (E), 1997, pp.959-961.

[4] "Users' Guide to the Neutron Beam Facilities at the High Flux Reactor (HFR)", (YOUTSOS, A.G., Ed.) EUR 128083 EN, 1998, pp. 1-24.

[5] YOUTSOS, A.G., Neutron Diffraction Alive at HFR-Petten, *Neutron News,* Vol. **9**, No. 2, 1998, pp.11-12.

[6] OHMS C., Youtsos, A.G., "Residual stress measurements in structural components by neutron diffraction", *Journal of Textures and Microstructures,* Vol. **33**, 1999, pp. 243-262.

[7] European Project "RESTAND 1st Annual Progress Report", EC-JRC-IE, Petten, The Netherlands, (YOUTSOS, A.G., OHMS, C., eds), January 1999.

[8] YOUTSOS, A.G.,Mid Term Project Report on European Project entitled "RESTAND" (Residual Stress Standard using Neutron Diffraction), EC-JRC-IE, Petten, The Netherlands,(1999).

[9] OHMS, C., YOUTSOS, A.G., BONTENBAL, A., MULDER, F.M., "Neutron Diffraction Facilities at the High Flux Reactor, Petten", *Physica B: Physics of Condensed Matter*, **276-278**, pp. 160-161 (2000).

[10] OHMS, C., YOUTSOS, A.G., IDSERT, P.V.D., Th. TIMKE, "Residual Stress Measurements in Thick Structural Weldments by Means of Neutron Diffraction", *Materials Science Forum*, **347-349**, pp. 658-663 (2000).

[11] YOUTSOS, A.G., OHMS, C., "Residual Stresses in Interface Controlled Materials by Neutron Diffraction", *Materials Science Forum*, **347-349**, pp. 524-529(2000).

[12] BOURCHARD, P.J., LEGGATT, R.H., GEORGE, D., BATE, S.K., YOUTSOS, A.G., "Thermal Relaxation of Residual Stresses in Thick Section Type 316 Stainless Steel Girth Welds", Proceedings of *ICRS-6 6th International Conference on Residual Stresses*, Vol. **2**, IOM Communications Ltd., London, pp.972-979 (2000).

[13] 2nd Annual Progress Report on European Project entitled "RESTAND" (Residual Stress Standard using Neutron Diffraction), (YOUTSOS, A.G., OHMS, C., eds) EC-JRC-IE, Petten, The Netherlands, March 2000.

[14] YOUTSOS, A.G., OHMS, C., HUBBARD, C., "VAMAS TWA 20 Workshops held at ORNL and JRC Petten", *Neutron News*, Vol. **11** No. 2, pp. 2-4 (2000).

[15] JOHNSON, M.W., DAYMOND, M.R., OHMS, C., YOUTSOS, A.G., "Neutron Diffraction Measurements of Residual Stress in a Shrink-fit Ring and Plug", Chapter on Strain Data and Analysis in VAMAS Report No. 38, (Webster, G.A., Ed) ISSN 1016-2186, NPL, pp. 19-32 (2000).

[16] OHMS, C., YOUTSOS, A.G., "Neutron Diffraction Measurements of Residual Stress in a Shrink-fit Ring and Plug", in Chapter on "Individual laboratory measurements in VAMAS Report No. 38, (Webster, G.A., Ed), ISSN 1016-2186, NPL, pp. 59-65 (2000).

[17] GIGOUT, D., BACZMANSKI, A., OHMS, C., YOUTSOS, A.G., LODINI, A., "Residual Stresses in Austeno-Ferritic Steel – Neutron Diffraction and Modelling", *Journal of Neutron Research*, **9**, pp. 65-70 (2001).

[18] YOUTSOS, A.G., OHMS, C., "Testing method for residual stress determination based on neutron diffraction", *Draft Standard*, CEN/TC 138/AHG7 N2, Petten, The Netherlands, , pp. 1-49 April 2001.

[19] YOUTSOS, A.G., OHMS, C., 3rd Annual Report on European Project entitled "RESTAND" (residual stress standard based on neutron diffraction), EC-JRC-IE, Petten, The Netherlands, July 2001.

[20] YOUTSOS, A.G., OHMS, C., in "ISO – Technology Trends Assessment: Polycrystalline materials – Determination of residual stresses by neutron diffraction", Eds. G.A. Webster, R.W. Wimpory, Reference number ISO/TTA 3 2001(E), ISO, Geneva, pp. 33-37 (2001).

[21] OHMS, C., YOUTSOS, A.G., "Neutron Diffraction assisted Residual Stress Analysis in Welded Structures", in *Recent Advances in Experimental Mechanics*, (Gdoutos, E.E., Ed) Kluwer Academic Publishers, Dordrecht, Netherlands p. 515-526 (2002)

[22] WEBSTER, G.A., YOUTSOS, A.G., OHMS, C., WIMPORY, R.C., "Draft Standard for the Measurement of Residual Stresses by Neutron Diffraction", in *Recent Advances in Experimental Mechanics*, (Gdoutos, E.E., Ed) Kluwer Academic Publishers, Dordrecht, Netherlands, p.467-476 (2002)

[23] YOUTSOS, A.G., OHMS, C., Final Report on European Project entitled "RESTAND" (residual stress standard based on neutron diffraction, EC-JRC-IE, Petten, The Netherlands, (April 2002).

[24] YOUTSOS A.G., OHMS, C., Final Technological Implementation Plan on European Project entitled "RESTAND" (residual stress standard based on neutron diffraction), EC-JRC-IE, Petten, Netherlands, (April 2002).

[25] OHMS, C., YOUTSOS, A.G., IDSERT, P.V.D., "Structural Integrity Assessment based on the HFR Petten Neutron Beam Facilities", Applied Physics A, 75, p. 1443-1445 (2002).

[26] YOUTSOS, A.G., OHMS, C., "European Standardization Activities on Residual Stress Analysis by Neutron Diffraction", *Applied Physics A, 75, p. 1715-1718 (2002).*

[27] GRRIPENBERG, H. KEINANEN, H., OHMS, C., HANNINEN, H., STEFANESCU, D., SMITH, D., "Prediction and Measurement of Residual Stresses in Cladded Steel", *Materials Science Forum*, **404-407**, p. 861-866 (2002).

Activities at Safari-1 research reactor on residual stress measurements

A. Venter
Necsa Limited, Pretoria, South Africa

Abstract. The beam-line facilities of Safari-1 are developed and made available though collaborative projects to the higher education sector, other governmental funded institutions and industry. These facilities play an integral role in the training of scientists and engineers up to post-graduate level.Within this scenario, the residual strain facility assumes a pivotal role as well as provides a specialized capability to the materials engineering industries. An overview is given of the residual strain instrument at Necsa, its application to typical projects, as well as improvements identified from its use over a number of years.

1.   Introduction

Necsa (South African Nuclear Energy Corporation) owns and operates the Safari-1 (South African Fundamental Atomic Research Institute) 20MW research reactor [1] that is located 30 km west of Pretoria. It is a 20 MW tank-in-pool type reactor design, moderated and cooled by light water, and has been in continuous operation since 1965. The reactor is similar in design and layout to the Studsvik reactor in Sweden and the Petten reactor in the Netherlands. The in-core and pool-side facilities are dedicated primarily to commercial activities [2]. As part of a new initiative, the beam-line facilities are made available to users from academia. The focus is to establish an active neutron scattering community in South Africa with academia playing an integral part with the initiation and collaboration of long term research programs. Beam time is awarded on the merits of scientific project proposals.

The layout of the Safari-1 neutron diffraction facility is shown in Fig.1. It is unique in that a single radial beam line from the reactor core delivers the neutrons to three independent instruments in the reactor hall. This is accomplished by having crystal monochromators for each instrument downstream along the primary beam. All three units are housed in the same monochromator chamber, which is enclosed by one-meter thick high density concrete. Each diffractometer workstation has its own point of origin within the monochromator shield to provide optimal flexibility and take-off angle selections. The primary neutron beam is filtered through a sapphire filter to reduce fast neutron contamination.

Three diffractometer workstations exist:

- A residual strain instrument

- A four-circle Huber diffractometer for single crystal studies

- A multi detector powder diffraction instrument, which is being upgraded to a vertical array of horizontal position sensitive detectors (PSD) 600 mm in length.

To accommodate the diverse fields of application requested by the user community the facilities are being upgraded. The most important aspects being addressed are improvements to the monochromator beam optics and neutron detection efficiencies to speed up data acquisition rates. Substantial increases in the neutron flux on the sample have been obtained through the implementation of focused monochromator units [3].
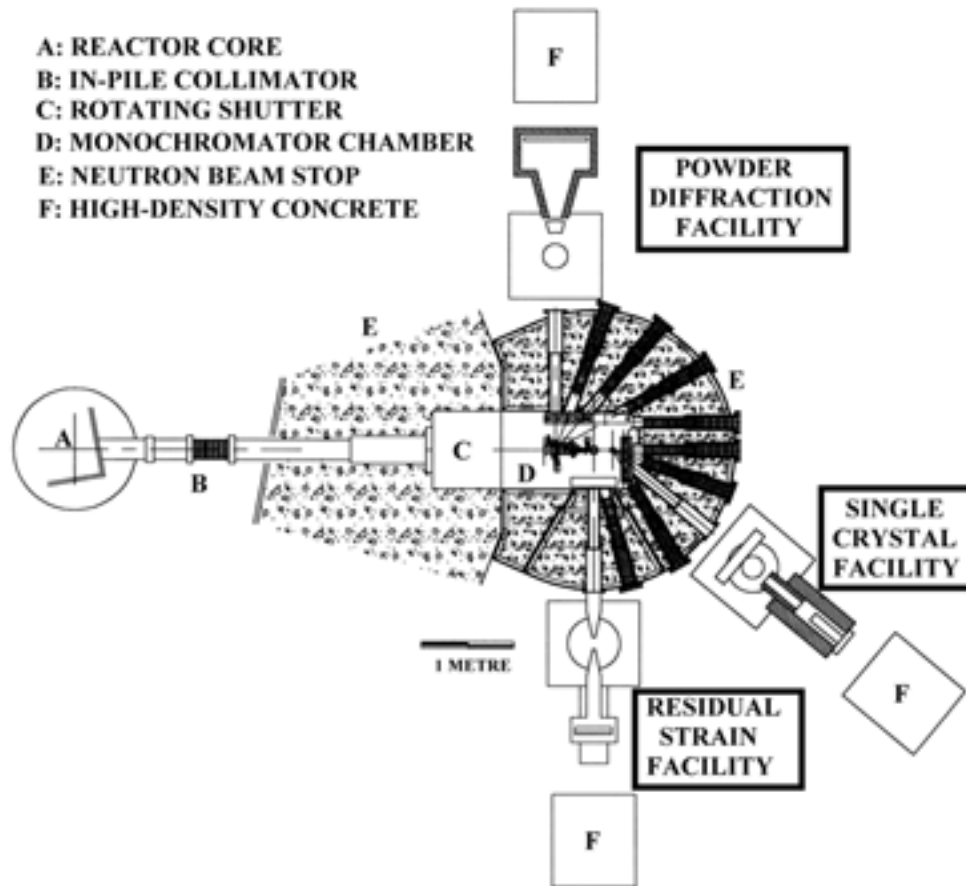
A: REACTOR CORE
B: IN-PILE COLLIMATOR
C: ROTATING SHUTTER
D: MONOCHROMATOR CHAMBER
E: NEUTRON BEAM STOP
F: HIGH-DENSITY CONCRETE

POWDER DIFFRACTION FACILITY

SINGLE CRYSTAL FACILITY

RESIDUAL STRAIN FACILITY

1 METRE

Figure 1. Schematic representation of the neutron diffraction facility at the Safari-1 research reactor.

2. Residual strain instrument

A dedicated residual strain instrument exists. The instrument is an adapted 2-axis diffractometer that has been equipped with a XYZ orthogonal stage that has a carrying capacity of 300kg and enables sample translations of 150mm in each direction and a 100mm long one-dimensional linear position sensitive detector from ODRELA. At a sample-detector distance of 1000mm the detector covers an angular extent of 5.7° that enables the simultaneous measurement of a complete Bragg peak. The detector is shielded with 50% loading of B_4C in epoxy mixture. The beam defining optics is done with apertures manufactured from BN positioned close to the sample. Figure 2 displays views of the instrument.

A recent upgrade to the instrument is the incorporation of a focused Si-multiwafer monochromator [3]. By selective minimization of the instrument-resolution function, shown in Fig 3B, over a small angular extent in 2θ leads to a substantial increase in the neutron intensity on the sample at detector angles close to 90˚ (Fig 3C). This unit enables investigation at deeper depths into materials or alternatively reducing the size of the sampling volume.
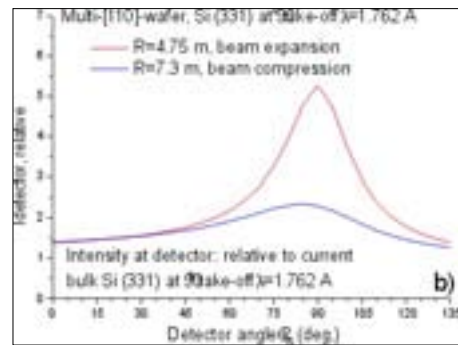
52

Figure 2. Views of the residual strain instrument.
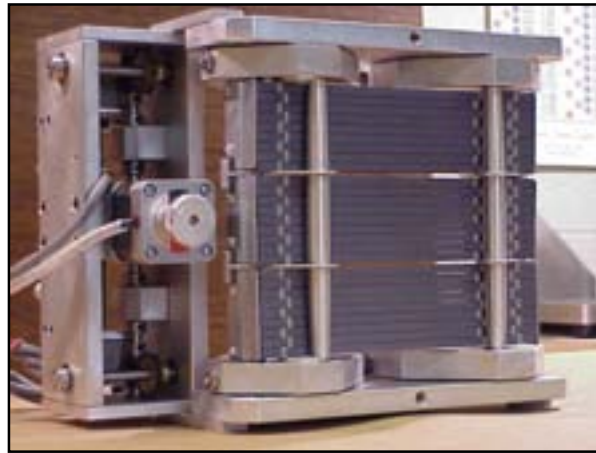
(A)
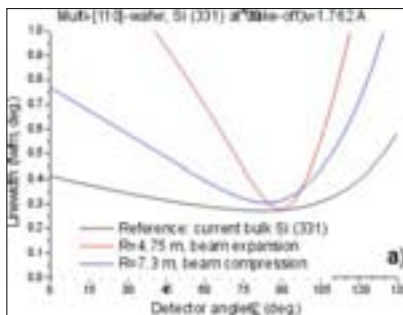
(B)

(C)

Figure 3. A: Picture of the Si-multiwafer monochromator unit with the performance characteristics shown in B and C.

2.1 Fields of application of the facility

The facility has been one of the participating facilities in the international benchmarking of the neutron residual strain measurement method as part of the VAMAS TWA-20 initiative [4].

Many student projects are run to train engineering graduates in the advantages of the method as well as to inform academics on new technological developments. This in effect leads to the training of future clients. Typical projects entail participation in short-term projects such as: Comparison of residual stresses: neutron diffraction with FEM analyses and Studies of inter-granular residual stains under cyclic uniaxial loading conditions.

Investigations of the residual strains in various engineering applications such as autofrettage [5-7] and welded structures have been performed and are discussed here. Fig. 4 shows results from the investigation of autofrettaged (AF) thick walled steel tubes in which remaining lifetime predictions were done based on inputs on the experimentally determined plastic boundary from neutron-diffraction measurements [6]. It is possible to identify the plastic boundary from the assessment of the full-width at half maximum (FWHM) values of the Bragg peaks (Fig.4A). The regions of increased FWHM are ascribed to material that had yielded plastically. Significant broadening of the Bragg peaks from their values in the outer section of the wall signifies material regions that had yielded plastically.
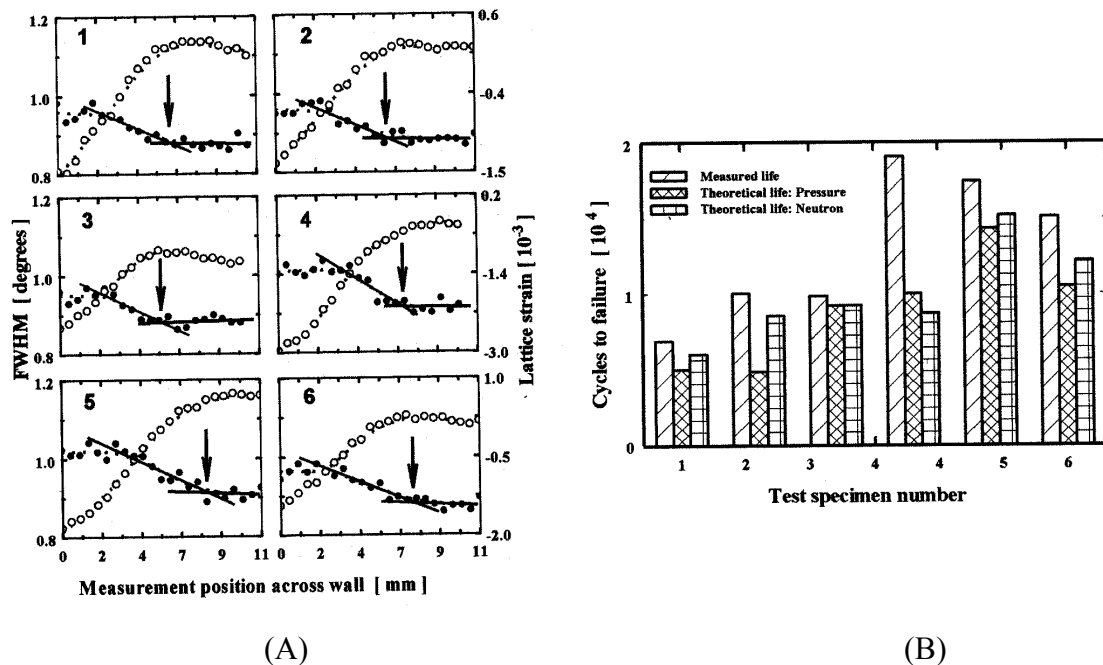

(A)　　　　　　　　　　　　　　　(B)

Figure 4. Curves A: Presentation of the FWHM (●) and the residual hoop strain (○) profiles across the walls of different samples that failed during fatigue measurements to determine the remaining lifetimes of AF cylinders. A wide range of configurations was covered with multiple internal radial elliptic shaped cracks. The linear extrapolations of the FWHM dependences in the region surrounding the plastic radii are indicated by the solid lines with the plastic radii indicated by the arrows; Curves B: Comparison of the theoretical fatigue calculations, based on input parameters such as the plastic boundaries, with the experimental results.

The hoop residual strain distributions at the corresponding positions across the wall of the samples are also indicated. Remaining lifetime predictions based on inputs on the plastic boundaries from the neutron diffraction investigation were found to show good correlation to the actual measured lifetimes. As the neutron diffraction investigation was done on the components after failure, this method thus provides an assessment method for post-mortem

studies of failed components to ascertain whether the AF treatment had been applied correctly.

Figure5 shows the redistribution of residual strains resulting in AF samples from the introduction of holes machined at 50% of the plastic boundary [7].
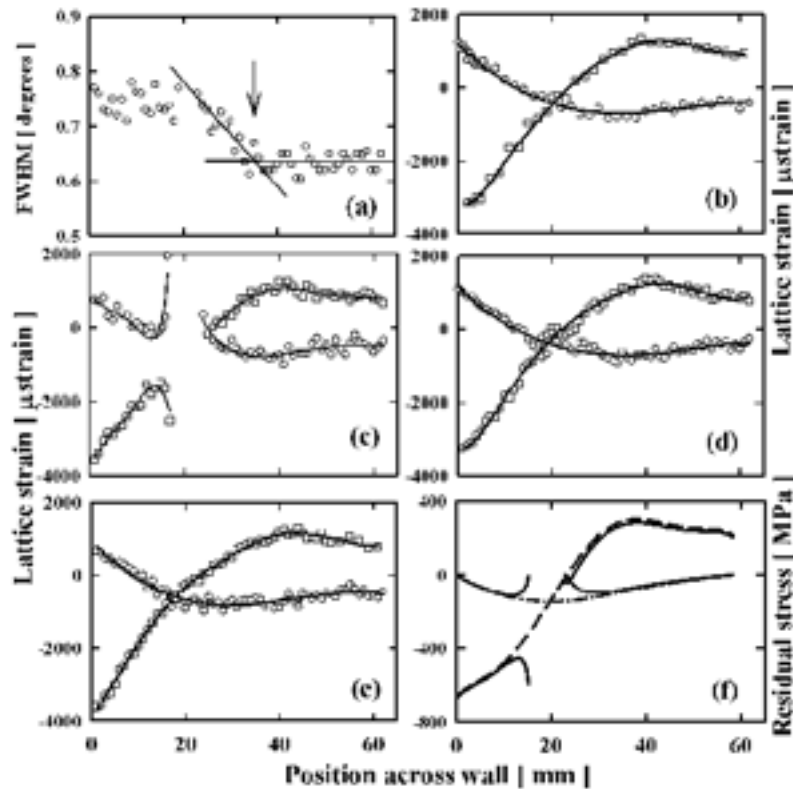

Figure 5 Graph (a) shows the identification of the plastic boundary from the FWHM values with graph (b) indicating the hoop (squares) and radial (circles) residual strain profiles in the solid sample. Graphs (c), (d) and (e) show the redistribution in the residual strains measured along radial lines at angles of 0°, 3.75° and 7.5° that result from the machining of the holes. Graph (f) shows a comparison of the FEM analysis of the residual stresses along 0° in the solid sample (solid curves) and the predicted redistribution after machining the holes (dotted curves).

Profiles measured along a line extending through a hole, machined to be coincident with the measurement positions of the solid sample of Figure 5b, are given in Figure 5c. The machining of the holes is seen to cause a substantial, but localized redistribution of both the hoop and radial residual strain profiles. On the internal bore side thereof the redistribution is seen to occur very close to the edge of the hole. This is expected due to the dominance of the compressive residual strains from the autofrettage treatment at this region in the tube wall. As the hole is approached the hoop strain becomes increasingly compressive, while the radial strains become tensile. On moving outwards radially from the hole, the residual strain redistribution is less dramatic but extends much further. The magnitudes of the hoop and radial strains are decreased with respect to the equivalent profiles in the solid section up to the plastic boundary.

Residual strain profiles along a line offset 3.25° from the 0° reference line are shown in Figure 5d. The redistribution is seen as deviations in the profiles at the proximity of the holes. The rest of the profiles essentially remain unchanged. Residual strain profiles along lines 7.5° offset from the 0° reference line (bisecting two holes), Fig.5e, do not show obvious redistribution and is largely similar to the residual strain profiles observed in the solid sample. Fig.5f displays the theoretical simulations of the residual hoop stress dependences in the solid sample and the predicted relaxation along a line through a hole (0°) from the insertion of the cooling channels. These results are similar to the dependences calculated from the measured strains.

The neutron diffraction method is indispensable in the investigation of the residual strains in welded structures and components. Substantial residual strains are induced during welding due to the inhomogeneous heating within the material bulk. Fig.6A displays a typical T-butt weld geometry. Through the application of the neutron diffraction method, information on the residual strain distribution can be obtained of the various components of strain and at different depths into the base-plate section as well as locations from the weld. Fig.6B shows the longitudinal strain distribution within the base-plate section. An important conclusion of this result is that the magnitudes of the strain values in weld 'A' are smaller than those in weld 'B'. This results from the heat input during weld B that partially annealed the residual strains that existed in weld 'A'. Subsequently this method furthermore provides an accurate technique for the optimization of welding and annealing procedures.
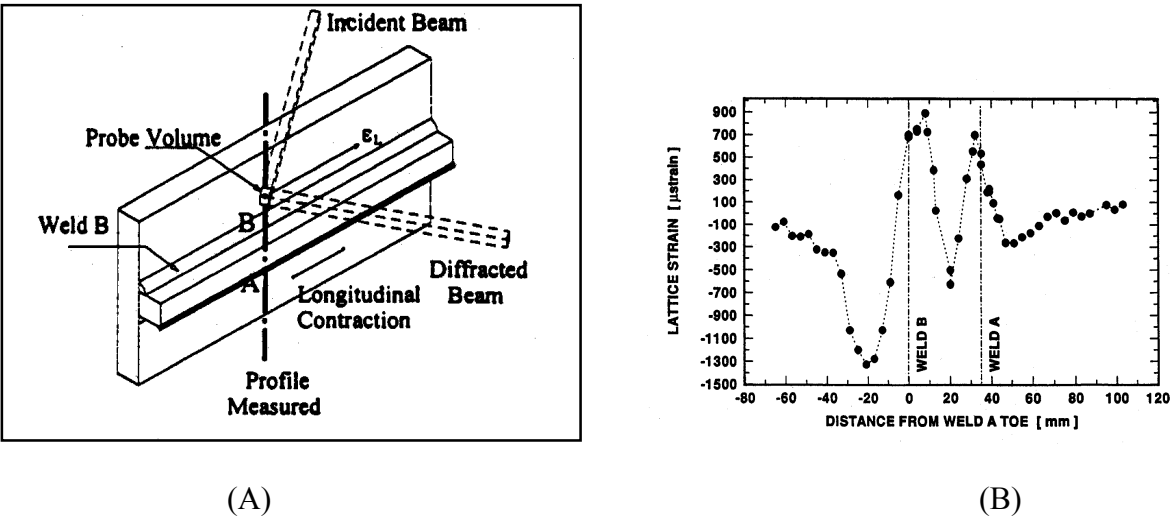

(A)   (B)

Figure 6. A: T-butt welded geometry investigated with neutron diffraction; B: residual strain distribution along the base-plate section.

Results from an analogous application, Thermit welds, used in the joining of railway rails are shown in Figure 7. Notwithstanding the large bulk and effective neutron path lengths though the different rail regions, the residual strain distributions across the Thermit welds could be measured non-destructively. The aim of this project was to participate in the development of the mould geometry used to contain the molten material during the joining process. Figure 7B shows the residual strain distributions across a Thermit weld at various heights along the web section of the rail.

56

(A)
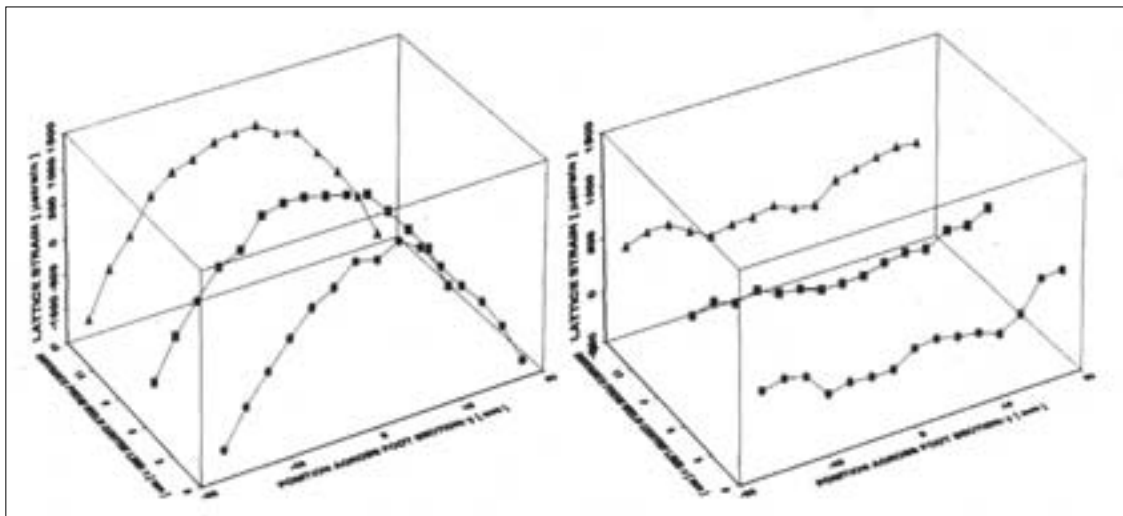
(B)

Figure 7. A: Various rail sections used in the investigation of railway rails. The location and magnitude of the Thermit weld in a rail section is shown; B: Residual strain distributions across Thermit welds in the web section of railway rails.

Future projects envisaged:

- Post-mortem studies of failed AF tubes in conjunction with FEM
- Influence of annealing on autofrettage process
- Fundamental study of material properties under reverse yielding
- Tensile yielding followed by compression yielding
- Studies with universities, student projects
- Exploiting the synergy with laboratory based X rays.

2.2 Improvements to be implemented at the Necsa facility

Based on experience in the implementation and use of the neutron residual strain measurement method at the Necsa facility a number of essential upgrades to the facility have been identified and listed here:

- Smaller sampling volumes especially for the investigation of samples that have steep residual strain profiles. This can be accomplished by the reduction in background, improved beam optics, larger 2D detector, in which larger vertical acceptance angles are employed, etc.
- Improved aperture geometries. To assist with sample setup and repositioning, automation of aperture size adjustments, as well as being able to retract the slits during sample repositioning all lead to the optimisation of instrument setup times.
- Improved instrument calibration and alignment procedures. Substantial time goes into the setting up of measurements. A number of possibilities can be implemented to automate or assist in speeding up this process. Solutions include the implementation of an integrated camera systems above the sample position, or the incorporation of the standardised software for the off-line planning and setting up of experiments which can be transferred with large accuracy to the physical instrument with the aid of fiducial points. The latter is being developed at a number of facilities such as ENGIN-X (ISIS), FaME38 and SALSA (ILL).
- Devise a remedy to extend the application of the method closer to sample surfaces. This can be addressed by software corrections or the implementation of a radial collimator.
- Incorporation of an in-situ loading frame of at least 50kN capacity for the investigation of fundamental properties of materials during loading in the plastic region. One specific application is the setting up of elasto-plastic self-consistent models. By incorporating the capability to apply uniaxial compression would enable the investigation of materials under reverse yielding (tensile yield followed by compressive yielding). By incorporating a heating mechanism of the sample under loading conditions creep phenomena can be investigated in-situ.
- To eetermination of principal strains and directions. This becomes possible when a χ-ring can be incorporated onto the instrument.

2.3. Conclusion

This paper underlines an important peaceful utilization of nuclear activities that has major technological advantages in material and component development though the assessment of not only detrimental residual strain situations, but also beneficial residual strain conditions. Within the South African scenario, the availability of this capability forms a key role in the research and industry communities with skills and product developments. It enhances the scope of Necsa and SA in the field of non-destructive evaluation of materials and components. International collaboration with other neutron diffraction facilities is an important avenue to pursue in the development and upgrading of the Necsa facility.

REFERENCES

[1] de BEER, F.C., STRYDOM, W.J., Neutron Radiography at Safari-1 in South Africa, Non-destructive Test Evaluation, **16,** 163, (2001).

[2] STRYDOM, W.J., VENTER, A.M., FRANKLYN, C.B., de BEER, F.C., The Role of Safari-1 in Industry and Academia. Physica Scripta **T97** 45 (2002).

[3] POPOVICI, M., STOICA, A., HUBBARD, C., SPOONER, S., PRASK, H., GNAEUPEL-HAROLD, T., GEHRING, P., ERWIN, R., Multi-wafer focusing neutron monochromators and applications, Neutron Optics, (J.L. WOOD and I.S. ANDERSON eds.), Proceedings of SPIE **4509**, 21-32 (2001).

[4] Neutron Diffraction Measurements of Residual Stress in a Shrink-fit Ring and Plug, VAMAS Report no 38 (ISSN 1016-2186) Technical Working Area 20 (WEBSTER, G.A., ed) (2000).

[5] VENTER, A.M.,de SWARDT, R.R., KYRIACOU, S.J., Comparative Measurements on Autofrettaged Cylinders with large Bauschinger Reverse Yielding Zones. Journal of Strain Analysis, **35,** 459, (2000)

[6] De SWARDT, R.R., VENTER, A.M., VAN DER WATT, M.W, Fatigues investigations on autofrettaged steel cylinders based on neutron diffraction measurements. Applied Phys **A74** [Suppl.], S1412-S1414 (2002)

[7] VENTER, A.M., de SWARDT, R.R., "Investigation of autofrettaged thick-walled cylinders with axial holes machined", accepted for publication in Journal of Neutron Research (2004).

The dedicated residual stress diffractometers E3/E7 at HMI Berlin and Stress-Spec at FRM II

R. P. Schneider*, T. Poeste*'**, H. Freydank*, M. Hofmann***
*   Hahn-Meitner-Institut Berlin, Germany
**   Institute for Materials Science and Technology, Germany
*** TU Munich, FRM II, Garching, Germany

Abstract. Most recent engineering progresses are due to the development of new materials and innovations in their processing and treatments. Material technologies, like the study of metals, alloys, ceramics and composites, especially non-destructive analyses of residual stresses profiles and textures, have gained increasing importance.

The dedicated residual stress diffractometers E3 and E7 at BENSC and Stress-Spec at FRM II are equipped with new two-dimensional position sensitive detectors. Sophisticated monochromators as bent silicon crystals yield a large gain of the diffractometers efficiency for strain measurements. Various equipments for sample positioning are available, e.g. an Eulerian cradle and translation tables carrying samples up to 300kg and 1000mm in diameter. Gauge volume can be adjusted by a new computer controlled variable slit-system. In-situ residual stress analyses can be performed within industrial components during mechanical or thermal loading (up to 2000K). The specially designed software ZET.DAT does rapid data visualization as well as evaluation. The linear powder-like diffraction pattern is calculated by summation over the scattering angle dependent Debye-Scherrer lines on the two-dimensional planar area detector. A large amount of beam time is exclusively used for industrial research.

1.   Introduction

The neutron diffractometer E3 at beam tube T2 of the BER II reactor has been dedicated to residual stress analyses for several years. In the framework of the Berlin Neutron Scattering Centre (BENSC), user groups from universities and research institutes have performed residual stress analyses the diffractometer by. For these groups beam-time is allocated on the basis of a peer-reviewed proposal system. Further beam-time contingents are dedicated to applied research for industry. The instrument E7 is completely used for industrial research. Among the components that were investigated are crankshafts, impellers, turbine blades, pistons, cylinder heads, and welds. Stress-Spec at FRM II, Garching, will start operation during 2004 [1]. All three instruments are quite similarly designed.

2.   Instrumental Setup

For easy and accurate handling of samples on the diffractometer, goniometers together with a translation device for precise x-y-z movements of heavy components have been installed at the diffractometers. The goniometer consists of two heavy-duty omega–circles manufactured by Huber, Rimsting, Germany (Figure 1), which can carry loads up to 1000 kg. For precise x-y-z translations of heavy components on the diffractometer a translation device has been constructed and manufactured. The z – translation is performed using four mandrels, thus, stabilizing the table against torsion, buckling and tilting. The table can carry components as heavy as 300 kg. Its accuracy of positioning is about 6μm (see Figure 2).

The detector system of E3 consists of a position sensitive area detector (30cmx30cm) manufactured by DENEX, with a resolution of approximately 1.5 mm. E7 and Stress-Spec actually use a 20x20cm detector build by EMBL. The angular resolution obtained depends on the distance between the sample and the detector; the best angular resolution obtainable is about 1”. The detector is housed in a sandwich – architecture made of Cadmium, boron car-
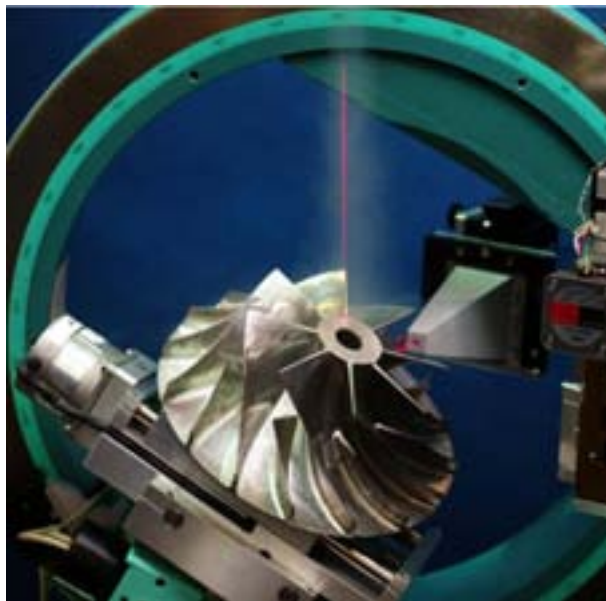
Figure 1. An MTU impeller on the materials research diffractometer E3 equipped with a HUBER Eulerian cradle. The lasers are displaying the actually investigated gauge volume defined by the slit system.

Figure 2. An X-Y-Z translation device is mounted on a HUBER sample table to move the sample (here: MTU turbine wheel) through the gauge volume defined by the slit system.

bide and polyethylene. The distance between sample and detector has been designed to be variable in order to enable an optimisation of the count rate and resolution for different sample diameters. Space in the diffractometer is large enough to accommodate samples and components of up to 1000 mm in diameter. A precise movement of the whole goniometer, the

detector and slit system, is guaranteed by the use of air cushions on a very accurate granite tanzboden (see Figure 3). [2-4]
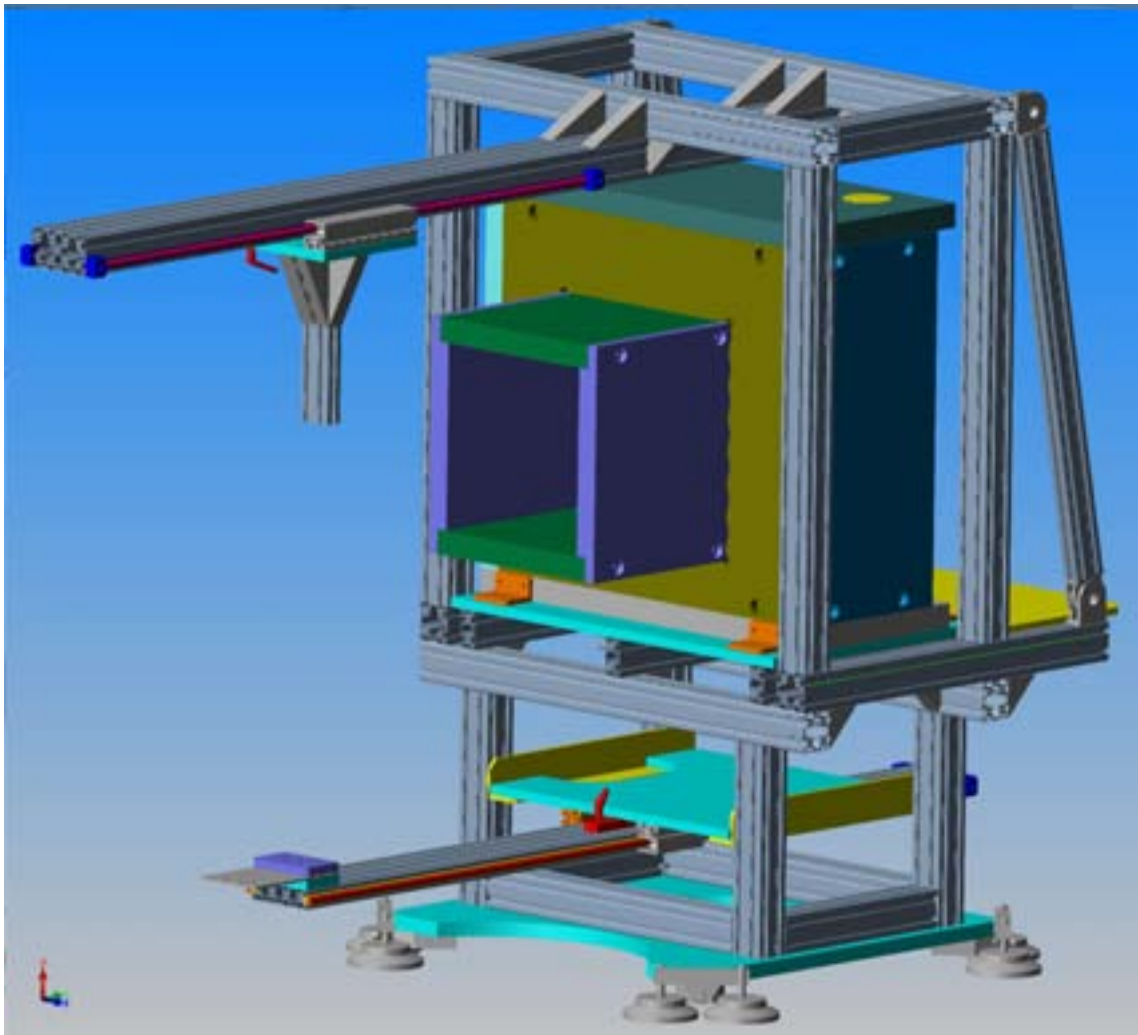

Figure 3. Construction of the detector shielding and setup at the instrument E3.

The 30cm x 30cm position sensitive detector is shielded by 10cm of polyethylene, 5 mm of boron carbide and 1mm of cadmium from the surrounding fast and thermal neutron background. The complete setup is build by using ITEM profiles and can be moved on air cushions over a very accurate granite tanzboden. A rail system on top of the detector guides the secondary slit system. Another rail on the bottom connects the detector to the sample table and allows the variation of the sample-detector distance between 1m and 1.5m.

At the Berlin instruments E3 (E7) flat copper **monochromators** are used providing a wavelength of 0.137nm (0.186nm) at a take of angle of 65° (90°). New monochromators consisting of bent silicon crystals are designed in cooperation with Pavol Mikula, Rez, and will be in use presumably in summer 2004 at both the instruments. At the FRM II instrument Stress-Spec we have a bent silicon monochromator build by Mihai Popovici (see fig. 4), a vertically focusing germanium monochromator and a double focusing PG monochromator [5-9].
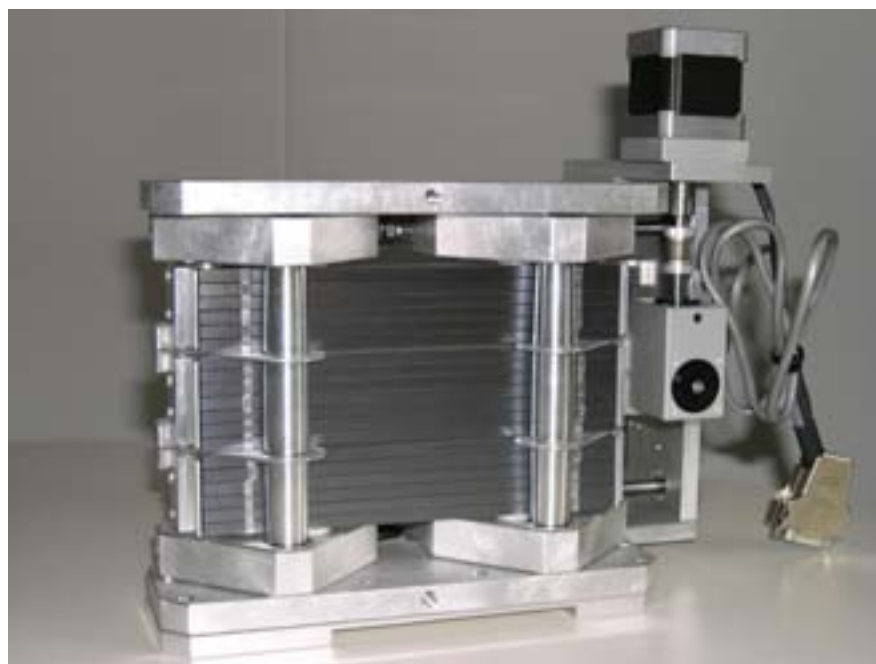
Figure 4. Focusing monochromator assembly

For the determination of the gauge volume within the sample a motorized slit system has been developed, which can be aligned to the neutron beam automatically during the instrument calibration procedure. The design of the slit system has taken into account the necessity to enable measurements on different sized samples and components with slits almost touching the sample surface and thus guaranteeing the best definition of the gauge volume possible. The slit size is defined by plates that can be translated within two grooves, which point together at an angle of about 30°. A micrometer screw can adjust the horizontal size of the secondary slit, very accurately. From the slit towards the detector housing a shielding system guides the diffracted beam in order to reduce instrument background.

A new designed cradle for heavy loads up to 50kg enables automatic sample orientation and thus strain scans without manual sample tilts and reorientations during the experiment cycle (see Figure 5).

For the instrument alignment it is obvious that very precise positioning of standards (slits or rods) on the diffractometer table is indispensable. For this reason instead of a theodolite a high resolution camera system with telecentrical lenses (Figure 6) is mounted with its optical axis perpendicular to the beam. By image processing the sample positioning can be done automatically. A ^{3}He detector tube at low gas pressure is positioned in the primary beam at the beam stop for the automatic adjustment of the primary slit using a vertically slit standard centred on the sample table. Additionally it can be used for a very fast and easy determination of absorption coefficients.

The especially designed software ZET.DAT does the data visualization and evaluation as well as the instrument calibration. The linear diffraction pattern is calculated by summation over the scattering angle dependent Debye-Scherrer lines on the flat area detector (see Figures 7, 8 and 9).
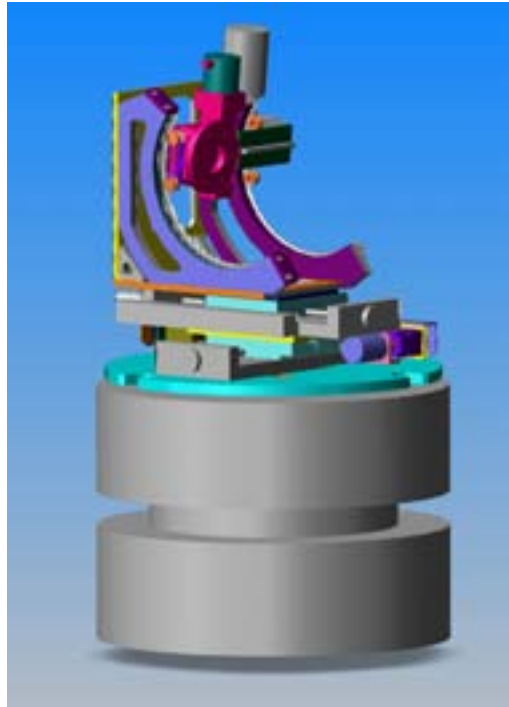
Figure 5. A new cradle is designed to tilt samples up to 50kg in a range from -5° to 100° and can presumably be used at E3/E7/Stress-Spec from summer 2004.

Figure 6. A high resolution camera (JAI M4+) together with telecentrical optics (JENMETA 1:1) allows very accurate sample positioning on the sample table.
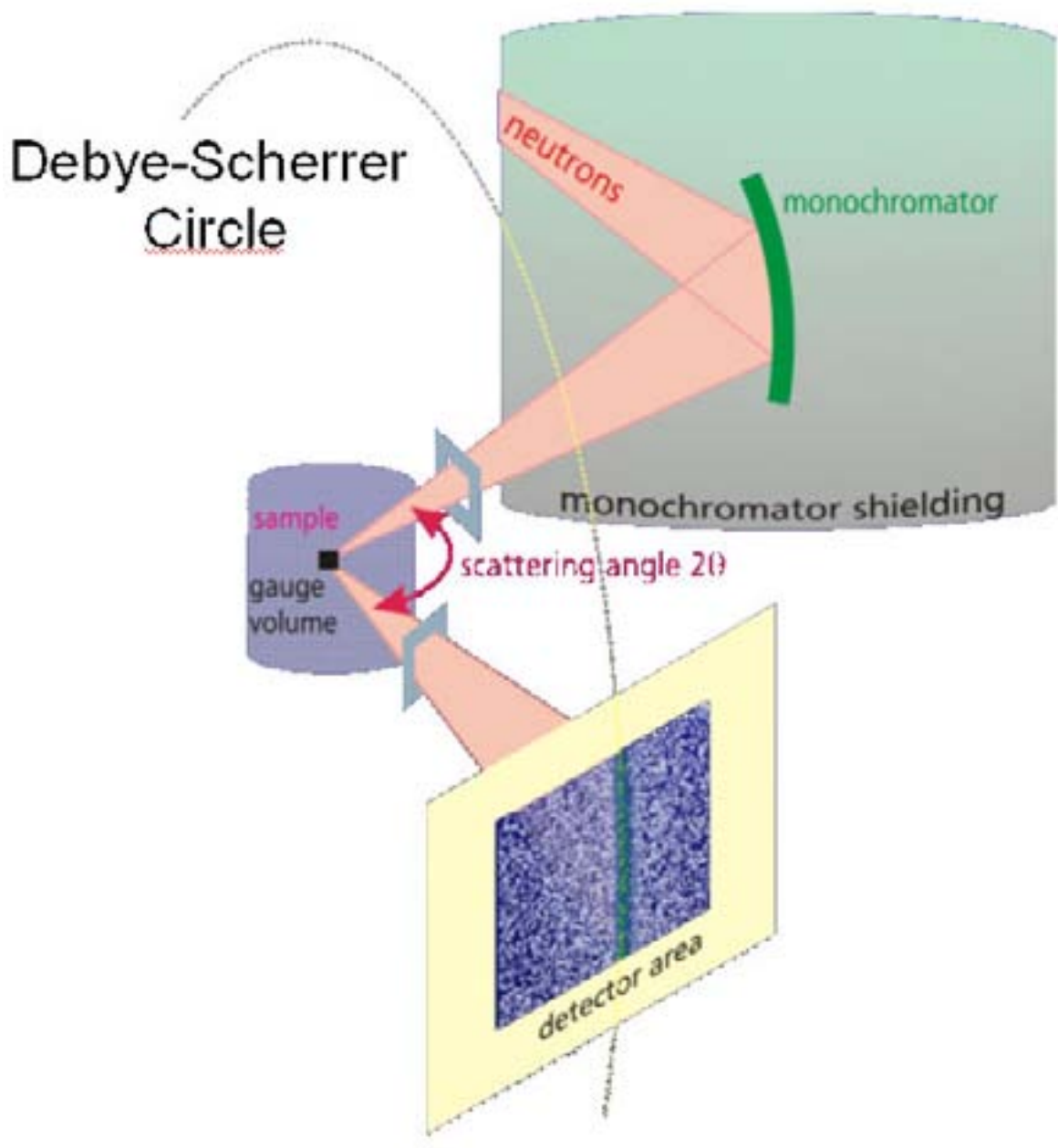
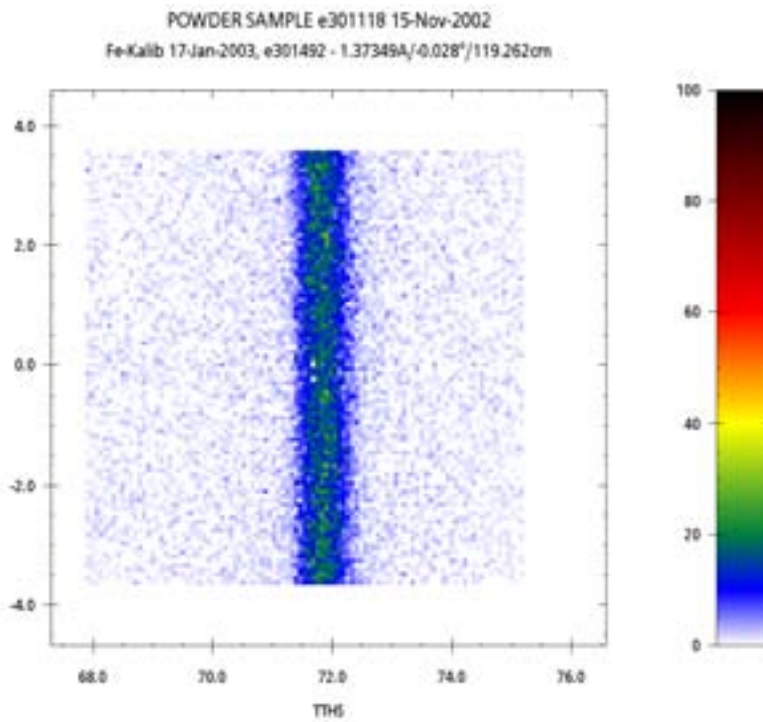*Figure 7. Intensity distribution on a two-dimensional position sensitive detector.*

Fe-Kalib 17-Jan-2003, e301492 - 1.37349A/-0.028°/119.262cm

Figure 8. Colour coded intensity distribution of a Debye-Scherrer line on the area detector as visualized by ZET.DAT.

POWDER SAMPLE e301118 15-Nov-2002

Gaussian Fit Results

Parameter	Value
TTHS	71.896(3)
d-value	1.170(2)
width	0.273(2)
magnitude	2170(20)
area	1490(30)

CARESS and Calibration

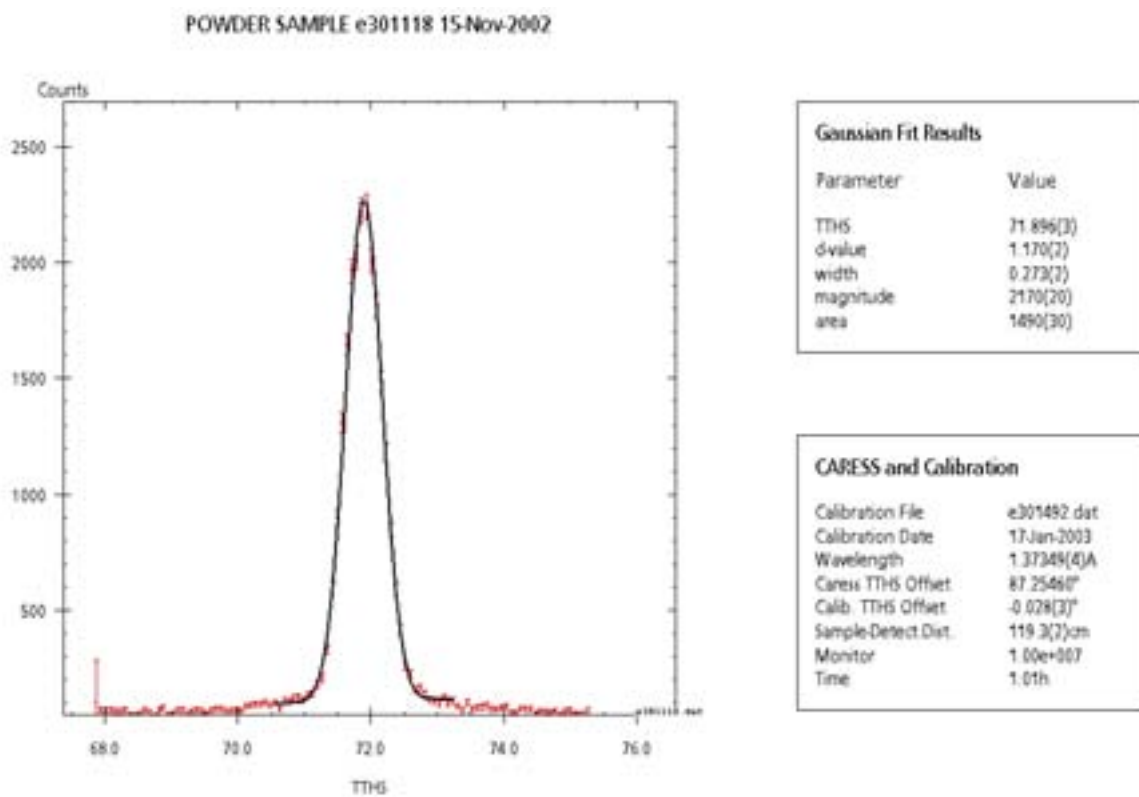|	
Calibration File	e301492.dat
Calibration Date	17-Jan-2003
Wavelength	1.37349(4)A
Caress TTHS Offset	87.25460°
Calib. TTHS Offset	-0.028(3)°
Sample-Detect.Dist.	119.3(2)cm
Monitor	1.00e+007
Time	1.01h

Figure 9. Bragg reflection of an iron sample measured at E3 together with the evaluation output of ZET.DAT

By loading a standard powder data set (iron, silicon) the instrumental calibration parameters are calculated and software automatically corrects all following data evaluations. *ZET.DAT* is developed for MS Windows platforms and allows data exchange by the MS Windows clipboard. Thus any other software like *Jandel peakfit* or *Origin* can be used to evaluate the measured data.

In order to carry out in-situ experiments a high temperature furnace is available which allows diffraction measurements at temperatures up to 2000K (see fig. 10). For the future we intend to improve our possibilities of in-situ measurements, e.g. it is planned to design a tensile rig with variable sample temperature.

Figure 10. The high temperature furnace mounted on the sample table of E7.

2.1 Example

Recently a Volkswagen crankshaft was investigated by neutron diffraction. The stresses within the deep rolled zone of the large end bearing have been of interest. Experiments carried out at the instrument E7 proved the validity of destructive X ray measurements. A slice 2cm thick was cut out of the crankshaft and a strain scan with high resolution was done (see fig. 11) [10]

2.2 Conclusion

The dedicated residual stress neutron diffractometer, in operation at BENSE, is described with its special features like focussing monochromator, goniometers and position sensitive detector. Two such instruments are designed for neutron beams at BENSE, Berlin and FRM-II, Munich. The diffractometer in operation at BENSE has special sample environment facilities like high temperature furnace and in-situ measurements can be performed on it. The results of an experiment on an industrial sample are shown to demonstrate the capability of the instrument.
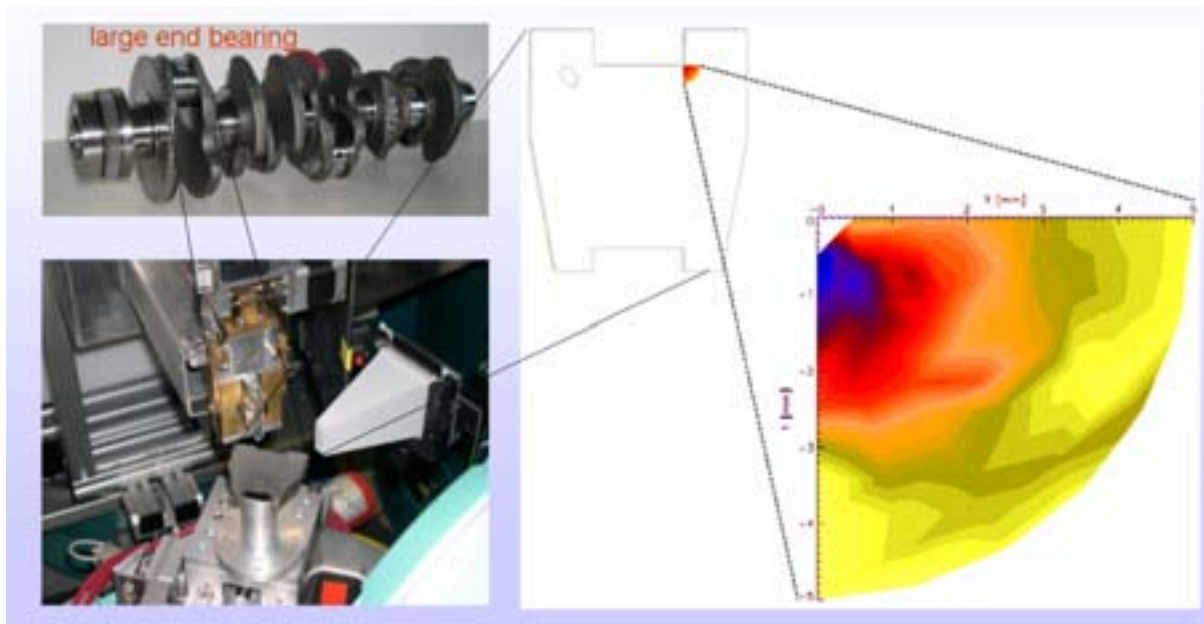
Figure 11. Investigation of residual stress distributions within the deep rolled zone of the large end bearing of a Volkswagen crankshaft. (Diploma thesis of Peter Lemke, TU Berlin)

REFERENCES

[1] MAYER, H.M.; PYZALLA, A.; REIMERS, W, "Construction of the new material science neutron diffractometer STRESS-SPEC", Materials Science Forum, **347-349**, p.29-33 (2000).

[2] MARMOTTI, M.; HAESE-SEILLER, M.; KAMPMANN, R, "Two-dimensional position-sensitive gaseous detectors for high-resolution neutron and X ray diffraction", Applied Physics A (Materials Science Processing), A**74**, suppl., pt.1, p.S252-4 (2002).

[3] MARMOTTI, M.; BURMESTER, J.; HAESE-SEILLER, M.; KAMPMANN, R "Two-dimensional position-sensitive detectors for high resolution diffraction with neutrons and high energy synchrotron radiation", Nuclear Instruments & Methods in Physics Research, Section A (Accelerators, Spectrometers, Detectors and Associated Equipment), **477**, no.1-3, p.347-52 (2002).

[4] MARMOTTI, M., HAESE-SEILLER, M., KAMPMANN, R., "Two-dimensional position-sensitive 3He-neutron detector for reflectometry and high-resolution diffractometry", Physica B **276-278**, p.210-11 (2000).

[5] MIKULA, P., "symmetric diffraction geometry of the bent crystal monochromator - A way to improve the properties of strain diffractometers", Applied Physics A (Materials Science Processing), A**74**, suppl., pt.1, p.S204-6 (2002).

[6] TANAKA, I., NIIMURA, N., MIKULA, P., "An elastically bent silicon monochromator for a neutron diffractometer", Journal of Applied Crystallography, **32**, pt.3, p.525-9 (1999).

[7] ONO, M., MIKULA, P., HARIJO, S.; SAROUN, J.; YONEDA, K.; SAWANO, J.; SAKURAI, Y.; KOBAYASHI, T., "Focusing bent perfect-crystal neutron monochromator -a key to high-resolution stress/strain measurement studies of polycrystalline materials", Materials Science Forum **321-324**, pt.1, p.296-301 (2000).

[8]   YELON, W.B.; BERLINER, R., POPOVICI, M., "A perfect match for high resolution neutron powder diffraction: position sensitive detection and focusing monochromators", Physica B **241-243**, p.237-9 (1997).

[9]   POPOVICI, M., HERWIG, K.W., BERLINER, R., YELON, W.B., " High-resolution neutron scattering with commercial thin silicon wafers as focusing monochromators", Physica B **241-243**, p.216-18 (1997).

[10] PETER LEMKE, Diploma thesis, Central Laboratory, Volkswagen (2003).

Residual stress measurement at Budapest Neutron Center

T. Gyula

Research Institute for Solid State Physics and Optics, Budapest, Hungary

Abstract. The use of residual stress measurements of different construction element and recent possibilities of Budapest Neutron Centre are presented. The details investigated already: gas turbine wheel, axial compressor blade, turbine blade and plastically deformed stainless steel. We demonstrated the use of a neutron scattering (SANS, residual stress, diffraction) for the materials behavior investigation in order to analyze the processes going on under the different mechanical loading. The direction of possible instrumental development is presented.

1.   Budapest Neutron Centre

The research reactor in Budapest (Figure 1) was first put into operation in 1959. A full-scale reconstruction and upgrading project started in 1986, aiming at the substitution of aged components, the enhancement of reactor safety, and the increase of reactor power to 10MW. The reactor reached first criticality on 12 December 1992. The regular operation was resumed on 25 November 1993. The Budapest Research Reactor is a tank type reactor, moderated and cooled by light water. The cold neutron source was installed on the tangential beam tubes. Irradiations may be carried out by inserting samples into the special vertical channels into the 51special vertical channels. The reactor was operated in 1994 for over 3700 hours; in 1995 about 4000 hours are foreseen. The timetable corresponds to the various requirements. The reactor has 10 horizontal beam tubes (8 radial and 2 tangential ones).

The reactor serves for basic and applied research (condensed matter, radiochemistry, biological irradiations, reactor technology), technological and commercial applications (production of radioisotopes, neutron radiography, activation analysis, pressure vessel surveillance), education and training: (undergraduates, Ph.D. students, IAEA training courses, etc.).

Figure 1. The Budapest Research Reactor.

1.1 Cold Neutron Experimental Stations at the Budapest Research Reactor
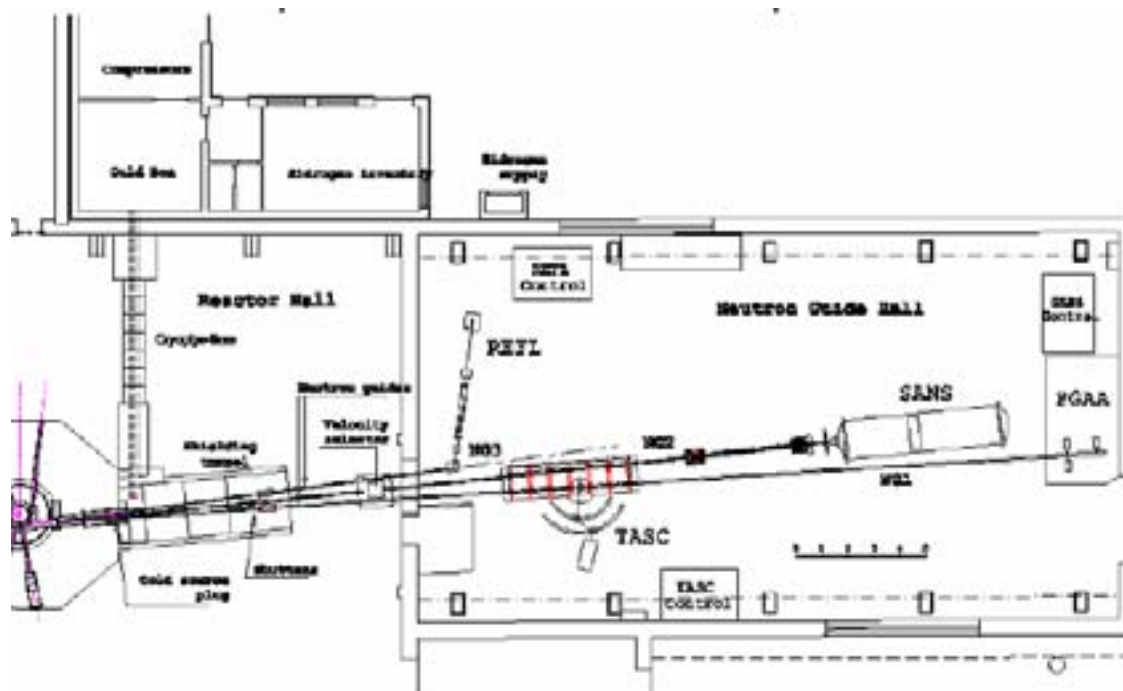

Figure 2. The neutron guide hall at Budapest Reactor Center.

Residual stress measurements were carried out on the cold neutron triple axis spectrometer (Figure 3), which is set up in the guide hall (Figure 2.) for low background, having a 2D area detector (Figure 5) and a focusing monochromator (Figure 4). Space is available for heavy samples.

Figure 3. Layout of the spectrometer.

1.2 The main parameters of the spectrometer

|	
Beam tube	neutron guide No.1
Monochromator	
Focusing	Focusing vertical pyrolitic graphite 90x80 mm (24min mosaicity)
Analyser:	Flat pyrolitic graphite 50x90 mm (24min mosaicity)/Ge monocrystal (15min mosaicity)
Collimations	45', 30', 15'
monochromator angle	$36 < 2\theta < 126^0$
scattering angle	$-120^0 < 2\Phi < 70^0$
analyser angle	$-40^0 < 2\theta < 120^0$
Range of crystal Orientation	$0^0 < 2\theta < 360^0$
Angular resolution	0.01^0
Flux at specimen	2×10^6 n/cm^2/sec
Beam size	25x90 mm^2
Momentum transfer	$0 - 2.7$ Å^{-1}
Energy transfer	0 - 9 meV
Characteristic resol (3.3Å)	120-150 μeV
Sample environment	closed cycle refrigerator; cryostat (liquid. N2), Magnet up to 2T, (max scattering angle 100) furnace up to 1000^{0}C, Thermostat (-20 ^{o} C-100 ^{o} C)
Detector	190x190 mm 2D detector, type MK the MK 200N-1 type, 2 Delay-Line type
Control and data collection	Daffodil (LLB) /PC / OPEN Hungary

Figure 4. Focusing PG monochromator.
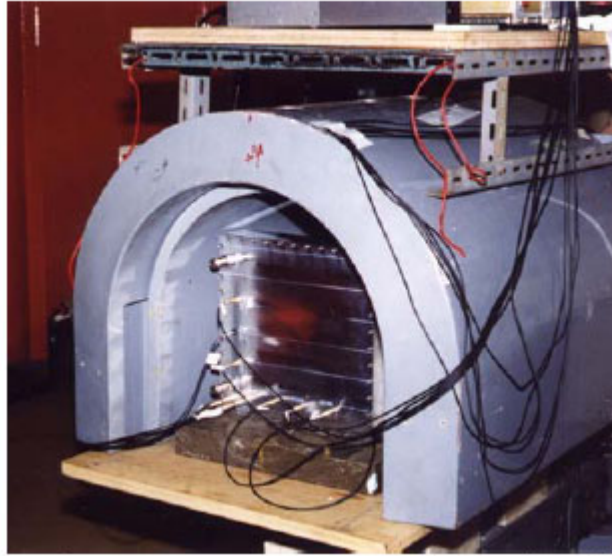
Figure 5. The new 180x180mm area detector installed in the spectrometer detector shielding.

2.   Selected measurements

High-resolution diffraction for residual stress determination in a NiCrMoV wheel of the axial compressor of a heavy-duty gas turbine (Figure 6 and Figure 7)

Figure 6. The material NiCrMoV high-strength-low-alloy steel with reference to the ASTM A 471 (type 2) The wheel experimented, as bladed, ~2500 0-peak cycles, with some 102% over speed ones, and operated at a temperature ~300 °C.

A preceding SANS investigation has revealed the absence of precipitates texture and a low concentration of nano-defects in the material, as compared to analogous steels after thermal

treatment, where an intense formation is induced of precipitates which volume fraction exceeded ~ 1 %. [1]
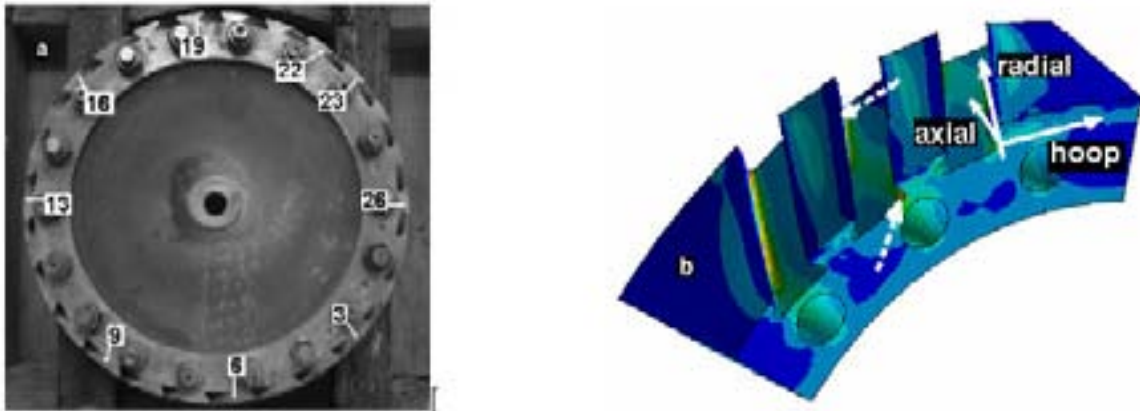

Figure 7. Wheel of the axial compressor of a heavy-duty gas turbine. Identification of the investigated locations (a), and FEM detail (b) with the local coordinate system and the evaluation of the maximum stresses areas (see the outlined arrows).

Measurements along three directions (radial, hoop and axial) of each considered point have been performed, at wavelength $\lambda = 0.28$ nm.

Gaussian peaks over a linear background have been obtained, over the peak Fe (110).

Figures 8 (a & b) and 9 show tensile RS. Hoop stresses, in general, result higher than the radial ones, and they are in the range $\sim$50 - 200 MPa, reaching their max value in correspondence of the location 19 ($\sigma_{19hoop} = 190.7$ MPa).
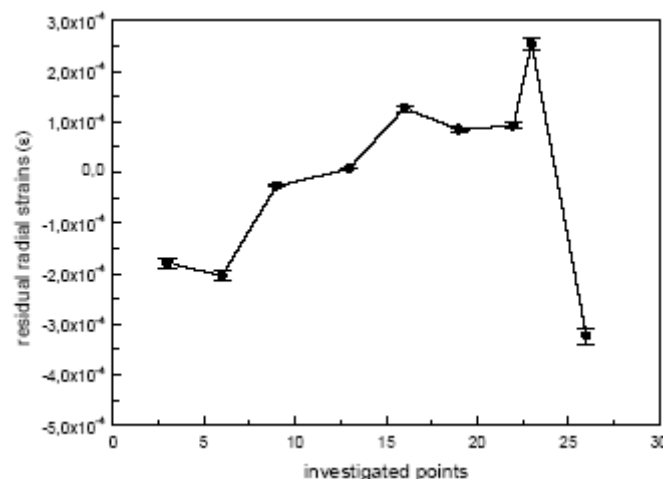

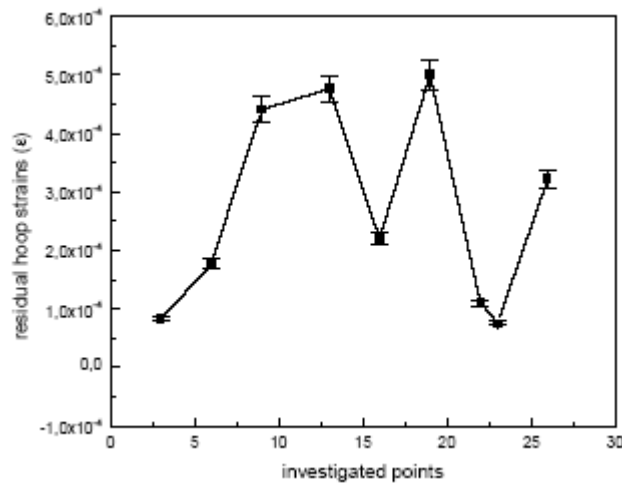*Figure 8a. Elastic residual strains for radial direction.*

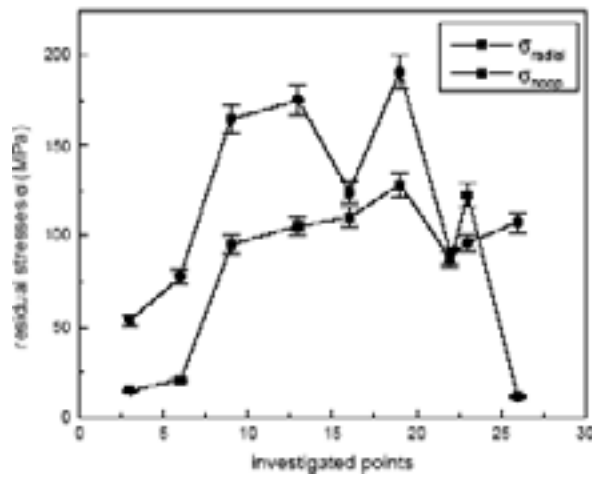*Figure 8b. Elastic residual strains for hoop direction.*

Figure 9. RS values for radial and hoop directions.

Radial stresses are in the range ~10 - 130 MPa, showing their max value in correspondence of the same location 19 (σ_{19rad} = 128,7 MPa) and their min. values in correspondence of the contiguous locations 3, 6 and 26. The same RS are firstly due to the manufacturing process, and successively changed by the operating cycles fatigue and thermal effects. In future an investigation of a new wheel by the same adopted technique allows comparing the obtained RS data between new and operated material,

2.1   *Stainless steels X18H10T*

We have examined a series of plastically deformed stainless steels X18H10T (with composition given in Table 1), commonly used in the WWR-type Nuclear power plants. The SANS results are shown in Figure 10.

Table 1. Chemical composition of steel X18H10T (GOST 5632-72)

element	C	Mn	Cr	Ni	Ti	Fe
concentr,% wt.	0.08-0.12	1-2	17-19	9-11	0.4-0.7	67.18-72.52

76

The SANS intensity distribution I(q) for plastically deformed steel

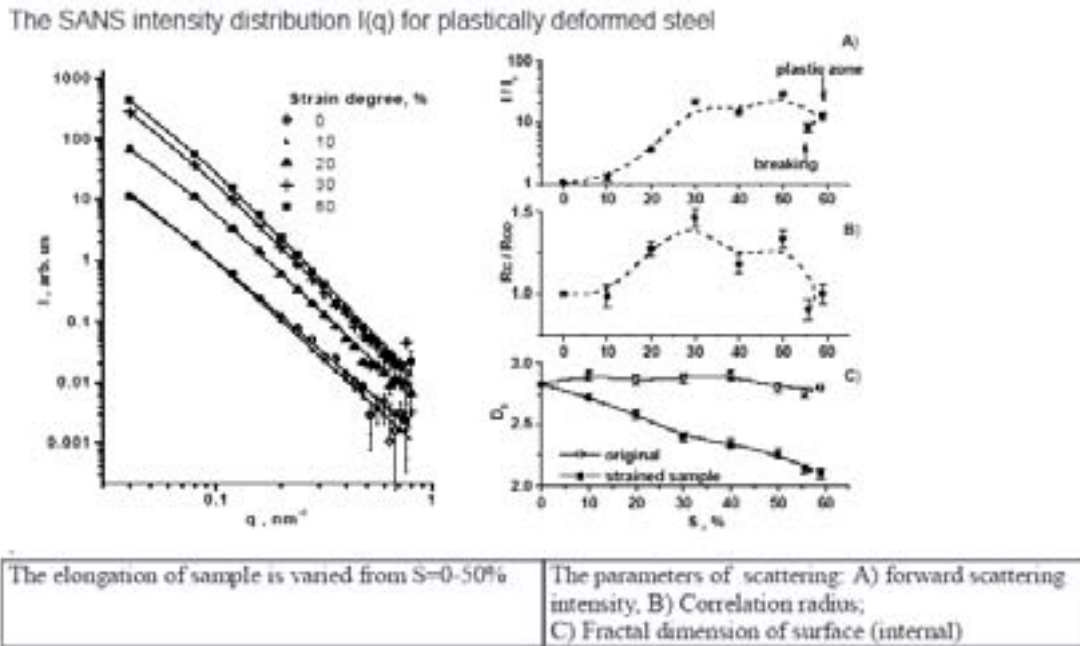| The elongation of sample is varied from S=0-50%	The parameters of scattering: A) forward scattering intensity, B) Correlation radius; C) Fractal dimension of surface (internal)

Figure 10. Results of the SANS experiment on X18H10T (Steel).

After the SANS measurement we investigated the residual stress in the deformed samples at λ=0.286 nm on BNC TASC spectrometer. We detected an austenite- martensite phase transition by plastic deformation (Fig 11 and Fig. 12).

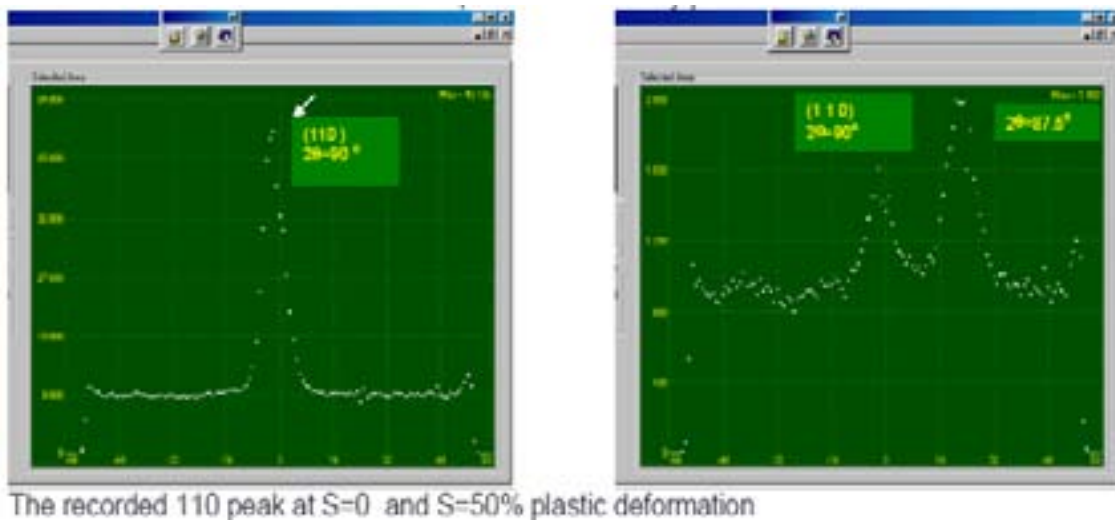The recorded 110 peak at S=0 and S=50% plastic deformation
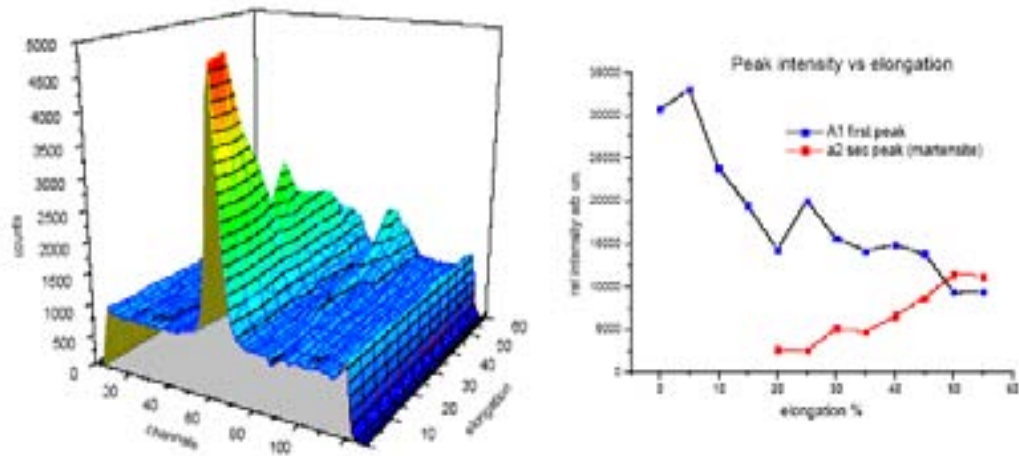
Figure 11. Phase transformation in plastically deformed X18H10T steel.

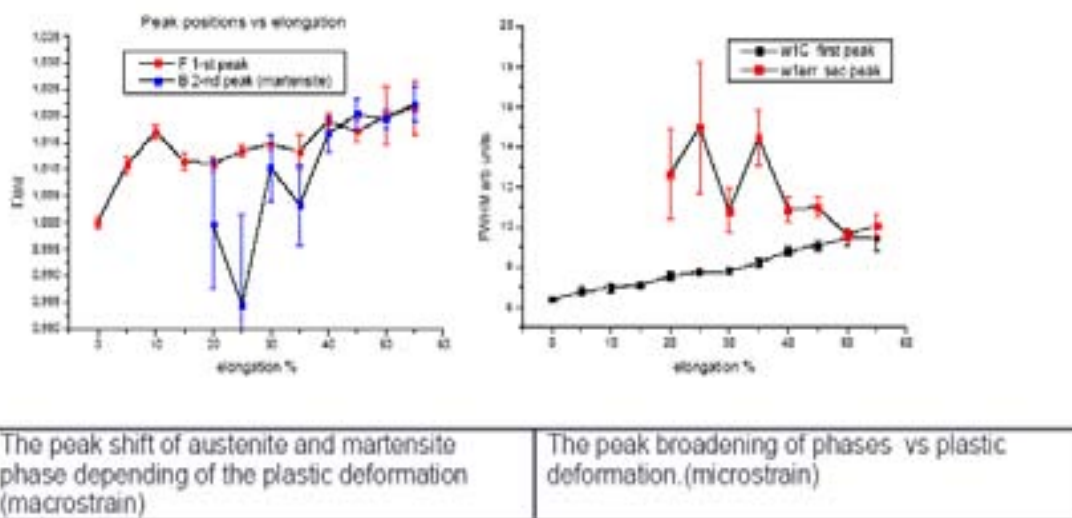Fig The austenite- martensite transformation by plastic deformation of plastically deformed X18H10T steel

The peak shift of austenite and martensite phase depending of the plastic deformation (macrostrain)	The peak broadening of phases vs plastic deformation.(microstrain)

Figure 12. *Intensity distribution, shift in peak position and half width variation as a function of plastic deformation*

In order to explain the results of two-phase stress measurements a theoretical description of residual stress in complex material is needed.

3.   Theory

The interplanar distance d was evaluated by using the Bragg law:
$$n \lambda = 2\, d \sin \theta \tag{1}$$
The corresponding lattice strain by using the following relation:
$$\sigma = (d_0 - d) / d = d\theta \cot g\, \theta \tag{2}$$
Where d_0 is the interplanar distance of a stress-free reference material.

3.1 Materials containing two phases (composite or alloy)

Stresses (cubic system) in the directions *ijk = xyz* can be calculated by Hook's law:

$$\sigma_i = (E/(1-2\nu)(1+\nu)) [(1-\nu)\varepsilon_i + \nu(\varepsilon_j \, \varepsilon_k)] \tag{3}$$

E the Young's modulus, ν are Poisson's ratio of the material.

ε_i, ε_j, ε_k are strains in the principal directions.

For a composite material, the total measured stress σ_{tot}, averaged over the gauge volume in each phase can be split into three contributions:

- A macrostress (σ_{macro}), which varies smoothly through many grains;
- an elastic mismatch microstrain (σ_{mE}), varying on a scale of the inhomogeneous structure due to difference in elastic constants of the two phases and representing the load transfer to the stiffer phase (e.g. C reinforcement in phase A);
- Thermal mismatch microstrain (σ_{mT}), which is due in difference of the thermal expansion coefficients of the two phases.

Thus the following tensor relation for two-phase system (*i* A, C):

$$\sigma^i_{tot} = \sigma_{macro} + \sigma^i_{mE} + \sigma^i_{mT}$$

The macrostress can be calculated from the measured stress σ_{tot} in both phases as:

$$\sigma_{macro} = f\,\sigma_{Ctot} + (1-f)\sigma_{A\,tot},$$

f is the relative volume fraction of the C reinforcement.

The elastic mismatch microstress is related to the macro-stress by means of:

$$\sigma^i_{mE} = B^i\sigma_{macro}$$

Where B^i is a tensor, which depends on the reinforcement particle shape and on the elastic constants of the two phases. (This question is more or less open and needs some development).

4. Conclusion

The powder diffractometer and small angle neutron scattering spectrometer with their applications for materials studies are presented. The new instrument installed on a beam line of the reactor with focussing monochromator and position sensitive detector is described. Results on phase transformation by plastic deformation are shown for illustration. The equipment is used to study industrial components like compressor wheel for the measurement of residual stresses produced due to manufacturing processes and which undergo changes by running over various cycles of operation.

REFERENCE

[1] ROGANTE, M., BATTISTELLA, P., CESARI, F.G., CESCHINI, G.F., RETFALVI, E., LEBEDEV: V., "*SANS-study of the nano-defects in a NiCrMoV component for nuclear/traditional energy applications*", Proc. of 1st Int. Conf. on Materials & Tribology 2002, Dublin, Sept. 12-13, 2002, (KENNEDY, D.M., Ed), Publ. DIT, Dublin, p.30 (2002).

Current status and forecast of the residual stress program at the NIST reactor

T. Gnäupel-Herold
National Institute of Standards and Technology, United States of America

Abstract. Together with other leading instruments in the field the BT8 Residual Stress Diffractometer at the NCNR has undergone a rapid development since commissioning in 1995. As of now, the peak performance is increased by a factor eight, thus enabling measurements at larger information depths and higher spatial resolutions. The design of the instrument, its experimental capabilities and projected future requirements will be discussed. The new experimental capabilities open the field to new users and type of experiments ranging from stresses in bulk rails with some 80 mm thickness down to sheet metal, electron beam welds, and coatings with required spatial resolutions < 0.5 mm. These experiments will be discussed in some detail with respect to relevance, user interest and instrumental requirements. With the increased demand on the instrumental performance there is also a rising demand for a broadened scope of capabilities for stress measurements other than neutron diffraction.

1. THE NIST REACTOR AND THE BT8 RESIDUAL STRESS DIFFRACTOMETER

1.1 Neutron Instruments at the NIST Centre for Neutron Research

The NBS reactor reached its first criticality in December 1967. The reactor is heavy water moderated with a core that is horizontally split at the beam tube level for background reduction. In the following 18 years the reactor was operating at 10 MW until its upgrade to 20 MW operation in 1985. The power upgrade was accompanied by transformation into a national user facility for neutron scattering experiments with 38+11 days reactor cycles. Another major step was the commissioning of the liquid hydrogen cold source in 1994, which increased the output of long wavelength neutrons by more than one order of magnitude. Since then, the NIST Centre for Neutron Research has become the most frequented user facility in the United States with continuing neutron instrument upgrades and completely new designs such as the next generation triple axis spectrometers as well as several new cold neutron spectrometers. Today, there are seven thermal neutron instruments and 12 cold neutron instruments, all of which are available for user experiments (Figures 1 and 2).
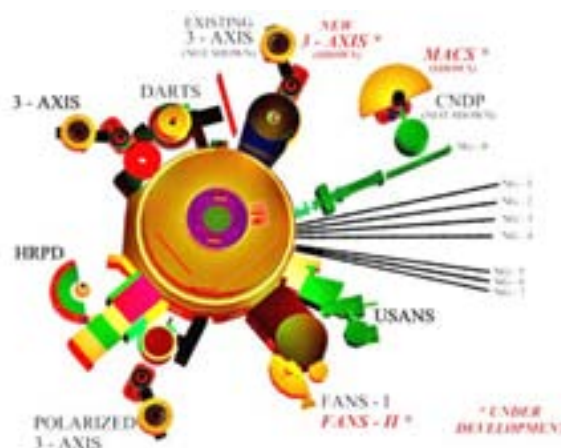

Figure 1. Thermal neutron instruments at the NCNR. Acronyms: DARTS – Residual Stress Diffractometer, HRPD – High Resolution Powder Diffractometer, FANS – Filter Analyser Neutron Spectrometer, USANS – Ultra Small Angle Neutron Spectrometer, MACS – Multi-Analyser Crystal Spectrometer.
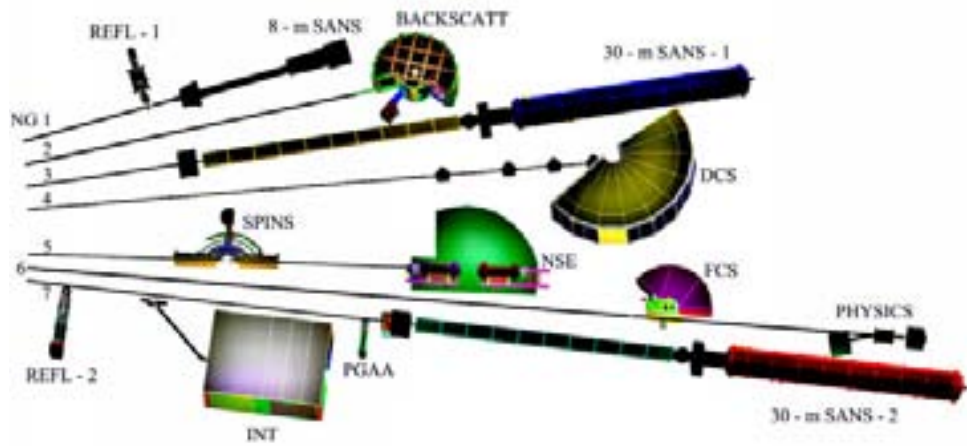
Figure 2. Cold neutron instruments at the NCNR.

1.1.1 The Residual Stress Diffractometer

The BT8 Residual Stress Diffractometer is the centrepiece of the stress measurement program at the NCNR which depending on the experimental demands covers the entire range of spatial resolutions and information depths accessible through diffraction (Figure 3). Neutron diffraction and lab X ray diffraction are available in-house. Synchrotron diffraction is available through collaborations with major synchrotron sources such as the Advanced Photon Source.
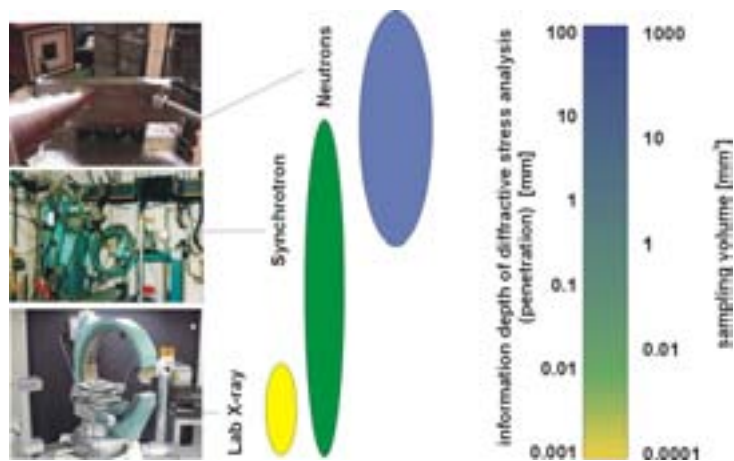

Figure 3. Diffraction techniques used for residual stress analysis.

The BT8 diffractometer was commissioned in 1996 as a dedicated residual stress instrument. A rendering of its CAD drawing is shown in Figure 4.
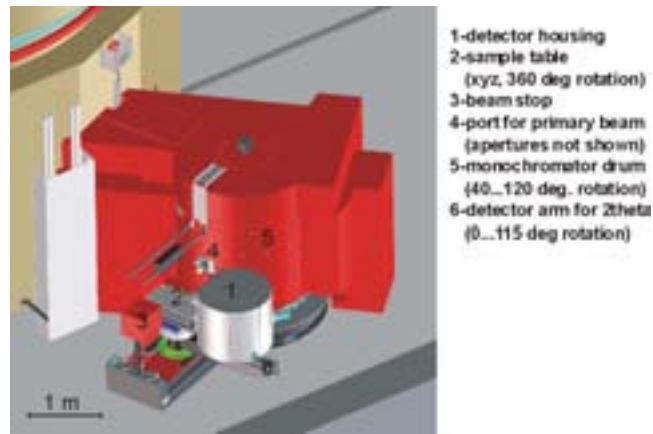
Figure 4. Layout of the BT8 Residual Stress Diffractometer.

The main feature of the instrument is its versatility. Through the variable take-off angle (2theta monochromator) and the available monochromator options the wavelength can be adjusted continuously between 0.08 to 0.32 nm. This is important because it allows bringing the diffraction angle $2\theta_{sample}$ for almost any sample d-spacing close to 90° for optimal spatial resolution. The adjustable curvature of the double focusing Si-monochromator (Figure 5) allows the fine-tuning of the Figure-of-Merit for keeping the counting time at a minimum.
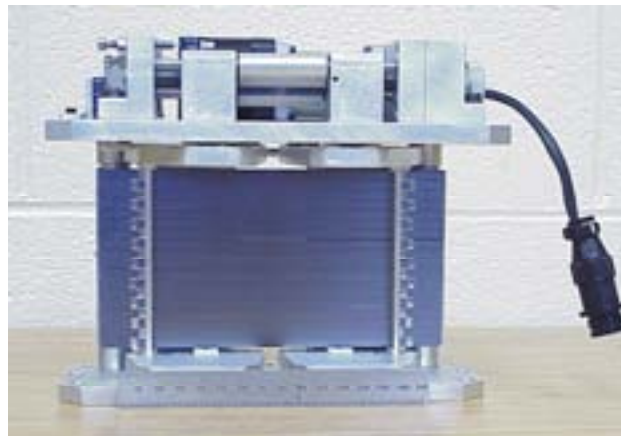

Figure 5.   Double focusing monochromator. The vertical curvature is fixed while the horizontal curvature is variable by bending stacks of thin silicon wafer blades in [001] orientation. The gain is achieved both by spatial focusing and 'wavelength focusing'.

Specimens up to 150 kg weight can be fit onto the experiment table. The allowable specimen dimensions depend on the gauge volume locations. The gauge volume size can be up to 6x6x20 mm^3. The more important lower limit depends on materials properties such as scattering length and absorption. Under certain circumstances such as favourable textures gauge volume sizes of 0.1 mm^3 have been achieved. The combined effects of the available instrument flux and the Figure-of-Merit of the monochromator can be conveniently summarized in the performance curve in Fig.8.6 which shows the counting time necessary for a certain depth at a given gauge volume size for the two common engineering materials aluminium and steel. The data are normalized to ($\Delta\varepsilon$) $\Delta d/d=10^{-4}$ as the relative accuracy of the position of the peak measured.
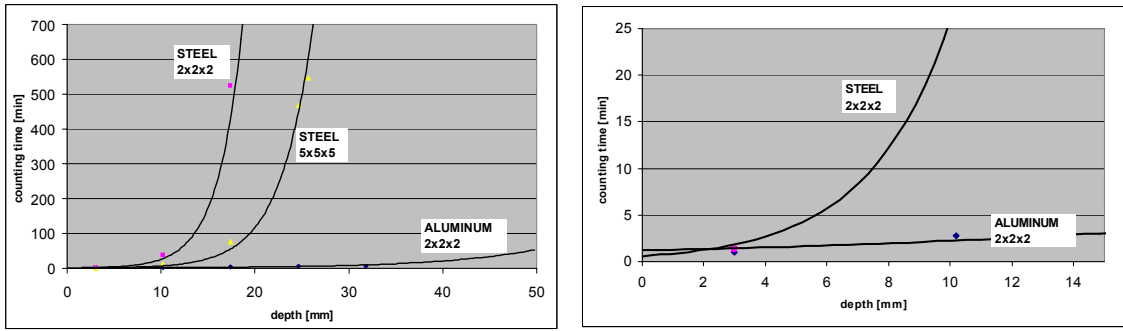
Figure 6. Depth dependent counting time for Al (311) vs. steel (211) at $2\theta=90°$ and $\Delta\varepsilon=10^{-4}$. The graph of the right is a zoom of the left graph.

Another important feature emphasized in instrument design is a low instrumental background rather than high primary beam intensity. This is especially useful for experiments with low intensities times where low signal to noise ratios can significantly prolong the counting time.

1.2 Instrumental demands of current experiments

Instrument development is largely driven by the demands of experiments which themselves reflect current needs and interests in mechanical and materials engineering. The experiments conducted on BT8 in the last two years as shown in Fig.7 typically deal with four major issues:

- Deep penetration for large samples (rails)
- Very small sampling volumes for steep gradients (springback)
- Coarse grained materials with medium sampling volume sizes (stainless steel, aluminium)
- Lineup of samples with complicated shape (rails, I-beams)

The following examples highlight these issues while at the same time it is shown that these problems are often interconnected.
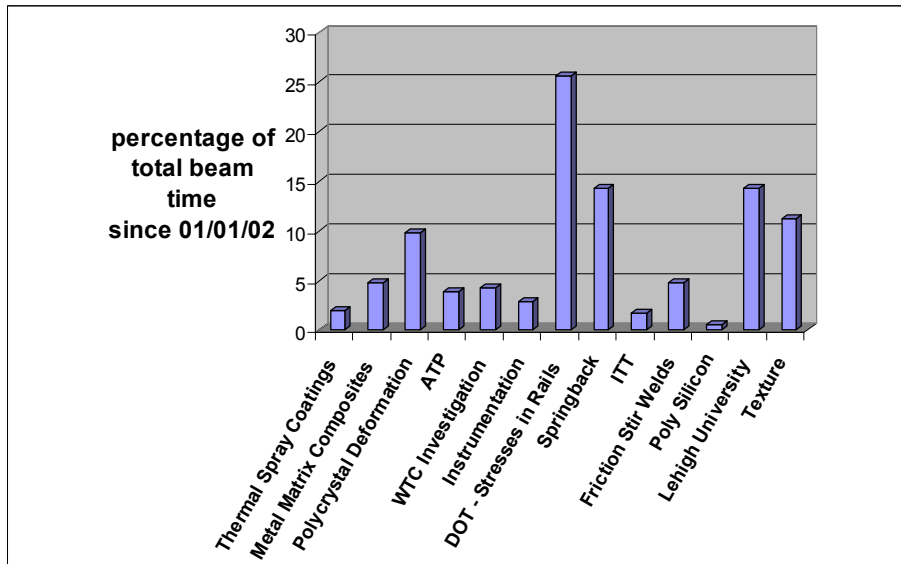

Figure 7. Experiments conducted on the BT8 Residual Stress Diffractometer since 2002.

1.2.1 Stresses in Rails

Residual stresses in rails and the dependence of the stresses on service history, on surface conditioning and material strength have been the subject of a long-standing interest. The demands for rail safety and longevity on one side and increased tonnages and accumulated gross weight on the other side increase steadily. At the same time, the effects of increased axle loads and car speeds on rail integrity are not completely understood. However, it is established that the level of residual stresses in the railhead increases with the accumulated tonnage, which can lead to the formation of catastrophic cracks in the rail. Thus, the non-destructive measurement of these stresses is of great importance both to provide necessary data for failure models and to establish a benchmark to which the results of other – mostly destructive - methods can be compared.

The difficulties associated with this experiment become clear in Fig.8.8. The specimen is heavy (35 kg); the region of interest (head section in the mid-plane) has no straight faces for easy position measurement, and extremely long neutron paths because of a maximum width of the head of 75 mm.
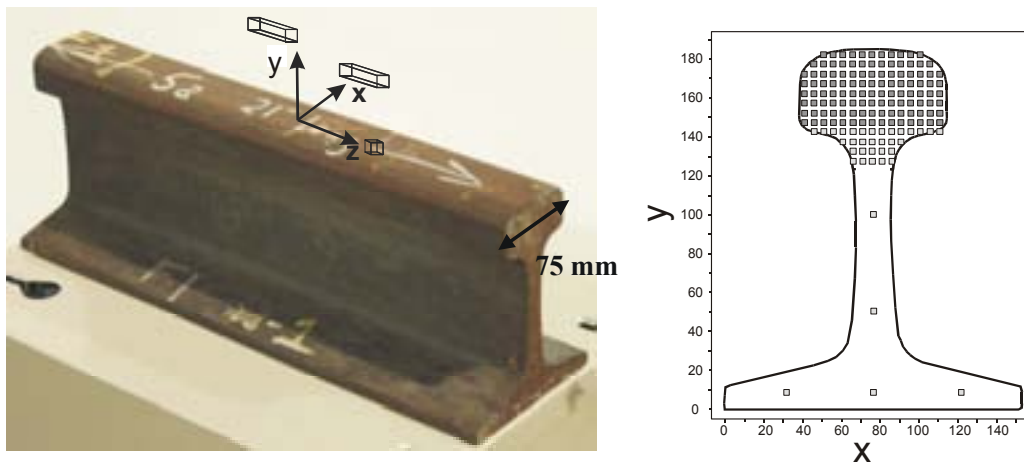

Figure 8. Left: Section of a rail (North American profile). The length (53 cm) was chosen such that the longitudinal stresses are preserved. The sketch on the right shows the measurement locations and relative dimensions of the gauge volumes.

From previous measurements on rail slices it was known that because of steep stress gradients the size of the sampling volume in the XY-plane should not exceed 5 mm. Also, it was determined that a 5 mm spacing of measurement locations was required. Thus, for measuring the three principal directions and the xy-shear component a total of 568 measurements were necessary to obtain a stress map of sufficient detail.

Steel is a strong neutron absorber, which makes measurements with more than $\approx$70 mm neutron path prohibitive. Applicable measures for reducing the beam path in the railhead are a reduced diffraction angle for the longitudinal component ($2\theta \approx 60°$), tilting the specimen, and an increased diffraction angle ($2\theta \approx 100°$) for the y- and x-component (Figure 9).
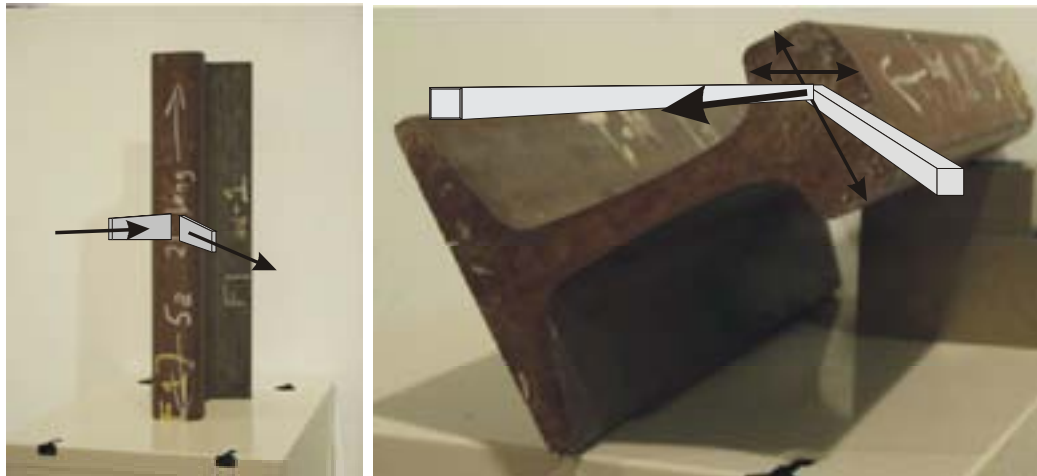
Figure 9. Approximate specimen orientation for the z-direction (left) and for the longitudinal direction (right).

A small coupon from the rail was used for the d_0-reference measurements at the two diffraction angles. This allows the calculation of strains and stresses as shown in Fig. 10.

σ_{xx}

Max: 455 MPa
Min: -403 MPa

σ_{zz}

Max: 427 MPa
Min: -165 MPa

σ_{yy}

Max: 345 MPa
Min: -476 MPa

σ_{xy}
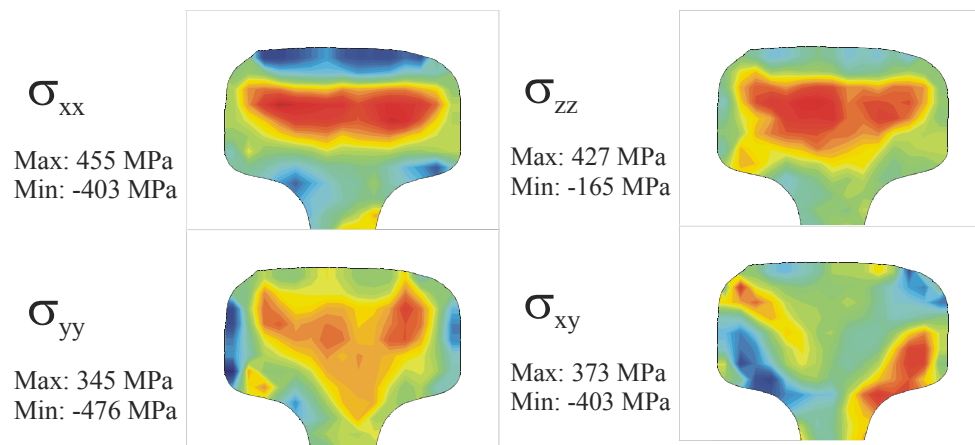
Max: 373 MPa
Min: -403 MPa

Figure 10. Result of the stress measurement on the intact rail piece.

While the results for the x-, y- and xy-stress components confirm previous measurements on thin rail slices (6 mm thickness), the main focus of this experiment were the longitudinal stresses for which there were no previous results available that were obtained non-destructively. The great success of this measurement highlights the unique advantages of neutron diffraction residual stress analysis to provide reliable and unambiguous results for critical materials problems.

Future experiments are already at the planning stage, and they will focus on residual stresses in wheels. The problems of path length and absorption will remain the same with an even heavier specimen.

1.2.2 Springback

It was shown in the previous section what is necessary to measure stresses on a large, bulky and absorbing piece of material. At the other extreme end of the scale one has small, thin specimens which require gauge volumes > 1 mm^3 which pose additional limitations arising

from partial illumination near surfaces and beam divergence. Springback stresses in sheet metal represent an excellent example for such an experimental problem because one typically has to expect high strain gradients over the range of 1 .3 mm (sheet thickness), thus requiring spatial resolutions of the order of 0.1…0.5 mm in order to provide the necessary resolution.

Springback is the elastic shape change of sheet metal after forming and removal from the die. In the automotive industry the poor predictability of springback has always been a problem but it was somewhat alleviated by the use of rather thick walled, low strength steels. Due to the increasing need for weight reduction there is a major shift underway to use thinner high strength steels and aluminum alloys. In both cases these materials exhibit larger springback magnitudes, thus making an accurate prediction all the more necessary in order to avoid costly re-design of the stamping tool.

An accurate prediction of springback means first of all the accurate prediction of the residual stresses that create springback. However, it was found that there were no sufficiently accurate previous experimental data on springback available that would allow benchmarking finite element calculations.

In order to conduct such a measurement a deep drawn cup was chosen as a standard test specimen (Figure 11). Measurements were to be performed in the mid-section of the cup.

Figure 11. Standard test specimen for the measurement of springback stresses. Left: intact cup; middle: sectioned cup with mid-section as the actual specimen; right: split mid-ring for measuring the ring opening.

The main advantage of the cup is that it encompasses all the main features of sheet metal stamping such as large bi-axial strains and large springback magnitudes. The latter is measured by splitting the mid-ring open and measuring the ring opening.

The experimental demand for the diffraction measurement is to measure at least eight through-thickness locations in three directions as shown in Figure 12.

Several of the above ring samples were investigated both by synchrotron diffraction and by neutron diffraction. Synchrotron radiation is generally well suited for aluminum because of the low absorption compared to steel. Neutron diffraction, on the other hand, is better suited for steel because of the large scattering length of iron, and the path lengths in the sheet are small.
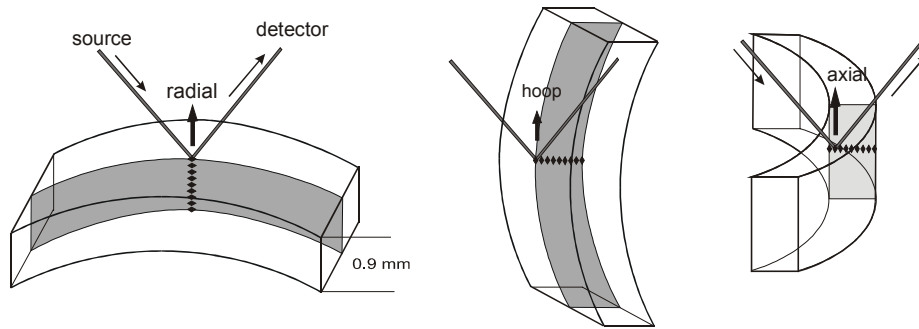
Figure 12. Orientation of a ring section and location of sampling volumes for a diffraction measurement of through-thickness stresses. This scheme is applicable both for synchrotron diffraction and for neutron diffraction.

The extreme demands for spatial resolution in this type of measurement are at the limit of what neutron diffraction can currently achieve. These experiments are made possible to some extent by taking advantage of preferred orientation, which, for selected specimen directions, can substantially boost intensity. This allows in return reducing proportionally the gauge volume size. Typical texture strengths for rolled and deep drawn sheet material are four to eight times random orientation. In these directions, gauge volume sizes down to 0.1 mm^3 are possible. Fig. 13 shows pole figure that were measured at locations that correspond to the rolling direction (RD), the transverse direction (TD) and the intermediate direction at 45° between both. The red regions represent directions of high intensity where strain measurements should be done.
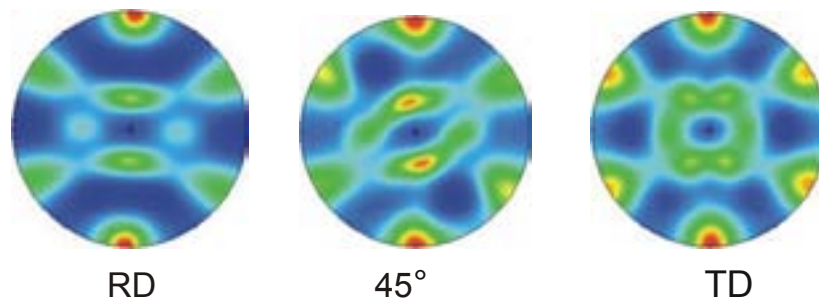

RD   45°   TD

Figure 13. (011) pole figures from locations that correspond to the rolling direction (RD), the transverse direction (TD) and the intermediate direction at 45° between both.

The results of the diffractive stress analysis on several rings made of Al6022 and AISI1010 are shown in Figure 14.

Counting times with such small gauge volume sizes can be as little as 10 min if the measurement is done in preferred directions.

Springback continues to draw considerable attention, especially in the car industry. Having established an optimal strategy for these measurements opens up the possibility of more routine measurements as well as the option of investigating the effect of parameters such as yield strength, pre-strain or lubricant on the through-thickness stresses. Overall, sheet metal specimens with preferred orientation are excellent examples for experiments where neutron diffraction provides much needed results for current engineering problems.
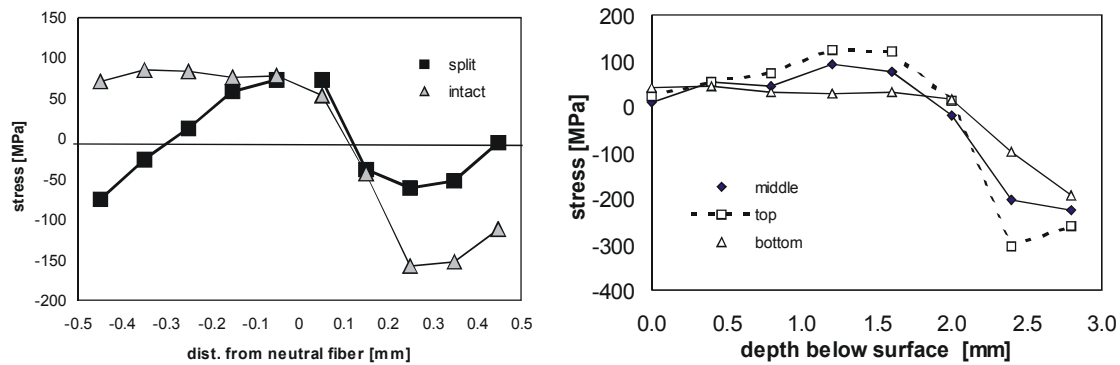
Figure 14. Circumferential stresses in Al6022 rings (left) and in mild steel (right). Also shown on the left are the stresses after splitting the ring. On the right, results are shown also for rings cut at different vertical positions.

1.3 Outlook

Future development efforts are concentrated on instrumental improvements in two areas: increasing the intensity of the primary beam and increasing detector coverage. The two areas have a major effect on the duration of an experiment and they translate directly into the ability of the neutron instrument to keep up with demand.

The neutron flux before the monochromator cannot be increased as it depends primarily on the reactor. Thus, the main source of increase is the use of a larger beam port to increase the active area of the double focusing monochromator. It is estimated that together with the use of germanium as monochromator material the intensity can be more than doubled without sacrificing resolution. However, no beam port is currently available to allow the use of this option.

Currently, increased detector coverage is the most effective use of funds because the benefit is immediately available. It is planned to use up to three vertically stacked position sensitive detectors simultaneously. This upgrade is currently being implemented, thus providing a threefold increase in detected intensity.

BIBLIOGRAPHY

POPOVICI, M., STOICA, A.D., HUBBARD, C.R., SPOONER, S., PRASK, H.J., GNAEUPEL-HEROLD, T., GEHRING, P.M., ERWIN, R.W., *Multi-wafer focusing neutron monochromators and applications*, in: Neutron Optics (WOOD, JAMES L., ANDERSON, IAN S.Eds) Proceedings of SPIE, Volume 4509, pp. 21-32 (2001).

GNAEUPEL-HEROLD, T., PRASK, H.J., MAGIERA, J., *Effect of Grinding Strategy on Accumulation of Damage in Rails: Neutron Diffraction Investigation of Residual Stresses in Transverse and Oblique cut Rail Slices*, Proceedings of the 6th International Conference on Residual Stresses (ICRS-6), Oxford, July 10-12, 2000, p 879-888, ISBN I-86125-123-8

PRASK, H. J., BRAND, P.C., GNAEUPEL-HEROLD, T., HICHO, G.E., *Determination of Residual Stresses Using Neutron Diffraction: Tank-Car Welds and Rail Slices*, in Topics on Non-destructive Evaluation Series: Volume 5, Non-destructive testing and Evaluation for the

Railroad Industry, (REIS, H., BARKAN, C., Eds), (ASNT, Columbus, OH), pp 199-211 (2002)

GNAEUPEL-HEROLD, T., PRASK, H.J., FIELDS, R.J., FOECKE, T.J., XIA, Z.C., LIENERT, U., *A Synchrotron Study of Residual Stresses in a Al6022 Deep Drawn Cup*, Mat. Sci. Eng. **A366**, 104-113 (2004)

LIST OF PARTICIPANTS

Gnäupel-Herold, T.   NIST Center for Neutron Research,
Bureau Dr. Stop 8562,
Gaithersburg, MD 20899-8562,
United States of America
Phone: 301-975-5380
Fax: + 1 301-921-9847
Email: tg-h@nist.gov

Mikula, P.   Neutron Physics Laboratory,
Nuclear Physics Institute of ASCR,
Rez near Prague 25068, Czech Republic
Phone: + 42 0 2 2094141 / + 42 0 2 6617 3553
Fax: + 420 2 20941130   / + 420 2 20940220
E-mail: mikula@ujf.cas.cz

Paranjpe, S.K.   International Atomic Energy Agency,
Wagramer Strasse 5,
1220, Vienna, Austria
Phone: + 43 1 260021751
Fax: + 43 1 26007 21751
E-mail: S.K.Paranjpe@iaea.org

Schneider, R.   Hahn-Meitner-Institute,
BENSE,
Glienicker Strasse 100,
14109 Berlin, Germany
E-mail: Schneider-r@hmi.de

Teixeira, J.   Centre National De La Recherche Scientifique
Laboratoire Leon Brillouin,
CEA Saclay – 91191 Gif-Sur-Yvette Cedex, France
Phone: +33 1 6908 6650
Fax: +33 1 6908 8261
E-mail: teix@llb.saclay.cea.fr

Torok, G.   Research Institute for Solid State Physics and Optics,
Neutron Spectroscopy Department,
Konkoly Thege str 29-33,
H1121 Budapest, Hungary
Phone: +36-1-392 2222 ext 1439
Fax +36-1-392-2501
E-mail: torok@power.szfki.kfki.hu

Venter, A.   NECSA, Atomic Energy Corporation of S.A Ltd,
Building No. 1800, P.O. Box 582,
Pretoria 001
Phone: + 27 12 31 66058
Fax: + 27 12 31 65956
E-mail: amventer@aec.co.za

Youtsos, A.G.   HFR/Neutron Methods Sector,
Joint Research Centre, Institute for Energy,
Westerduinweg 3, NL 1755 LE Petten,
Netherlands
Phone: + 31 224 565 262
Fax: + 31 224 561 384
E-mail: anastasius.YOUTSOS@cec.eu.int